

Estimating distinguishability measures on quantum computers

Rochisha Agarwal,¹ Soorya Rethinasamy,² Kunal Sharma,³ and Mark M. Wilde²

¹*Department of Physics, Indian Institute of Technology Roorkee, Roorkee, Uttarakhand, India*

²*Hearne Institute for Theoretical Physics, Department of Physics and Astronomy,
and Center for Computation and Technology, Louisiana State University, Baton Rouge, Louisiana 70803, USA*

³*Joint Center for Quantum Information and Computer Science,
University of Maryland, College Park, Maryland 20742, USA*

(Dated: April 18, 2022)

The performance of a quantum information processing protocol is ultimately judged by distinguishability measures that quantify how distinguishable the actual result of the protocol is from the ideal case. The most prominent distinguishability measures are those based on the fidelity and trace distance, due to their physical interpretations. In this paper, we propose and review several algorithms for estimating distinguishability measures based on trace distance and fidelity. The algorithms can be used for distinguishing quantum states, channels, and strategies (the last also known in the literature as “quantum combs”). The fidelity-based algorithms offer novel physical interpretations of these distinguishability measures in terms of the maximum probability with which a single prover (or competing provers) can convince a verifier to accept the outcome of an associated computation. We simulate many of these algorithms by using a variational approach with parameterized quantum circuits. We find that the simulations converge well in both the noiseless and noisy scenarios, for all examples considered. Furthermore, the noisy simulations exhibit a parameter noise resilience.

CONTENTS

I. Introduction	1	IV. Performance evaluation of algorithms using a noiseless and noisy quantum simulator	26
II. Estimating fidelity	3	A. Ansatz	26
A. Estimating fidelity of pure states	3	B. Test states and channels	26
B. Estimating fidelity when one state is pure and the other is mixed	4	C. Fidelity of states	26
C. Estimating fidelity of arbitrary states	5	D. Trace distance of states	27
1. Controlled unitary and Bell state overlap	6	E. Fidelity of channels	27
2. Generalized swap test	8	F. Diamond distance of channels	28
3. Variational algorithm with Bell measurements	9	G. Multiple state discrimination	29
4. Variational algorithm for Fuchs–Caves measurement	11	V. Generating fixed points of quantum channels	29
D. Estimating fidelity of channels	12	VI. Conclusion	30
E. Estimating fidelity of strategies	14	Acknowledgments	31
F. Alternate methods of estimating the fidelity of channels and strategies	16	References	31
G. Estimating maximum output fidelity of channels	17	A. Approximate fixed points and Deutschian closed timelike curves	34
H. Generalization to multiple states	18		
I. Generalization to multiple channels and strategies	20		
III. Estimating trace distance, diamond distance, and strategy distance	22		
A. Estimating trace distance	22		
B. Estimating diamond distance	23		
C. Estimating strategy distance	23		
D. Estimating minimum trace distance of channels	24		
E. Generalization to multiple states, channels, and strategies	24		

I. INTRODUCTION

In quantum information processing, it is essential to quantify the performance of protocols by using distinguishability measures. It is typically the case that there is an ideal state to prepare or an ideal channel to simulate, but in practice, we can only realize approximations, due to experimental error. Two commonly employed distinguishability measures for states are the trace distance [Hel67, Hel69] and the fidelity [Uhl76]. The former has an operational interpretation as the distinguishing advantage in the optimal success probability when trying to distinguish two states that are chosen uniformly at random. The latter has an operational meaning as

the maximum probability that a purification of one state could pass a test for being a purification of the other (this is known as Uhlmann’s transition probability [Uhl76]). These distinguishability measures have generalizations to quantum channels, in the form of the diamond distance [Kit97] and the fidelity of channels [GLN05], as well as to strategies (sequences of channels), in the form of the strategy distance [CDP08, CDP09, Gut12] and the fidelity of strategies [GRS18]. Each of these measures are generalized by the generalized divergence of states [SW12], channels [LKDW18], and strategies [WW19]. The operational interpretations of these latter distinguishability measures are similar to the aforementioned ones, but the corresponding protocols involve more steps that are used in the distinguishing process.

Both the trace distance and the fidelity can be computed by means of semi-definite programming [Wat13], so that they can be estimated accurately with a runtime that is polynomial in the dimension of the states. The same is true for the diamond distance [Wat09b], fidelity of channels [YF17, KW21], the strategy distance [CDP08, CDP09, Gut12], and the fidelity of strategies [GRS18]. While this method of estimating these quantities is reasonable for states, channels, and strategies of small dimension, its computational complexity actually increases exponentially with the number of qubits involved, due to the well known fact that Hilbert-space dimension grows exponentially with the number of qubits.

In this paper, we provide several quantum algorithms for estimating these distinguishability measures. Some of the algorithms rely on interaction with a quantum prover, in which case they are not necessarily efficiently computable even on a quantum computer. In fact, the computational hardness results of [Wat02, RW05, Wat09c] lend credence to the belief that estimating these quantities reliably is not generally possible in polynomial time on a quantum computer. However, as we show in our paper, by replacing the quantum prover with a parameterized circuit (see [CAB+20, BCLK+21] for reviews of variational algorithms), it is possible in some cases to estimate these quantities reliably. Identifying precise conditions under which a quantum computer can estimate these quantities efficiently is an interesting open question that we leave for future research. Already in [WZC+21], it was shown that estimating the fidelity of two quantum states is possible in quantum polynomial time when one of the states is low rank. See also [CPCC20, CSZW20, TV21] for variational algorithms that estimate fidelity of states and [CSZW20, LLSL21] for variational algorithms to estimate trace distance. It is open to determine conditions under which precise estimation is possible for channel and strategy distinguishability measures.

One of the other results of our paper is that the problem of estimating the fidelity between a mixed state and a pure state is a BQP-complete promise problem (see [Wat09a, VW16] for reviews of quantum computational complexity theory). The aforementioned result follows

by demonstrating that there is an efficient quantum algorithm for this task and by showing a reduction from an arbitrary BQP algorithm to one for this task. Thus, if we believe that there is a separation between the computational power of classical and quantum computers, then this fidelity estimation problem is one for which a quantum computer has an advantage. Several BQP-complete promise problems are known, including approximating the Jones polynomial [AJL06], estimating quadratically signed weight enumerators [KL01], estimating diagonal entries of powers of sparse matrices [JW07], a problem related to matrix inversion [HHL09], and deciding whether a pure bipartite state is entangled [GHMW15]. See [Zha12] for a 2012 review of BQP-complete promise problems.

Lastly, we perform noiseless and noisy simulations of several of the algorithms provided. We find that in the noiseless scenario, all algorithms converge to the true known value of the distinguishability measure under consideration. In the noisy simulations, the algorithms converge well, and the parameters obtained exhibit a noise resilience, as put forward in [SKCC20]; i.e., the relevant quantity can be accurately estimated by inputting the parameters learned from the noisy simulator into the noiseless simulator.

In the rest of the paper, we provide details of the algorithms and results mentioned above. In particular, our paper proceeds as follows:

1. The various subsections of Section II are about estimating fidelity of states, channels, and strategies. We begin in Section II A by establishing two quantum algorithms for estimating the fidelity of pure states, one of which is based on a state overlap test (Algorithm 1) and another that employs Bell state preparation and measurement along with a controlled unitary (Algorithm 2).
2. In Section II B, we generalize Algorithm 1 to estimate the fidelity of a pure state and a mixed state (see Algorithm 3), and we prove that the promise version of this problem is BQP-complete (Theorem 1).
3. In Section II C, we establish several quantum algorithms for estimating the fidelity of two arbitrary states. Algorithm 4 generalizes Algorithm 2. Algorithm 5 generalizes the well known swap test to the case of arbitrary states. Algorithm 6 is a variational algorithm that employs Bell measurements, as a generalization of the approach in [GEC13, SCC19] for pure states. Algorithm 7 is another variational algorithm that attempts to simulate a fidelity-achieving measurement, such as the Fuchs–Caves measurement [FC95], in order to estimate the fidelity.
4. In Section II D, we generalize Algorithm 4 to a quantum algorithm for estimating the fidelity of

quantum channels (see Algorithm 8). This algorithm involves interaction with competing quantum provers, and interestingly, its acceptance probability is directly related to the fidelity of channels, thus giving the latter an operational meaning. Later, we replace the provers with parameterized circuits and arrive at a method for estimating fidelity of channels.

5. In Section II E, we generalize the aforementioned approach in order to estimate the fidelity of strategies (a strategy is a sequence of quantum channels and thus generalizes the notion of a quantum channel).
6. In Section II F, we briefly discuss alternative methods for estimating the fidelity of channels and strategies, based on the approaches from Section II C for estimating the fidelity of states.
7. Section II G introduces a method for estimating the maximum output fidelity of two quantum channels, which has an application to generating a fixed point of a quantum channel (as discussed later on in Section V).
8. In Sections II H and III, we generalize the whole development above to the case of testing similarity of arbitrary ensembles of states, channels, or strategies. We find that the acceptance probability of the corresponding algorithms is related to the secrecy measure from [KRS09], which can be understood as a measure of similarity of the states in an ensemble. We then establish generalizations of this measure for an ensemble of channels and an ensemble of strategies and remark how this has applications in private quantum reading [BDW18, DBW20].
9. We then move on in Section III to estimating trace-distance-based measures, for states, channels, and strategies. We stress that these various algorithms were already known, and our goal here is to investigate their performance using a variational approach. In Sections III A, III B, and III C, Algorithms 14, 15, and 16 provide methods for estimating the trace distance of states, the diamond distance of channels, and the strategy distance of strategies, respectively.
10. In Section III D, we provide two different but related algorithms for estimating the minimum trace distance between two quantum channels. The related approaches employ competing provers to do so.
11. In Section III E, we generalize the whole development for trace-distance based algorithms to the case of multiple states, channels, and strategies.
12. In Section IV, we discuss the results of numerical simulations of Algorithms 4–8, Algorithms 14–15, and Algorithm 19. We use both noiseless and

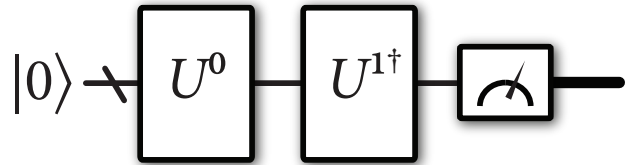


FIG. 1. This figure depicts Algorithm 1 for estimating the fidelity of pure states generated by quantum circuits U^0 and U^1 .

noisy quantum simulators and a variational approach with parameterized circuits.

We finally conclude in Section VI with a summary and some open questions.

II. ESTIMATING FIDELITY

A. Estimating fidelity of pure states

We begin by outlining two simple quantum algorithms for estimating fidelity when both states are pure. A standard approach for doing so is to use the swap test [BCWdW01] or Bell measurements [GEC13, SCC19]. The approaches that we discuss below are different from these approaches. The first algorithm is a special case of that proposed in [Wat02] (see also [CSZW20]), as well as a special case of Algorithm 3 presented later. See also [LLB18]. The second algorithm involves a Bell-state preparation and projection, as well as controlled interactions, and it is a special case of Algorithm 4 presented later. We list both of these algorithms here for completeness and because later algorithms build upon them.

Suppose that the goal is to estimate the fidelity of pure states ψ^0 and ψ^1 , and we are given access to quantum circuits U^0 and U^1 that prepare these states when acting on the all-zeros state. We now detail a first quantum algorithm for estimating the fidelity

$$F(\psi^0, \psi^1) := |\langle \psi^1 | \psi^0 \rangle|^2. \quad (1)$$

Algorithm 1 *The algorithm proceeds as follows:*

1. Act with the circuit U^0 on the all-zeros state $|0\rangle$.
2. Act with $U^{1\dagger}$ and perform a measurement of all qubits in the computational basis.
3. Accept if and only if the all-zeros outcome is observed.

Algorithm 1 is depicted in Figure 1. The acceptance probability of Algorithm 1 is precisely equal to $|\langle 0 | U^{1\dagger} U^0 | 0 \rangle|^2$, which by definition is equal to the fidelity

in (1). In fact, Algorithm 1 is a quantum computational implementation of the well known operational interpretation of the fidelity as the probability that the state ψ^0 passes a test for being the state ψ^1 .

Our next quantum algorithm for estimating fidelity makes use of a Bell-state preparation and projection. Its acceptance probability is equal to

$$\frac{1}{2} \left(1 + \sqrt{F}(\psi^0, \psi^1) \right) \quad (2)$$

and thus gives a way to estimate the fidelity through repetition. It is a variational algorithm that optimizes over a phase ϕ and makes use of the fact that

$$\max_{\phi \in [0, 2\pi]} \text{Re}[e^{i\phi} \langle \psi^0 | \psi^1 \rangle] = |\langle \psi^0 | \psi^1 \rangle|. \quad (3)$$

Let S denote the quantum system in which the states ψ^0 and ψ^1 are prepared.

Algorithm 2 *The algorithm proceeds as follows:*

1. Prepare a Bell state

$$|\Phi\rangle_{T'T} := \frac{1}{\sqrt{2}}(|00\rangle_{T'T} + |11\rangle_{T'T}) \quad (4)$$

on registers T' and T and prepare system S in the all-zeros state $|0\rangle_S$.

2. Using the circuits U_S^0 and U_S^1 , perform the following controlled unitary:

$$\sum_{i \in \{0,1\}} |i\rangle\langle i|_T \otimes U_S^i. \quad (5)$$

3. Act with the following unitary on system T' :

$$\begin{bmatrix} 1 & 0 \\ 0 & e^{i\phi} \end{bmatrix}. \quad (6)$$

4. Perform a Bell measurement

$$\{\Phi_{T'T}, I_{T'T} - \Phi_{T'T}\} \quad (7)$$

on systems T' and T . Accept if and only if the outcome $\Phi_{T'T}$ occurs.

Figure 2 depicts Algorithm 2. After Step 3 of Algorithm 2, the overall state is as follows:

$$\frac{1}{\sqrt{2}} \sum_{j \in \{0,1\}} |jj\rangle_{T'T} e^{ij\phi} |\psi^j\rangle_S, \quad (8)$$

and the acceptance probability is equal to

$$\left\| \langle \Phi |_{T'T} \left(\frac{1}{\sqrt{2}} \sum_{j \in \{0,1\}} |jj\rangle_{T'T} e^{ij\phi} |\psi^j\rangle_S \right) \right\|_2^2$$

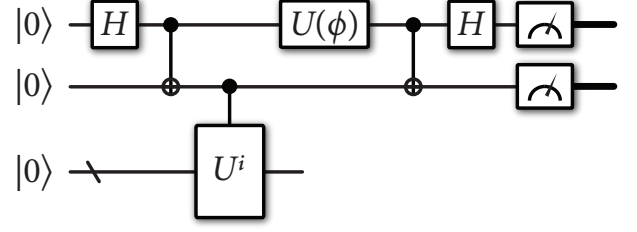


FIG. 2. This figure depicts Algorithm 2 for estimating the fidelity of pure states generated by quantum circuits U^0 and U^1 . The third gate with U^i in the box is defined in (5).

$$= \frac{1}{4} \left\| \sum_{j,k \in \{0,1\}} \langle kk | jj \rangle_{T'T} e^{ij\phi} |\psi^j\rangle_S \right\|_2^2 \quad (9)$$

$$= \frac{1}{4} \left\| \sum_{j \in \{0,1\}} e^{ij\phi} |\psi^j\rangle_S \right\|_2^2 \quad (10)$$

$$= \frac{1}{4} (2 + 2 \text{Re}[e^{i\phi} \langle \psi^0 | \psi^1 \rangle]). \quad (11)$$

By choosing the optimal phase ϕ in (3), we find that the acceptance probability is equal to the expression in (2). Note that, through repetition, we can execute Algorithm 2 in a variational way to learn the optimal value of ϕ .

B. Estimating fidelity when one state is pure and the other is mixed

In this section, we outline a simple quantum algorithm that estimates the fidelity between a mixed state ρ_S and a pure state ψ_S . It is a straightforward generalization of Algorithm 1. We also prove that a promise version of this problem is a BQP-complete promise problem.

Let U_{RS}^ρ be a quantum circuit that generates a purification φ_{RS} of ρ_S when acting on the all-zeros state of systems RS , and let U_S^ψ be a circuit that generates ψ_S when acting on the all-zeros state.

Algorithm 3 *The algorithm proceeds as follows:*

1. Act on the all-zeros state $|0\rangle_{RS}$ with the circuit U_{RS}^ρ .
2. Act with $U_S^{\psi^\dagger}$ on system S and perform a measurement of all qubits of system S in the computational basis.
3. Accept if and only if the all-zeros outcome is observed.

Figure 3 depicts Algorithm 3. The acceptance probability of Algorithm 3 is equal to the fidelity $F(\psi, \rho) =$

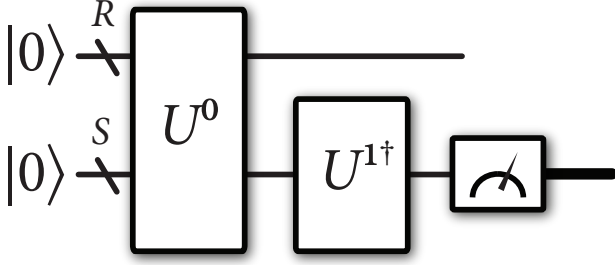


FIG. 3. This figure depicts Algorithm 3 for estimating the fidelity of a mixed state generated by a quantum circuit U^0 and a pure state generated by U^1 .

$\langle\psi|\rho|\psi\rangle$, which follows because

$$\begin{aligned} & \left\| \langle 0|_S U_S^{\psi^\dagger} U_{RS}^\rho |0\rangle_{RS} \right\|_2^2 \\ &= \|\langle\psi|_S|\varphi\rangle_{RS}\|_2^2 \end{aligned} \quad (12)$$

$$= \text{Tr}[(I_R \otimes |\psi\rangle\langle\psi|_S) |\varphi\rangle\langle\varphi|_{RS}] \quad (13)$$

$$= \text{Tr}[|\psi\rangle\langle\psi|_S \rho_S] \quad (14)$$

$$= \langle\psi|\rho|\psi\rangle. \quad (15)$$

We note here that it is not strictly necessary to have access to the reference system R of $|\varphi\rangle_{RS}$ in order to execute Algorithm 3. It is only necessary to have some method of generating the reduced state ρ_S .

As we show now, the promise problem version of estimating the fidelity of a pure state and a mixed state is BQP-complete. In what follows, we provide a detailed argument for this claim. The meaning of this result is that the problem can be solved efficiently on a quantum computer (as witnessed by Algorithm 3), and this problem furthermore captures the full power of polynomial-time quantum computation. Refs. [Wat09a, VW16] provide reviews of basic concepts in quantum computational complexity theory.

Problem 1 ((α, β) -Fidelity-Pure-Mixed) *Let α and β be such that $0 \leq \alpha < \beta \leq 1$. Given are descriptions of circuits U_{RS}^ρ and U_S^ψ that prepare a purification of a mixed state ρ_S and a pure state ψ_S , respectively. Decide which of the following holds.*

$$\text{Yes: } F(\rho_S, \psi_S) \geq 1 - \alpha, \quad (16)$$

$$\text{No: } F(\rho_S, \psi_S) \leq 1 - \beta. \quad (17)$$

Theorem 1 *The promise problem Fidelity-Pure-Mixed is BQP-complete.*

1. (α, β) -Fidelity-Pure-Mixed is in BQP for all $\alpha < \beta$. (It is implicit that the gap between α and β is larger than an inverse polynomial in the input length.)
2. $(\varepsilon, 1 - \varepsilon)$ -Fidelity-Pure-Mixed is BQP-hard, even when ε decays exponentially in the input length.

Thus, (α, β) -Fidelity-Pure-Mixed is BQP-complete for all (α, β) such that $0 < \alpha < \beta < 1$.

Proof. The containment of (α, β) -Fidelity-Pure-Mixed in BQP is a direct consequence of Algorithm 3. So we focus on proving the hardness result. Let L be an arbitrary promise problem in BQP, and let $\{\phi_{DG}^x\}_x$ be a family of efficiently preparable pure states witnessing membership of L in BQP. System D is a decision qubit indicating acceptance or rejection of x , and system G is a garbage system that purifies D . Suppose that the family $\{\phi_{DG}^x\}_x$ has completeness $1 - \delta$ and soundness δ . If x is a yes-instance of L , then, by the definition of BQP, it follows that $\|\langle 1|_D|\phi^x\rangle_{DG}\|_2^2 \geq 1 - \delta$. On the other hand, if x is a no-instance of L , then $\|\langle 1|_D|\phi^x\rangle_{DG}\|_2^2 \leq \delta$. Since

$$\|\langle 1|_D|\phi^x\rangle_{DG}\|_2^2 = \langle 1|_D \text{Tr}_G[\phi_{DG}^x] |1\rangle_D \quad (18)$$

$$= F(|1\rangle\langle 1|_D, \text{Tr}_G[\phi_{DG}^x]), \quad (19)$$

it follows directly that this is an instance of $(1 - \delta, \delta)$ -Fidelity-Pure-Mixed, given that the reduced state $\text{Tr}_G[\phi_{DG}^x]$ can be prepared efficiently, as well as the state $|1\rangle\langle 1|_D$. The desired hardness result then follows because $\text{BQP}(c, s) \subseteq \text{BQP}(\delta, 1 - \delta)$, for every δ exponentially small in the input length. ■

C. Estimating fidelity of arbitrary states

In this section, we outline several quantum algorithms for estimating the fidelity of arbitrary states on a quantum computer, some of which involve an interaction with a quantum prover (more precisely, the algorithms involving interaction with a prover are QSZK algorithms, where QSZK stands for “quantum statistical zero knowledge” [Wat02, Wat09c]). The algorithms are different from the algorithm proposed in [Wat02] (as also considered in [CSZW20]), which is based on Uhlmann’s formula for fidelity [Uhl76].

Suppose that the goal is to estimate the fidelity of states ρ_S^0 and ρ_S^1 , defined as [Uhl76]

$$F(\rho_S^0, \rho_S^1) := \left\| \sqrt{\rho_S^0} \sqrt{\rho_S^1} \right\|_1^2, \quad (20)$$

where the trace norm of an operator A is defined as $\|A\|_1 := \text{Tr}[\sqrt{A^\dagger A}]$. Suppose also that we are given access to quantum circuits U_{RS}^0 and U_{RS}^1 that prepare purifications ψ_{RS}^0 and ψ_{RS}^1 of ρ_S^0 and ρ_S^1 , respectively, when acting on the all-zeros state $|0\rangle_{RS}$. Let us recall Uhlmann’s formula for fidelity [Uhl76]:

$$F(\rho_S^0, \rho_S^1) = \max_{|\psi^0\rangle_{RS}, |\psi^1\rangle_{RS}} |\langle\psi^1|\psi^0\rangle_{RS}|^2, \quad (21)$$

where the optimization is over all purifications ψ_{RS}^0 and ψ_{RS}^1 of ρ_S^0 and ρ_S^1 , respectively. We note here that the fidelity can be computed by means of a semi-definite program [Wat13]. Also, the promise version of this problem, involving descriptions of quantum circuits as input,

is a QSZK-complete promise problem [Wat02], where QSZK stands for quantum statistical zero knowledge (see [Wat02, Wat09c] for details of this complexity class). Thus, it is unlikely that anyone will find a general purpose efficient quantum algorithm for estimating fidelity (i.e., one that does not involve interaction with an all-powerful prover).

1. Controlled unitary and Bell state overlap

We now detail a QSZK algorithm for estimating the following quantity:

$$\frac{1}{2} \left(1 + \sqrt{F}(\rho_S^0, \rho_S^1) \right). \quad (22)$$

It is a QSZK algorithm because, in the case that the fidelity $\sqrt{F}(\rho_S^0, \rho_S^1) \approx 1$, the verifier does not learn anything by interacting with the prover (i.e., the verifier only learns that the algorithm accepts with high probability). This algorithm is somewhat similar to the quantum algorithm proposed in [CHM⁺16], which was used for estimating a quantity known as fidelity of recovery [SW15]. It is also similar to the algorithm described in Figure 3 of [KW00]. It can be understood as a generalization of Algorithm 2 from pure states to arbitrary states.

Algorithm 4 *The algorithm proceeds as follows:*

1. The verifier prepares a Bell state

$$|\Phi\rangle_{T'T} := \frac{1}{\sqrt{2}}(|00\rangle_{T'T} + |11\rangle_{T'T}) \quad (23)$$

on registers T' and T and prepares systems RS in the all-zeros state $|0\rangle_{RS}$.

2. Using the circuits U_{RS}^0 and U_{RS}^1 , the verifier performs the following controlled unitary:

$$\sum_{i \in \{0,1\}} |i\rangle\langle i|_T \otimes U_{RS}^i. \quad (24)$$

3. The verifier transmits systems T' and R to the prover.

4. The prover prepares a system F in the $|0\rangle_F$ state and acts on systems T' , R , and F with a unitary $P_{T'RF \rightarrow T''F'}$ to produce the output systems T'' and F' , where T'' is a qubit system.

5. The prover sends system T'' to the verifier, who then performs a Bell measurement

$$\{\Phi_{T''T}, I_{T''T} - \Phi_{T''T}\} \quad (25)$$

on systems T'' and T . The verifier accepts if and only if the outcome $\Phi_{T''T}$ occurs.

Figure 4 depicts Algorithm 4.

Theorem 2 *The acceptance probability of Algorithm 4 is equal to*

$$\frac{1}{2} \left(1 + \sqrt{F}(\rho_S^0, \rho_S^1) \right). \quad (26)$$

Proof. After Step 1 of Algorithm 4, the global state is

$$|\Phi\rangle_{T'T}|0\rangle_{RS}. \quad (27)$$

After Step 2 of Algorithm 4, it is

$$\frac{1}{\sqrt{2}} \sum_{i \in \{0,1\}} |i\rangle_{T'} |i\rangle_T |\psi^i\rangle_{RS}. \quad (28)$$

After Step 4 of Algorithm 4, it is

$$P_{T'RF \rightarrow T''F'} \left(\frac{1}{\sqrt{2}} \sum_{i \in \{0,1\}} |i\rangle_{T'} |i\rangle_T |\psi^i\rangle_{RS} |0\rangle_F \right). \quad (29)$$

For a fixed unitary $P \equiv P_{T'RF \rightarrow T''F'}$ of the prover, the acceptance probability is then

$$\begin{aligned} & \left\| \langle \Phi |_{T''T} P \left(\frac{1}{\sqrt{2}} \sum_{i \in \{0,1\}} |i\rangle_{T'} |i\rangle_T |\psi^i\rangle_{RS} |0\rangle_F \right) \right\|_2^2 \\ &= \frac{1}{2} \left\| \langle \Phi |_{T''T} P \sum_{i \in \{0,1\}} |i\rangle_{T'} |i\rangle_T |\psi^i\rangle_{RS} |0\rangle_F \right\|_2^2. \end{aligned} \quad (30)$$

In a quantum interactive proof, the prover is trying to maximize the probability that the verifier accepts. So the acceptance probability of Algorithm 4 is given by

$$\max_{P_{T'RF \rightarrow T''F'}} \frac{1}{2} \left\| \langle \Phi |_{T''T} P \sum_{i \in \{0,1\}} |i\rangle_{T'} |i\rangle_T |\psi^i\rangle_{RS} |0\rangle_F \right\|_2^2. \quad (31)$$

Setting

$$P_{R \rightarrow F'}^0 := \langle 0 |_{T''} P_{T'RF \rightarrow T''F'} |0\rangle_{T'} |0\rangle_F, \quad (32)$$

$$P_{R \rightarrow F'}^1 := \langle 1 |_{T''} P_{T'RF \rightarrow T''F'} |1\rangle_{T'} |0\rangle_F, \quad (33)$$

we have that

$$\begin{aligned} & \frac{1}{2} \left\| \langle \Phi |_{T''T} P \sum_{i \in \{0,1\}} |i\rangle_{T'} |i\rangle_T |\psi^i\rangle_{RS} |0\rangle_F \right\|_2^2 \\ &= \frac{1}{4} \left\| \sum_{i \in \{0,1\}} P_{R \rightarrow F'}^i |\psi^i\rangle_{RS} \right\|_2^2 \end{aligned} \quad (34)$$

$$= \frac{1}{4} \sum_{i,j \in \{0,1\}} \langle \psi^i |_{RS} (P_{R \rightarrow F'}^i)^\dagger P_{R \rightarrow F'}^j |\psi^j\rangle_{RS} \quad (35)$$

$$\leq \frac{1}{2} \left(1 + \text{Re} \{ \langle \psi^0 |_{RS} (P_{R \rightarrow F'}^0)^\dagger P_{R \rightarrow F'}^1 |\psi^1\rangle_{RS} \} \right) \quad (36)$$

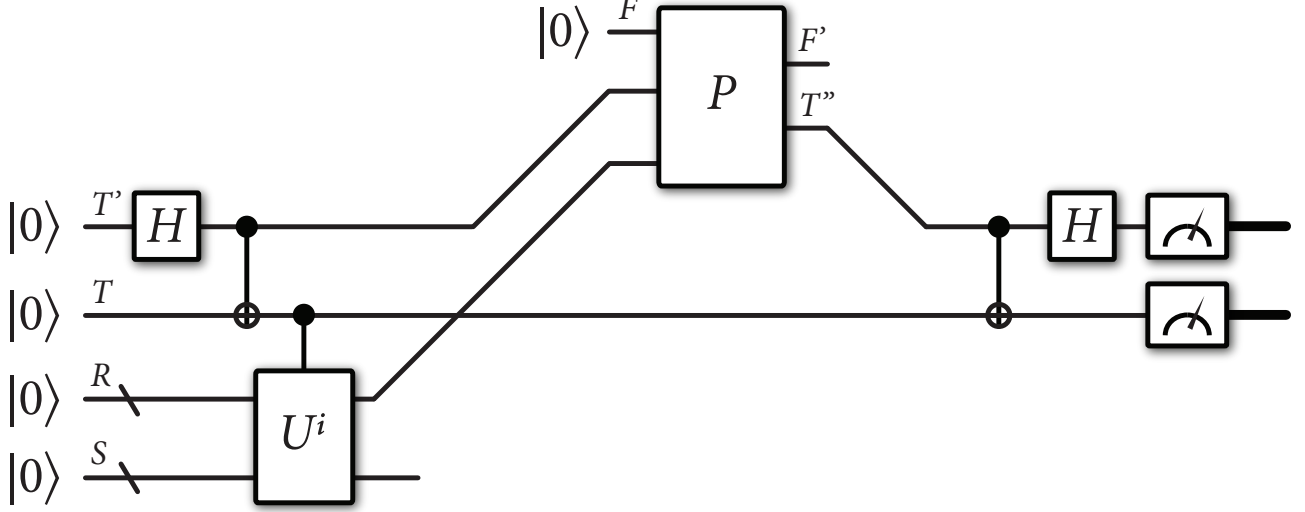


FIG. 4. This figure depicts Algorithm 4 for estimating the fidelity of mixed states generated by quantum circuits U_{RS}^0 and U_{RS}^1 .

$$\leq \frac{1}{2} (1 + |\langle \psi^0 |_{RS} (P_{R \rightarrow F'}^0)^\dagger P_{R \rightarrow F'}^1 | \psi^1 \rangle_{RS}|). \quad (37)$$

The first inequality follows because $P_{R \rightarrow F'}^i$ is a contraction for $i \in \{0, 1\}$, so that $(P_{R \rightarrow F'}^i)^\dagger P_{R \rightarrow F'}^i \leq I_{F'}$. Then consider that

$$\begin{aligned} & |\langle \psi^0 |_{RS} (P_{R \rightarrow F'}^0)^\dagger P_{R \rightarrow F'}^1 | \psi^1 \rangle_{RS}| \\ & \leq \max_{P^0, P^1} \left\{ |\langle \psi^0 |_{RS} (P_{R \rightarrow F'}^0)^\dagger P_{R \rightarrow F'}^1 | \psi^1 \rangle_{RS}| \right. \\ & \quad \left. : \|P^i\|_\infty \leq 1 \forall i \right\} \end{aligned} \quad (38)$$

$$= \sqrt{F}(\rho_S^0, \rho_S^1). \quad (39)$$

The last line is a consequence of the following reasoning (which is the same as that employed in Section III in [CHM⁺16]). The inequality

$$\begin{aligned} & \max_{P^0, P^1} \left\{ |\langle \psi^0 |_{RS} (P_{R \rightarrow F'}^0)^\dagger P_{R \rightarrow F'}^1 | \psi^1 \rangle_{RS}| \right\} \\ & \quad : \|P^i\|_\infty \leq 1 \forall i \\ & \geq \sqrt{F}(\rho_S^0, \rho_S^1) \end{aligned} \quad (40)$$

holds because the isometries $P_{R \rightarrow F'}^0$ and $P_{R \rightarrow F'}^1$ that achieve the maximum for the fidelity are each contractions and the optimization is conducted over all contractions. The opposite inequality

$$\begin{aligned} & \max_{P^0, P^1} \left\{ |\langle \psi^0 |_{RS} (P_{R \rightarrow F'}^0)^\dagger P_{R \rightarrow F'}^1 | \psi^1 \rangle_{RS}| \right\} \\ & \quad : \|P^i\|_\infty \leq 1 \forall i \\ & \leq \sqrt{F}(\rho_S^0, \rho_S^1) \end{aligned} \quad (41)$$

is a consequence of the fact that every contraction can be written as a convex combination of isometries [Zha11, Theorem 5.10]. Indeed, this means that, for each $i \in \{0, 1\}$,

$$P_{R \rightarrow F'}^i = \sum_x p_i(x) W_{R \rightarrow F'}^{i,x}, \quad (42)$$

where $\{p_i(x)\}_x$ is a probability distribution and $W_{R \rightarrow F'}^{i,x}$ is an isometry, for each i and x . Then we find that

$$\begin{aligned} & |\langle \psi^0 |_{RS} (P_{R \rightarrow F'}^0)^\dagger P_{R \rightarrow F'}^1 | \psi^1 \rangle_{RS}| \\ & = \left| \langle \psi^0 |_{RS} \left(\sum_x p_0(x) W_{R \rightarrow F'}^{0,x} \right)^\dagger \times \right. \\ & \quad \left. \left(\sum_{x'} p_1(x') W_{R \rightarrow F'}^{1,x'} \right) | \psi^1 \rangle_{RS} \right| \end{aligned} \quad (43)$$

$$\begin{aligned} & = \left| \sum_{x,x'} p_0(x) p_1(x') \langle \psi^0 |_{RS} \left(W_{R \rightarrow F'}^{0,x} \right)^\dagger W_{R \rightarrow F'}^{1,x'} | \psi^1 \rangle_{RS} \right| \\ & \leq \sum_{x,x'} p_0(x) p_1(x') \left| \langle \psi^0 |_{RS} \left(W_{R \rightarrow F'}^{0,x} \right)^\dagger W_{R \rightarrow F'}^{1,x'} | \psi^1 \rangle_{RS} \right| \end{aligned} \quad (44)$$

$$\begin{aligned} & \leq \sum_{x,x'} p_0(x) p_1(x') \left| \langle \psi^0 |_{RS} \left(W_{R \rightarrow F'}^{0,x} \right)^\dagger W_{R \rightarrow F'}^{1,x'} | \psi^1 \rangle_{RS} \right| \\ & \leq \max_{x,x'} \left| \langle \psi^0 |_{RS} \left(W_{R \rightarrow F'}^{0,x} \right)^\dagger W_{R \rightarrow F'}^{1,x'} | \psi^1 \rangle_{RS} \right| \end{aligned} \quad (45)$$

$$\begin{aligned} & \leq \max_{x,x'} \left| \langle \psi^0 |_{RS} \left(W_{R \rightarrow F'}^{0,x} \right)^\dagger W_{R \rightarrow F'}^{1,x'} | \psi^1 \rangle_{RS} \right| \\ & \leq \sqrt{F}(\rho_S^0, \rho_S^1). \end{aligned} \quad (46)$$

$$\leq \sqrt{F}(\rho_S^0, \rho_S^1). \quad (47)$$

Thus, an upper bound on the acceptance probability of Algorithm 4 is as follows:

$$\frac{1}{2} (1 + \sqrt{F}(\rho_S^0, \rho_S^1)). \quad (48)$$

This upper bound can be achieved if the prover applies a unitary extension of the following isometry:

$$P_{T'R \rightarrow T''F'} = \sum_{i \in \{0,1\}} |i\rangle_{T''} \langle i|_{T'} \otimes P_{R \rightarrow F'}^i \otimes |0\rangle_{F'}, \quad (49)$$

where $P_{R \rightarrow F'}^0$ and $P_{R \rightarrow F'}^1$ are isometries achieving the maximum in the fidelity $F(\rho_S^0, \rho_S^1)$. ■

2. Generalized swap test

We now detail another quantum algorithm for estimating the fidelity of arbitrary states, which is a generalization of the well known swap test from [BCWdW01]. We note that this algorithm was used in [KW00, Figure 3] as part of their proof that QIP = QIP(3). A key difference between Algorithm 5 and [KW00, Figure 3] is that Algorithm 5 accepts if and only if both qubits at the end are measured to be in the all-zeros state, whereas it is written in [KW00, Figure 3] that their algorithm accepts if and only if the first qubit is measured to be in the zero state.

Algorithm 5 *The algorithm proceeds as follows:*

1. The verifier prepares a Bell state

$$|\Phi\rangle_{T'T} := \frac{1}{\sqrt{2}}(|00\rangle_{T'T} + |11\rangle_{T'T}) \quad (50)$$

on registers T' and T and prepares systems $R_1 S_1 R_2 S_2$ in the all-zeros state $|0\rangle_{R_1 S_1 R_2 S_2}$.

2. Using the circuits U_{RS}^0 and U_{RS}^1 , the verifier acts on $R_1 S_1 R_2 S_2$ to prepare the two pure states $|\psi^{\rho^0}\rangle_{R_1 S_1}$ and $|\psi^{\rho^1}\rangle_{R_2 S_2}$.
3. The verifier performs a controlled SWAP from qubit T to systems S_1 and S_2 , which applies identity if the control qubit is $|0\rangle$ and swaps S_1 with S_2 if the control qubit is $|1\rangle$.
4. The verifier transmits systems T' , R_1 , and R_2 to the prover.
5. The prover prepares a system F in the $|0\rangle_F$ state and acts on systems T' , R_1 , R_2 , and F with a unitary $P_{T'R_1 R_2 F \rightarrow T'' F'}$ to produce the output systems T'' and F' , where T'' is a qubit system.
6. The prover sends system T'' to the verifier, who then performs a Bell measurement

$$\{\Phi_{T''T}, I_{T''T} - \Phi_{T''T}\} \quad (51)$$

on systems T'' and T . The verifier accepts if and only if the outcome $\Phi_{T''T}$ occurs.

Figure 5 depicts Algorithm 5.

Theorem 3 *The acceptance probability of Algorithm 5 is equal to*

$$\frac{1}{2} (1 + F(\rho_S^0, \rho_S^1)). \quad (52)$$

Proof. After Step 1 of Algorithm 5, the global state is

$$|\Phi\rangle_{T'T} |0\rangle_{R_1 S_1 R_2 S_2}. \quad (53)$$

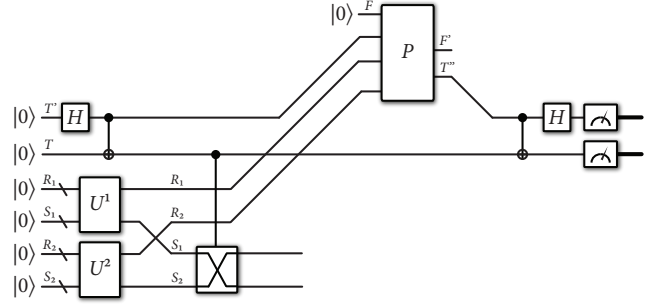


FIG. 5. This figure depicts Algorithm 5 for estimating the fidelity of mixed states generated by quantum circuits U_{RS}^0 and U_{RS}^1 . Algorithm 5 represents a generalization of the well known swap test for estimating the fidelity of pure states.

After Step 2, the global state is

$$|\Phi\rangle_{T'T} |\psi^{\rho^0}\rangle_{R_1 S_1} |\psi^{\rho^1}\rangle_{R_2 S_2}. \quad (54)$$

After Step 3, it becomes

$$\frac{1}{\sqrt{2}} |0\rangle_T |0\rangle_{T'} |\psi^{\rho^0}\rangle_{R_1 S_1} |\psi^{\rho^1}\rangle_{R_2 S_2} + \frac{1}{\sqrt{2}} |1\rangle_T |1\rangle_{T'} |\psi^{\rho^1}\rangle_{R_2 S_1} |\psi^{\rho^0}\rangle_{R_1 S_2}. \quad (55)$$

The verifier then sends systems T' , R_1 , and R_2 to the prover, who appends the state $|0\rangle_F$ and acts with a unitary $P_{T'R_1 R_2 F \rightarrow T'' F'}$. Without loss of generality, and for simplicity of the ensuing analysis, we can imagine that before applying the unitary $P_{T'R_1 R_2 F \rightarrow T'' F'}$, the prover applies a controlled SWAP to systems T' , R_1 , and R_2 , so that the state before applying $P_{T'R_1 R_2 F \rightarrow T'' F'}$ is as follows:

$$\frac{1}{\sqrt{2}} |0\rangle_T |0\rangle_{T'} |\psi^{\rho^0}\rangle_{R_1 S_1} |\psi^{\rho^1}\rangle_{R_2 S_2} + \frac{1}{\sqrt{2}} |1\rangle_T |1\rangle_{T'} |\psi^{\rho^1}\rangle_{R_1 S_1} |\psi^{\rho^0}\rangle_{R_2 S_2}. \quad (56)$$

This follows because the prover can apply arbitrary unitaries to his received systems, and one such possible unitary is to apply this controlled SWAP, undo it, and then apply $P_{T'R_1 R_2 F \rightarrow T'' F'}$. However, the latter two unitaries are a particular example of a unitary $P_{T'R_1 R_2 F \rightarrow T'' F'}$. So we proceed with the ensuing analysis assuming that the global state, before the prover applies $P_{T'R_1 R_2 F \rightarrow T'' F'}$, is given by (56). Note that the actions of tensoring in the state $|0\rangle_F$ and applying $P_{T'R_1 R_2 F \rightarrow T'' F'}$ together constitute an isometry

$$P_{T'R_1 R_2 \rightarrow T'' F'} := P_{T'R_1 R_2 F \rightarrow T'' F'} |0\rangle_F, \quad (57)$$

resulting in the state

$$\begin{aligned} & \frac{1}{\sqrt{2}} P_{T'R_1R_2 \rightarrow T''F'} |0\rangle_T |0\rangle_{T'} |\psi^{\rho^0}\rangle_{R_1S_1} |\psi^{\rho^1}\rangle_{R_2S_2} \\ & + \frac{1}{\sqrt{2}} P_{T'R_1R_2 \rightarrow T''F'} |1\rangle_T |1\rangle_{T'} |\psi^{\rho^1}\rangle_{R_1S_1} |\psi^{\rho^0}\rangle_{R_2S_2}. \end{aligned} \quad (58)$$

Let us set

$$P_{R_1R_2 \rightarrow F'}^{00} := \langle 0|_{T''} P_{T'R_1R_2 \rightarrow T''F'} |0\rangle_{T'}, \quad (59)$$

$$P_{R_1R_2 \rightarrow F'}^{11} := \langle 1|_{T''} P_{T'R_1R_2 \rightarrow T''F'} |1\rangle_{T'}. \quad (60)$$

The verifier finally performs a Bell measurement and accepts if and only if the outcome $\Phi_{T''T}$ occurs. The acceptance probability is then

$$\begin{aligned} & \left\| \langle \Phi|_{T''T} \frac{1}{\sqrt{2}} (|0\rangle_T P_{T'R_1R_2 \rightarrow T''F'} |0\rangle_{T'} |\psi^{\rho^0}\rangle_{R_1S_1} |\psi^{\rho^1}\rangle_{R_2S_2} + |1\rangle_T P_{T'R_1R_2 \rightarrow T''F'} |1\rangle_{T'} |\psi^{\rho^1}\rangle_{R_1S_1} |\psi^{\rho^0}\rangle_{R_2S_2}) \right\|_2^2 \\ & = \frac{1}{4} \left\| \langle 0|_{T''} P_{T'R_1R_2 \rightarrow T''F'} |0\rangle_{T'} |\psi^{\rho^0}\rangle_{R_1S_1} |\psi^{\rho^1}\rangle_{R_2S_2} + \langle 1|_{T''} P_{T'R_1R_2 \rightarrow T''F'} |1\rangle_{T'} |\psi^{\rho^1}\rangle_{R_1S_1} |\psi^{\rho^0}\rangle_{R_2S_2} \right\|_2^2 \end{aligned} \quad (61)$$

$$= \frac{1}{4} \left\| P_{R_1R_2 \rightarrow F'}^{00} |\psi^{\rho^0}\rangle_{R_1S_1} |\psi^{\rho^1}\rangle_{R_2S_2} + P_{R_1R_2 \rightarrow F'}^{11} |\psi^{\rho^1}\rangle_{R_1S_1} |\psi^{\rho^0}\rangle_{R_2S_2} \right\|_2^2 \quad (62)$$

$$= \frac{1}{4} \left(\begin{aligned} & \langle \psi^{\rho^0}|_{R_1S_1} \langle \psi^{\rho^1}|_{R_2S_2} (P_{R_1R_2 \rightarrow F'}^{00})^\dagger P_{R_1R_2 \rightarrow F'}^{00} |\psi^{\rho^0}\rangle_{R_1S_1} |\psi^{\rho^1}\rangle_{R_2S_2} \\ & + \langle \psi^{\rho^1}|_{R_1S_1} \langle \psi^{\rho^0}|_{R_2S_2} (P_{R_1R_2 \rightarrow F'}^{11})^\dagger P_{R_1R_2 \rightarrow F'}^{11} |\psi^{\rho^1}\rangle_{R_1S_1} |\psi^{\rho^0}\rangle_{R_2S_2} \\ & + \langle \psi^{\rho^0}|_{R_1S_1} \langle \psi^{\rho^1}|_{R_2S_2} (P_{R_1R_2 \rightarrow F'}^{00})^\dagger P_{R_1R_2 \rightarrow F'}^{11} |\psi^{\rho^1}\rangle_{R_1S_1} |\psi^{\rho^0}\rangle_{R_2S_2} \\ & + \langle \psi^{\rho^1}|_{R_1S_1} \langle \psi^{\rho^0}|_{R_2S_2} (P_{R_1R_2 \rightarrow F'}^{11})^\dagger P_{R_1R_2 \rightarrow F'}^{00} |\psi^{\rho^0}\rangle_{R_1S_1} |\psi^{\rho^1}\rangle_{R_2S_2} \end{aligned} \right) \quad (63)$$

$$\leq \frac{1}{4} \left(2 + 2 \operatorname{Re} \left\{ \langle \psi^{\rho^0}|_{R_1S_1} \langle \psi^{\rho^1}|_{R_2S_2} (P_{R_1R_2 \rightarrow F'}^{00})^\dagger P_{R_1R_2 \rightarrow F'}^{11} |\psi^{\rho^1}\rangle_{R_1S_1} |\psi^{\rho^0}\rangle_{R_2S_2} \right\} \right) \quad (64)$$

$$\leq \frac{1}{4} \left(2 + 2 \left| \langle \psi^{\rho^0}|_{R_1S_1} \langle \psi^{\rho^1}|_{R_2S_2} (P_{R_1R_2 \rightarrow F'}^{00})^\dagger P_{R_1R_2 \rightarrow F'}^{11} |\psi^{\rho^1}\rangle_{R_1S_1} |\psi^{\rho^0}\rangle_{R_2S_2} \right| \right) \quad (65)$$

$$= \frac{1}{2} \left(1 + \left| \langle \psi^{\rho^0}|_{R_1S_1} \langle \psi^{\rho^1}|_{R_2S_2} (P_{R_1R_2 \rightarrow F'}^{00})^\dagger P_{R_1R_2 \rightarrow F'}^{11} |\psi^{\rho^1}\rangle_{R_1S_1} |\psi^{\rho^0}\rangle_{R_2S_2} \right| \right) \quad (66)$$

$$\leq \frac{1}{2} \left(1 + \max_{U_{R_1R_2}} \left| \langle \psi^{\rho^0}|_{R_1S_1} \langle \psi^{\rho^1}|_{R_2S_2} U_{R_1R_2} |\psi^{\rho^1}\rangle_{R_1S_1} |\psi^{\rho^0}\rangle_{R_2S_2} \right| \right). \quad (67)$$

The steps given above follow for reasons very similar to those given in the proof of Theorem 2. Continuing, we find that

$$\text{Eq. (67)} = \frac{1}{2} \left(1 + \sqrt{F(\rho^0 \otimes \rho^1, \rho^1 \otimes \rho^0)} \right) \quad (68)$$

$$= \frac{1}{2} \left(1 + \sqrt{F(\rho^0, \rho^1) F(\rho^1, \rho^0)} \right) \quad (69)$$

$$= \frac{1}{2} \left(1 + F(\rho^0, \rho^1) \right), \quad (70)$$

where we used the multiplicativity of the fidelity for tensor-product states to get (69) and the symmetric property of fidelity to arrive at (70). Thus, we have established (52) as an upper bound on the acceptance probability. This upper bound can be achieved by setting $F' \simeq R_1R_2$ and

$$\begin{aligned} P_{T'R_1R_2 \rightarrow T''F'} & = |0\rangle_{T''} \langle 0|_{T'} \otimes I_{R_1R_2 \rightarrow F'} \otimes \langle 0|_F \quad (71) \\ & + |1\rangle_{T''} \langle 1|_{T'} \otimes U_{R_1} \otimes U_{R_2}^\dagger \otimes \langle 0|_F, \quad (72) \end{aligned}$$

where U_{R_1} is a unitary that achieves the fidelity for $F(\rho^0, \rho^1)$, so that

$$\sqrt{F(\rho^0, \rho^1)} = \langle \psi^{\rho^0}|_{R_1S_1} U_{R_1} |\psi^{\rho^1}\rangle_{R_1S_1}. \quad (73)$$

This concludes the proof. ■

3. Variational algorithm with Bell measurements

A third method for estimating the fidelity of arbitrary multi-qubit states is a variational algorithm that is based on a generalization of the approach outlined in [GEC13, SCC19]. The approach from [GEC13, SCC19] employs Bell measurements to estimate the expectation of the SWAP observable, which in turn allows for estimating the fidelity of multi-qubit pure states. See also [Bru04].

We begin in this section by recalling the basic idea from [GEC13, SCC19] for estimating fidelity of pure states. Let ψ_S and φ_S be m -qubit pure states of a system S (so that $S = S_1 \cdots S_m$, where each S_i is a qubit system, for $i \in \{1, \dots, m\}$). Let $F_{S\tilde{S}}$ denote the unitary swap operator that swaps systems S and \tilde{S} , and recall that

$$\operatorname{Tr}[F_{S\tilde{S}}(\psi_S \otimes \varphi_{\tilde{S}})] = |\langle \psi | \varphi \rangle|^2 = F(\psi_S, \varphi_S). \quad (74)$$

Consider that

$$F_{S\tilde{S}} = F_{S_1\tilde{S}_1} \otimes F_{S_2\tilde{S}_2} \otimes \cdots \otimes F_{S_m\tilde{S}_m}. \quad (75)$$

Now observe that

$$F_{S_i \bar{S}_i} = \sum_{x,z \in \{0,1\}} (-1)^{x \cdot z} \Phi_{S_i \bar{S}_i}^{x,z}, \quad (76)$$

where the Bell states are defined as

$$|\Phi^{0,0}\rangle := \frac{1}{\sqrt{2}} (|00\rangle + |11\rangle), \quad (77)$$

$$|\Phi^{0,1}\rangle := \frac{1}{\sqrt{2}} (|00\rangle - |11\rangle), \quad (78)$$

$$|\Phi^{1,0}\rangle := \frac{1}{\sqrt{2}} (|01\rangle + |10\rangle), \quad (79)$$

$$|\Phi^{1,1}\rangle := \frac{1}{\sqrt{2}} (|01\rangle - |10\rangle). \quad (80)$$

We then conclude that

$$\begin{aligned} & F(\psi_S, \varphi_{\bar{S}}) \\ &= \text{Tr} \left[\left(\bigotimes_{i=1}^m F_{S_i \bar{S}_i} \right) (\psi_S \otimes \varphi_{\bar{S}}) \right] \quad (81) \\ &= \text{Tr} \left[\left(\bigotimes_{i=1}^m \sum_{x_i, z_i \in \{0,1\}} (-1)^{x_i \cdot z_i} \Phi_{S_i \bar{S}_i}^{x_i, z_i} \right) (\psi_S \otimes \varphi_{\bar{S}}) \right] \quad (82) \\ &= \sum_{\substack{x_1, z_1, \dots, \\ x_m, z_m \in \{0,1\}}} (-1)^{\vec{x} \cdot \vec{z}} \text{Tr} \left[\left(\bigotimes_{i=1}^m \Phi_{S_i \bar{S}_i}^{x_i, z_i} \right) (\psi_S \otimes \varphi_{\bar{S}}) \right], \quad (83) \end{aligned}$$

where

$$\vec{x} \cdot \vec{z} \equiv \sum_{i=1}^m x_i \cdot z_i. \quad (84)$$

Thus, the approach of [GEC13, SCC19] is to estimate $F(\psi_S, \varphi_S)$ by repeatedly performing Bell measurements on corresponding qubits of ψ_S and $\varphi_{\bar{S}}$ followed by classical postprocessing of the outcomes. In particular, for $j \in \{1, \dots, n\}$, set $Y_j = (-1)^{\sum_{i=1}^m x_i \cdot z_i}$, where $x_1, z_1, \dots, x_m, z_m \in \{0,1\}$ are the outcomes of the Bell measurements on the j th iteration. Then set $\bar{Y}^n := \frac{1}{n} \sum_{j=1}^n Y_j$. By the Hoeffding inequality [Hoe63], for accuracy $\varepsilon \in (0,1)$ and failure probability $\delta \in (0,1)$, we are guaranteed that

$$\Pr[|\bar{Y}^n - F(\psi_S, \varphi_S)| \leq \varepsilon] \geq 1 - \delta, \quad (85)$$

as long as $n \geq \frac{2}{\varepsilon^2} \log(\frac{2}{\delta})$. Thus, the algorithm is polynomial in the inverse accuracy and logarithmic in the inverse failure probability.

We now form a simple generalization of this algorithm to estimate the fidelity of arbitrary states ρ_S^0 and ρ_S^1 , in which we perform a variational optimization over unitaries that act on the reference system of one of the states.

For $i \in \{0,1\}$, let U_{RS}^i be an m -qubit unitary that acts on $|0\rangle_{RS}$ to generate the m -qubit state $|\psi^{\rho^i}\rangle_{RS}$; i.e.,

$$|\psi^{\rho^i}\rangle_{RS} = U_{RS}^i |0\rangle_{RS}, \quad (86)$$

such that

$$\rho_S^i = \text{Tr}_R[|\psi^{\rho^i}\rangle\langle\psi^{\rho^i}|_{RS}]. \quad (87)$$

Algorithm 6 Set the error tolerance $\varepsilon > 0$. Set $\eta, \delta \in (0,1)$. The algorithm proceeds as follows:

1. Prepare systems $R_1 S_1 R_2 S_2$ in the all-zeros state $|0\rangle_{R_1 S_1 R_2 S_2}$.
2. Act with the circuits U_{RS}^0 and U_{RS}^1 on systems $R_1 S_1 R_2 S_2$ to prepare the two pure states $|\psi^{\rho^0}\rangle_{R_1 S_1}$ and $|\psi^{\rho^1}\rangle_{R_2 S_2}$.
3. Perform a unitary $V_{R_1}(\theta)$ on system R_1 .
4. For $j \in \{1, \dots, n\}$, where $n \geq \frac{2}{\eta^2} \log(\frac{2}{\delta})$, for $i \in \{1, \dots, m\}$, perform a Bell measurement on qubit i of system R_1 and qubit i of system R_2 , with outcomes x_R^i and z_R^i , and perform a Bell measurement on qubit i of system S_1 and qubit i of system S_2 , with outcomes x_S^i and z_S^i . Set $Y_j(\theta) = (-1)^{\sum_{i=1}^m x_R^i \cdot z_R^i + x_S^i \cdot z_S^i}$.
5. Set

$$\bar{Y}^n(\theta) := \frac{1}{n} \sum_{j=1}^n Y_j(\theta), \quad (88)$$

as an estimate of

$$F_\theta \equiv \left| \langle \psi^{\rho^1} |_{RS} V_R(\theta) \otimes I_S | \psi^{\rho^0} \rangle_{RS} \right|^2, \quad (89)$$

so that

$$\Pr[|\bar{Y}^n(\theta) - F_\theta| \leq \eta] \geq 1 - \delta. \quad (90)$$

6. Perform maximization of the reward function $\bar{Y}^n(\theta)$ and update the parameters in θ .
7. Repeat 1-6 until the reward function $\bar{Y}^n(\theta)$ converges with tolerance ε , so that $|\Delta \bar{Y}^n(\theta)| \leq \varepsilon$, or until some maximum number of iterations is reached. (Here $\Delta \bar{Y}^n(\theta)$ represents the difference in $\bar{Y}^n(\theta)$ from the previous and current iteration.)
8. Output the final $\bar{Y}^n(\theta)$ as an estimate of the fidelity $F(\rho_S^0, \rho_S^1)$.

Figure 6 depicts Algorithm 6. Since this is a variational algorithm, it is not guaranteed to converge or have a specified runtime, other than running for a maximum number of iterations. However, it is clearly a generalization of the algorithm from [GEC13, SCC19], in which we estimate the fidelity

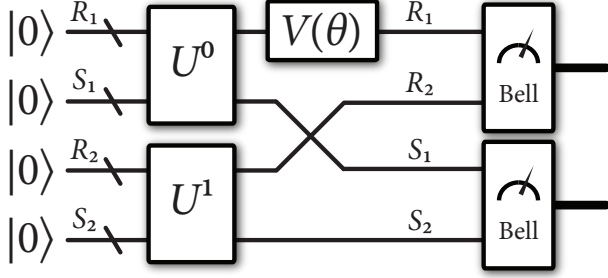


FIG. 6. This figure depicts Algorithm 6 for estimating the fidelity of quantum states generated by quantum circuits U_{RS}^0 and U_{RS}^1 .

$$\begin{aligned} & \left| \langle \psi^{\rho^1} |_{RS} V_R(\theta) \otimes I_S | \psi^{\rho^0} \rangle_{RS} \right|^2 \\ & = F(\psi_{RS}^{\rho^1}, V_R(\theta) \psi_{RS}^{\rho^0} V_R(\theta)^\dagger) \end{aligned} \quad (91)$$

at each iteration of the algorithm. If we could actually optimize over all possible unitaries acting on the reference system R , then the algorithm would indeed estimate the fidelity, as a consequence of Uhlmann’s theorem [Uhl76]:

$$F(\rho_S^0, \rho_S^1) = \sup_{V_R} F(\psi_{RS}^{\rho^1}, V_R \psi_{RS}^{\rho^0} V_R^\dagger). \quad (92)$$

However, by optimizing over only a subset of all unitaries, Algorithm 6 estimates a lower bound on the fidelity $F(\rho_S^0, \rho_S^1)$.

4. Variational algorithm for Fuchs–Caves measurement

Algorithm 4 from Section II C 1 is based on Uhlmann’s formula for fidelity in (21), and the same is true for Algorithm 5 from Section II C 2 and Algorithm 6 from Section II C 3. An alternate optimization formula for the fidelity of states ρ_S^0 and ρ_S^1 is as follows [FC95]:

$$F(\rho_S^0, \rho_S^1) = \left[\min_{\{\Lambda_S^x\}_x} \sum_x \sqrt{\text{Tr}[\Lambda_S^x \rho_S^0] \text{Tr}[\Lambda_S^x \rho_S^1]} \right]^2, \quad (93)$$

where the minimization is over every positive operator-valued measure $\{\Lambda_S^x\}_x$ (i.e., the operators satisfy $\Lambda_S^x \geq 0$ for all x and $\sum_x \Lambda_S^x = I_S$). A measurement achieving the optimal value of the fidelity is known as the Fuchs–Caves measurement [FC95] and has the form $\{|\varphi_x\rangle\langle\varphi_x|\}_x$, where $|\varphi_x\rangle$ is an eigenvector, with eigenvalue λ_x , of the following operator geometric mean of ρ^0 and $(\rho^1)^{-1}$ (also called “quantum likelihood ratio” operator in [Fuc96]):

$$M := (\rho^1)^{-1/2} \sqrt{(\rho^1)^{1/2} \rho^0 (\rho^1)^{1/2}} (\rho^1)^{-1/2}, \quad (94)$$

so that

$$M = \sum_x \lambda_x |\varphi_x\rangle\langle\varphi_x|. \quad (95)$$

That is, it is known from [FC95, Fuc96] that

$$F(\rho_S^0, \rho_S^1) = \left[\sum_x \sqrt{\text{Tr}[|\varphi_x\rangle\langle\varphi_x| \rho_S^0] \text{Tr}[|\varphi_x\rangle\langle\varphi_x| \rho_S^1]} \right]^2. \quad (96)$$

Thus, we can build a variational algorithm around this formulation of fidelity, with the idea being to optimize over parameterized measurements in an attempt to optimize the fidelity, while at the same time learn the Fuchs–Caves measurement (or a different fidelity-achieving measurement). In contrast to the other variational algorithms presented in previous sections, this alternate approach leads to an upper bound on the fidelity.

Before detailing the algorithm, recall the Naimark extension theorem [Nai40] (see also [Wil17, Wat18, KW20b]), which states that a general POVM $\{\Lambda_S^x\}_x$ with m outcomes, acting on a quantum state ρ of a d -dimensional system S , can be realized as a unitary interaction U_{SP} of the system S with an m -dimensional probe system P , followed by a projective measurement $\{|x\rangle\langle x|_P\}_x$ acting on the probe system. That is,

$$\text{Tr}[\Lambda_S^x \rho_S] = \text{Tr}[(I_S \otimes |x\rangle\langle x|_P) U_{SP} (\rho_S \otimes |0\rangle\langle 0|_P) U_{SP}^\dagger]. \quad (97)$$

It suffices to choose U_{SP} so that

$$U_{SP} |\psi\rangle_S |0\rangle_P = \sum_x \sqrt{\Lambda_S^x} |\psi\rangle_S |x\rangle_P. \quad (98)$$

Thus, we can express the optimization problem in (93) as follows:

$$F(\rho_S^0, \rho_S^1) = \left[\min_{U_{SP}} \sum_x \sqrt{\frac{\text{Tr}[(I_S \otimes |x\rangle\langle x|_P) U_{SP} (\rho_S^0 \otimes |0\rangle\langle 0|_P) U_{SP}^\dagger] \times \text{Tr}[(I_S \otimes |x\rangle\langle x|_P) U_{SP} (\rho_S^1 \otimes |0\rangle\langle 0|_P) U_{SP}^\dagger]}{\text{Tr}[(I_S \otimes |x\rangle\langle x|_P) U_{SP} (\rho_S^1 \otimes |0\rangle\langle 0|_P) U_{SP}^\dagger]}} \right]^2. \quad (99)$$

By replacing the optimization in (99) over all unitaries with an optimization over parameterized ones, we arrive at a variational algorithm for estimating fidelity:

Algorithm 7 Set $n \in \mathbb{N}$ and the error tolerance $\varepsilon > 0$. The algorithm proceeds as follows:

1. For $j \in \{1, \dots, n\}$, prepare system S_1 in the state $\rho_{S_1}^0$ and system S_2 in the state $\rho_{S_2}^1$, and prepare systems P_1 and P_2 in the all-zeros state $|0\rangle_{P_1} \otimes |0\rangle_{P_2}$.
2. Act with the circuit $U_{S_1 P_1}(\theta)$ on systems $S_1 P_1$ and act with the same circuit $U_{S_2 P_2}(\theta)$ on systems $S_2 P_2$.
3. Measure system P_1 in the computational basis and record the outcome as y_j , and measure system P_2 in the computational basis and record the outcome as z_j .

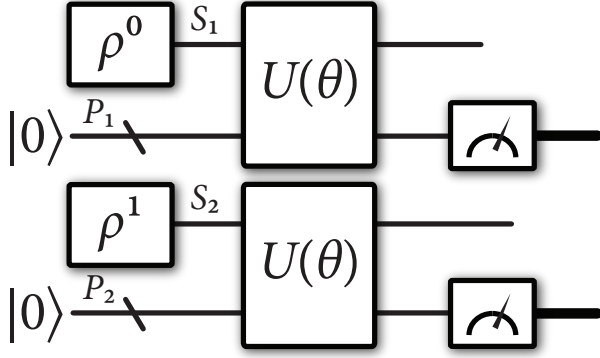


FIG. 7. This figure depicts Algorithm 7 for estimating the fidelity of quantum states ρ_S^0 and ρ_S^1 . The boxes enclosing ρ^0 and ρ^1 indicate that these are some mechanism by which these states are prepared.

4. Using the measurement data $\{y_j\}_{j=1}^n$ and $\{z_j\}_{j=1}^n$, calculate the empirical distributions $\tilde{p}_\theta(x)$ and $\tilde{q}_\theta(x)$, where $\tilde{p}_\theta(x)$ is the empirical distribution resulting from

$$p_\theta(x) :=$$

$$\text{Tr}[(I_S \otimes |x\rangle\langle x|_P) U_{SP}(\theta)(\rho_S^0 \otimes |0\rangle\langle 0|_P) U_{SP}^\dagger(\theta)], \quad (100)$$

and $\tilde{q}_\theta(x)$ is the empirical distribution resulting from

$$q_\theta(x) :=$$

$$\text{Tr}[(I_S \otimes |x\rangle\langle x|_P) U_{SP}(\theta)(\rho_S^1 \otimes |0\rangle\langle 0|_P) U_{SP}^\dagger(\theta)]. \quad (101)$$

5. Output

$$F(\tilde{p}_\theta, \tilde{q}_\theta) := \left[\sum_x \sqrt{\tilde{p}_\theta(x) \tilde{q}_\theta(x)} \right]^2 \quad (102)$$

as an estimate of $F(p_\theta, q_\theta)$.

6. Perform minimization of the cost function $F(\tilde{p}_\theta, \tilde{q}_\theta)$ and update the parameters in θ .
7. Repeat 1-6 until the cost function $F(\tilde{p}_\theta, \tilde{q}_\theta)$ converges with tolerance ε , so that $|\Delta F(\tilde{p}_\theta, \tilde{q}_\theta)| \leq \varepsilon$, or until some maximum number of iterations is reached. (Here $\Delta F(\tilde{p}_\theta, \tilde{q}_\theta)$ represents the difference in $F(\tilde{p}_\theta, \tilde{q}_\theta)$ from the previous and current iteration.)
8. Output the final value of $F(\tilde{p}_\theta, \tilde{q}_\theta)$ as an estimate of the fidelity $F(\rho_S^0, \rho_S^1)$.

Figure 7 depicts Algorithm 7. As before, since this is a variational algorithm, it is not guaranteed to converge or have a specified runtime, other than running for

a maximum number of iterations. One advantage of this algorithm is that it does not require purifications of the states ρ_S^0 and ρ_S^1 . All it requires is a circuit or method to prepare these states, and then it performs measurements on these states, in an attempt to learn an optimal measurement with respect to the cost function $F(\tilde{p}_\theta, \tilde{q}_\theta)$.

In Algorithm 7, we did not specify how large n should be in order to get a desired accuracy of the estimator in (102) for the classical fidelity $F(p_\theta, q_\theta)$. This estimator is called a ‘‘plug-in estimator’’ in the literature on this topic and it is a biased estimator, which however converges to $F(p_\theta, q_\theta)$ in the asymptotic limit $n \rightarrow \infty$. As a consequence of the estimator in (102) being biased, the Hoeffding inequality does not readily apply in this case. As far as we can tell, it is an open question to determine the rate of convergence of this estimator to $F(p_\theta, q_\theta)$. Related work on this topic has been considered in [JVHW15, AOST17].

D. Estimating fidelity of channels

In this section, we outline a method for estimating the fidelity of channels on a quantum computer, by means of an interaction with competing quantum provers [GW05, Gut05, GW07, Gut09, GW13]. The goal of one prover is to maximize the acceptance probability, while the goal of the other prover is to minimize the acceptance probability. We refer to the first prover as the max-prover and the second as the min-prover. The specific setting that we deal with is called a double quantum interactive proof (DQIP) [GW13], due to the fact that the min-prover goes first and then the max-prover goes last. The class of promise problems that can be solved in this model is equivalent to PSPACE [GW13], which is the class of problems that can be decided on a classical computer with polynomial memory.

Let us recall that the fidelity of channels $\mathcal{N}_{A \rightarrow B}^0$ and $\mathcal{N}_{A \rightarrow B}^1$ is defined as follows [GLN05]:

$$F(\mathcal{N}_{A \rightarrow B}^0, \mathcal{N}_{A \rightarrow B}^1) := \inf_{\rho_{RA}} F(\mathcal{N}_{A \rightarrow B}^0(\rho_{RA}), \mathcal{N}_{A \rightarrow B}^1(\rho_{RA})), \quad (103)$$

where the infimum is over every state ρ_{RA} , with the reference system R arbitrarily large. It is known that the infimum is achieved by a pure state ψ_{RA} with the reference system R isomorphic to the channel input system A , so that

$$F(\mathcal{N}_{A \rightarrow B}^0, \mathcal{N}_{A \rightarrow B}^1) := \min_{\psi_{RA}} F(\mathcal{N}_{A \rightarrow B}^0(\psi_{RA}), \mathcal{N}_{A \rightarrow B}^1(\psi_{RA})). \quad (104)$$

It is also known that it is possible to calculate the fidelity of channels by means of a semi-definite program [YF17, KW21], which provides a way to verify the output of our proposed algorithm for sufficiently small examples.

Suppose that the goal is to estimate the fidelity of channels $\mathcal{N}_{A \rightarrow B}^0$ and $\mathcal{N}_{A \rightarrow B}^1$, and we are given access to quantum circuits $U_{AE' \rightarrow BE}^0$ and $U_{AE' \rightarrow BE}^1$ that realize

isometric extensions of the channels $\mathcal{N}_{A \rightarrow B}^0$ and $\mathcal{N}_{A \rightarrow B}^1$, respectively, in the sense that

$$\mathcal{N}_{A \rightarrow B}^i(\omega_A) = \text{Tr}_E[U_{AE' \rightarrow BE}^i(\omega_A \otimes |0\rangle\langle 0|_{E'}) (U_{AE' \rightarrow BE}^i)^\dagger], \quad (105)$$

for $i \in \{0, 1\}$.

We now provide a DQIP algorithm for estimating the following quantity:

$$\frac{1}{2} \left(1 + \sqrt{F}(\mathcal{N}_{A \rightarrow B}^0, \mathcal{N}_{A \rightarrow B}^1) \right), \quad (106)$$

which is based in part on Algorithm 4 but instead features an optimization over input states of the min-prover.

Algorithm 8 *The algorithm proceeds as follows:*

1. The verifier prepares a Bell state

$$|\Phi\rangle_{T'T} := \frac{1}{\sqrt{2}}(|00\rangle_{T'T} + |11\rangle_{T'T}) \quad (107)$$

on registers T' and T and prepares system E' in the all-zeros state $|0\rangle_{E'}$.

2. The min-prover transmits the system A of the state $|\psi\rangle_{RA}$ to the verifier.
3. Using the circuits $U_{AE' \rightarrow BE}^0$ and $U_{AE' \rightarrow BE}^1$, the verifier performs the following controlled unitary:

$$\sum_{i \in \{0,1\}} |i\rangle\langle i|_T \otimes U_{AE' \rightarrow BE}^i. \quad (108)$$

4. The verifier transmits systems T' and E to the max-prover.
5. The max-prover prepares a system F in the $|0\rangle_F$ state and acts on systems T' , E , and F with a unitary $P_{T'EF \rightarrow T''F'}$ to produce the output systems T'' and F' , where T'' is a qubit system.
6. The max-prover sends system T'' to the verifier, who then performs a Bell measurement

$$\{\Phi_{T''T}, I_{T''T} - \Phi_{T''T}\} \quad (109)$$

on systems T'' and T . The verifier accepts if and only if the outcome $\Phi_{T''T}$ occurs.

Figure 8 depicts Algorithm 8.

Theorem 4 *The acceptance probability of Algorithm 8 is equal to*

$$\frac{1}{2} \left(1 + \sqrt{F}(\mathcal{N}_{A \rightarrow B}^0, \mathcal{N}_{A \rightarrow B}^1) \right). \quad (110)$$

Proof. After Step 1 of Algorithm 8, the global state is

$$|\Phi\rangle_{T'T} |\psi\rangle_{RA} |0\rangle_{E'}. \quad (111)$$

After Step 2 of Algorithm 8, it is

$$\frac{1}{\sqrt{2}} \sum_{i \in \{0,1\}} |i\rangle_{T'} |i\rangle_T U^i |\psi\rangle_{RA} |0\rangle_{E'}, \quad (112)$$

where $U^i \equiv U_{AE' \rightarrow BE}^i$ for $i \in \{0, 1\}$. After Step 4 of Algorithm 8, it is

$$P \left(\frac{1}{\sqrt{2}} \sum_{i \in \{0,1\}} |i\rangle_{T'} |i\rangle_T U^i |\psi\rangle_{RA} |00\rangle_{E'F} \right), \quad (113)$$

where $P \equiv P_{T'EF \rightarrow T''F'}$. For a fixed unitary $P_{T'EF \rightarrow T''F'}$ of the max-prover and fixed state $|\psi\rangle_{RA}$ of the min-prover, the acceptance probability is then

$$\begin{aligned} & \left\| \langle \Phi |_{T''T} P \left(\frac{1}{\sqrt{2}} \sum_{i \in \{0,1\}} |i\rangle_{T'} |i\rangle_T U^i |\psi\rangle_{RA} |00\rangle_{E'F} \right) \right\|_2^2 \\ &= \frac{1}{2} \left\| \langle \Phi |_{T''T} P \sum_{i \in \{0,1\}} |i\rangle_{T'} |i\rangle_T U^i |\psi\rangle_{RA} |00\rangle_{E'F} \right\|_2^2, \end{aligned} \quad (114)$$

In a competing-provers quantum interactive proof, the max-prover is trying to maximize the probability that the verifier accepts, while the min-prover is trying to minimize the acceptance probability. Since the max-prover plays second in this game, the acceptance probability of Algorithm 8 is given by

$$\min_{|\psi\rangle_{RA}} \max_P \frac{1}{2} \left\| \langle \Phi |_{T''T} P \sum_{i \in \{0,1\}} |ii\rangle_{T'T} U^i |\psi\rangle_{RA} |00\rangle_{E'F} \right\|_2^2. \quad (115)$$

Applying the analysis of Theorem 2, it follows that

$$\begin{aligned} & \max_P \frac{1}{2} \left\| \langle \Phi |_{T''T} P \sum_{i \in \{0,1\}} |ii\rangle_{T'T} U^i |\psi\rangle_{RA} |00\rangle_{E'F} \right\|_2^2 \\ &= \frac{1}{2} \left(1 + \sqrt{F}(\mathcal{N}_{A \rightarrow B}^0(\psi_{RA}), \mathcal{N}_{A \rightarrow B}^1(\psi_{RA})) \right). \end{aligned} \quad (116)$$

Thus, after applying the minimization over every input state ψ_{RA} , the claim in (110) follows. ■

Proposition 1 *An alternative expression for the acceptance probability of Algorithm 8 is*

$$\begin{aligned} & \min_{\rho_{RA}} \max_{\mathcal{P}_{T'E \rightarrow T''}} \text{Tr}[\Phi_{T''T} \mathcal{P}_{T'E \rightarrow T''}(\mathcal{M}_{A \rightarrow T'TBE}(\rho_{RA}))] \\ &= \max_{\mathcal{P}_{T'E \rightarrow T''}} \min_{\rho_{RA}} \text{Tr}[\Phi_{T''T} \mathcal{P}_{T'E \rightarrow T''}(\mathcal{M}_{A \rightarrow T'TBE}(\rho_{RA}))], \end{aligned} \quad (117)$$

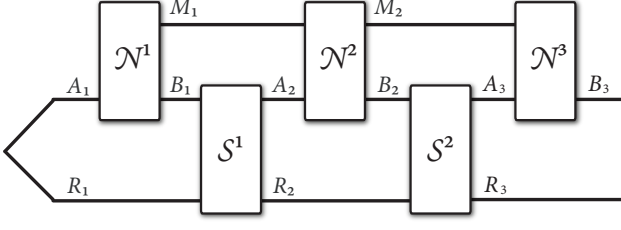


FIG. 9. Interaction of a three-turn strategy $\mathcal{N}^{(3)}$ with a two-turn co-strategy $\mathcal{S}^{(2)}$.

1. memory systems M_1, \dots, M_{n-1} , and
2. quantum channels $\mathcal{N}_{A_1 \rightarrow M_1 B_1}^1, \mathcal{N}_{M_1 A_2 \rightarrow M_2 B_2}^2, \dots, \mathcal{N}_{M_{n-2} A_{n-1} \rightarrow M_{n-1} B_{n-1}}^{n-1}$, and $\mathcal{N}_{M_{n-1} A_n \rightarrow B_n}^n$.

It is implicit that any of the systems involved can be trivial systems, which means that state preparation and measurements are included as special cases.

A co-strategy interacts with a strategy; co-strategies are in fact strategies also, but it is useful conceptually to provide an explicit means by which an agent can interact with a strategy. An $(n-1)$ -turn co-strategy $\mathcal{S}^{(n-1)}$, with input systems B_1, \dots, B_n and output systems A_1, \dots, A_n consists of the following:

1. memory systems R_1, \dots, R_n ,
2. a quantum state $\rho_{R_1 A_1}$, and
3. quantum channels $\mathcal{S}_{R_1 B_1 \rightarrow R_2 A_2}^1, \mathcal{S}_{R_2 B_2 \rightarrow R_3 A_3}^2, \dots, \mathcal{S}_{R_{n-1} B_{n-1} \rightarrow R_n A_n}^{n-1}$.

The result of the interaction of the strategy $\mathcal{N}^{(n)}$ with the co-strategy $\mathcal{S}^{(n-1)}$ is a quantum state on systems $R_n B_n$, and we employ the shorthand

$$\mathcal{N}^{(n)} \circ \mathcal{S}^{(n-1)} \quad (120)$$

to denote this quantum state. Figure 9 depicts a three-turn strategy interacting with a two-turn co-strategy.

Let $\mathcal{N}^{0,(n)}$ and $\mathcal{N}^{1,(n)}$ denote two compatible, n -turn quantum strategies, meaning that all systems involved in these strategies are the same but the channels that make up the strategies are possibly different. The fidelity of the strategies $\mathcal{N}^{0,(n)}$ and $\mathcal{N}^{1,(n)}$ is defined as [GRS18]

$$F(\mathcal{N}^{0,(n)}, \mathcal{N}^{1,(n)}) := \inf_{\mathcal{S}^{(n-1)}} F(\mathcal{N}^{0,(n)} \circ \mathcal{S}^{(n-1)}, \mathcal{N}^{1,(n)} \circ \mathcal{S}^{(n-1)}), \quad (121)$$

where the optimization is over every co-strategy $\mathcal{S}^{(n-1)}$. One can interpret the strategy fidelity in (121) as a generalization of the fidelity of channels in (103), in which the idea is to optimize the fidelity measure over all possible co-strategies that can be used to distinguish the

strategies $\mathcal{N}^{0,(n)}$ and $\mathcal{N}^{1,(n)}$. It follows from a standard data-processing argument that it suffices to perform the optimization in (121) over co-strategies involving an initial pure state $\rho_{R_1 A_1}$ and channels $\mathcal{S}_{R_1 B_1 \rightarrow R_2 A_2}^1, \mathcal{S}_{R_2 B_2 \rightarrow R_3 A_3}^2, \dots, \mathcal{S}_{R_{n-1} B_{n-1} \rightarrow R_n A_n}^{n-1}$ that are each isometric channels (these are called pure co-strategies in [GRS18]). We also note here that the measure in (121) is generalized by the generalized strategy divergence of [WW19].

The goal of this section is to delineate a DQIP algorithm for estimating the fidelity of strategies $\mathcal{N}^{0,(n)}$ and $\mathcal{N}^{1,(n)}$. To do so, we suppose that the verifier has access to unitary circuits that realize isometric extensions of all channels involved in the strategies. That is, for $i \in \{0, 1\}$, there exists a unitary channel $\mathcal{U}_{A_1 E'_1 \rightarrow M_1 B_1 E_1}^{i,1}$ such that

$$\mathcal{N}_{A_1 \rightarrow M_1 B_1}^{i,1}(\rho_{A_1}) = \text{Tr}_{E_1} [\mathcal{U}_{A_1 E'_1 \rightarrow M_1 B_1 E_1}^{i,1}(\rho_{A_1} \otimes |0\rangle\langle 0|_{E'_1})] \quad (122)$$

for every input state ρ_{A_1} ; for $j \in \{2, \dots, n-1\}$, there exists a unitary channel $\mathcal{U}_{M_{j-1} A_j E'_j \rightarrow M_j B_j E_j}^{i,j}$ such that

$$\mathcal{N}_{M_{j-1} A_j \rightarrow M_j B_j}^{i,j}(\rho_{A_j}) = \text{Tr}_{E_j} [\mathcal{U}_{M_{j-1} A_j E'_j \rightarrow M_j B_j E_j}^{i,j}(\rho_{A_j} \otimes |0\rangle\langle 0|_{E'_j})], \quad (123)$$

for every input state ρ_{A_j} ; and there exists a unitary channel $\mathcal{U}_{M_{n-1} A_n E'_n \rightarrow B_n E_n}^{i,n}$ such that

$$\mathcal{N}_{M_{n-1} A_n \rightarrow B_n}^{i,n}(\rho_{A_n}) = \text{Tr}_{E_n} [\mathcal{U}_{M_{n-1} A_n E'_n \rightarrow B_n E_n}^{i,n}(\rho_{A_n} \otimes |0\rangle\langle 0|_{E'_n})], \quad (124)$$

for every input state ρ_{A_n} . We use the notation $\mathcal{U}_{A_1 E'_1 \rightarrow M_1 B_1 E_1}^{i,1}, \mathcal{U}_{M_{j-1} A_j E'_j \rightarrow M_j B_j E_j}^{i,j}$, and $\mathcal{U}_{M_{n-1} A_n E'_n \rightarrow B_n E_n}^{i,n}$ to refer to the unitary circuits.

We now provide a DQIP algorithm for estimating the following quantity:

$$\frac{1}{2} \left(1 + \sqrt{F}(\mathcal{N}^{0,(n)}, \mathcal{N}^{1,(n)}) \right), \quad (125)$$

which is based in part on Algorithm 8 but instead features an optimization over all co-strategies of the min-prover.

Algorithm 9 *The algorithm proceeds as follows:*

1. The verifier prepares a Bell state

$$|\Phi\rangle_{T'T} := \frac{1}{\sqrt{2}}(|00\rangle_{T'T} + |11\rangle_{T'T}) \quad (126)$$

on registers T' and T and prepares systems $E'_1 \dots E'_n$ in the all-zeros state $|0\rangle_{E'_1 \dots E'_n}$.

2. The min-prover transmits the system A of the state $|\psi\rangle_{RA}$ to the verifier.

3. Using the circuits $U_{A_1 E'_1 \rightarrow M_1 B_1 E_1}^{0,1}$ and $U_{A_1 E'_1 \rightarrow M_1 B_1 E_1}^{1,1}$, the verifier performs the following controlled unitary:

$$\sum_{i \in \{0,1\}} |i\rangle\langle i|_T \otimes U_{A_1 E'_1 \rightarrow M_1 B_1 E_1}^{i,1}. \quad (127)$$

4. The verifier transmits system B_1 to the min-prover, who subsequently acts with the isometric quantum channel $\mathcal{S}_{R_1 B_1 \rightarrow R_2 A_2}^1$ and then sends system A_2 to the verifier.
5. For $j \in \{2, \dots, n-1\}$, using the circuits $U_{M_{j-1} A_j E'_j \rightarrow M_j B_j E_j}^{0,j}$ and $U_{M_{j-1} A_j E'_j \rightarrow M_j B_j E_j}^{1,j}$, the verifier performs the following controlled unitary:

$$\sum_{i \in \{0,1\}} |i\rangle\langle i|_T \otimes U_{M_{j-1} A_j E'_j \rightarrow M_j B_j E_j}^{i,j}. \quad (128)$$

The verifier transmits system B_j to the min-prover, who subsequently acts with the isometric quantum channel $\mathcal{S}_{R_j B_j \rightarrow R_{j+1} A_{j+1}}^j$ and then sends system A_{j+1} to the verifier.

6. Using the circuits $U_{M_{n-1} A_n E'_n \rightarrow B_n E_n}^{0,n}$ and $U_{M_{n-1} A_n E'_n \rightarrow B_n E_n}^{1,n}$, the verifier performs the following controlled unitary:

$$\sum_{i \in \{0,1\}} |i\rangle\langle i|_T \otimes U_{M_{n-1} A_n E'_n \rightarrow B_n E_n}^{i,n}. \quad (129)$$

7. The verifier transmits systems T' , E_1 , \dots , E_n to the max-prover.
8. The max-prover prepares a system F in the $|0\rangle_F$ state and acts on systems T' , E_1 , \dots , E_n , and F with a unitary $P_{T' E_1 \dots E_n F \rightarrow T'' F'}$ to produce the output systems T'' and F' , where T'' is a qubit system.
9. The max-prover sends system T'' to the verifier, who then performs a Bell measurement

$$\{\Phi_{T'' T}, I_{T'' T} - \Phi_{T'' T}\} \quad (130)$$

on systems T'' and T . The verifier accepts if and only if the outcome $\Phi_{T'' T}$ occurs.

Figure 10 depicts Algorithm 9.

Theorem 5 *The acceptance probability of Algorithm 9 is equal to*

$$\frac{1}{2} \left(1 + \sqrt{F}(\mathcal{N}^{0,(n)}, \mathcal{N}^{1,(n)}) \right), \quad (131)$$

where $\sqrt{F}(\mathcal{N}^{0,(n)}, \mathcal{N}^{1,(n)})$ is the strategy fidelity defined in (121).

Proof. After Step 1 of Algorithm 9, the global state is

$$|\Phi\rangle_{T' T} |\psi\rangle_{R A} |0\rangle_{E'^n}, \quad (132)$$

where we have employed the shorthand $E'^n \equiv E'_1 \dots E'_n$. After Step 6 of Algorithm 9, the global state is

$$|\varphi(\psi, \{S^j\}_{j=1}^{n-1})\rangle \equiv \frac{1}{\sqrt{2}} \sum_{i \in \{0,1\}} |i\rangle_{T'} |i\rangle_T U^{i,n-1} \prod_{j=1}^{n-1} (S^j U^{i,j}) |\psi\rangle_{R A} |0\rangle_{E'^n}, \quad (133)$$

where we have omitted many of the system labels for simplicity. After Step 8 of Algorithm 9, the global state is

$$P |\varphi(\psi, \{S^j\}_{j=1}^{n-1})\rangle. \quad (134)$$

For a fixed unitary P of the max-prover and a fixed pure co-strategy $(\psi, \{S^j\}_{j=1}^{n-1})$ of the min-prover, the acceptance probability is thus

$$\| \langle \Phi |_{T'' T} P |\varphi(\psi, \{S^j\}_{j=1}^{n-1})\rangle \|_2^2. \quad (135)$$

In a double-prover quantum interactive proof, the max-prover is trying to maximize the probability that the verifier accepts, while the min-prover is trying to minimize the acceptance probability. Since the max-prover plays second in this game, the acceptance probability of Algorithm 9 is given by

$$\min_{(\psi, \{S^j\}_{j=1}^{n-1})} \max_P \| \langle \Phi |_{T'' T} P |\varphi(\psi, \{S^j\}_{j=1}^{n-1})\rangle \|_2^2. \quad (136)$$

Applying the analysis of Theorem 2, it follows that

$$\begin{aligned} & \max_P \| \langle \Phi |_{T'' T} P |\varphi(\psi, \{S^j\}_{j=1}^{n-1})\rangle \|_2^2 \\ &= \frac{1}{2} \left(1 + \sqrt{F}(\mathcal{N}^{0,(n)} \circ \mathcal{S}^{(n-1)}, \mathcal{N}^{1,(n)} \circ \mathcal{S}^{(n-1)}) \right). \end{aligned} \quad (137)$$

Thus, after applying a minimization over every pure co-strategy $\mathcal{S}^{(n-1)}$, the claim in (131) follows. ■

F. Alternate methods of estimating the fidelity of channels and strategies

We note briefly here that other methods for estimating fidelity of channels can be based on Algorithms 5, 6, and 7. It is not clear how to phrase them in the language of quantum interactive proofs, in such a way that the acceptance probability is a simple function of the channel fidelity. However, we can employ variational algorithms in which we repeat the circuit for determining an optimal input state ψ_{RA} for the channel fidelity. Then these variational algorithms employ an extra minimization step

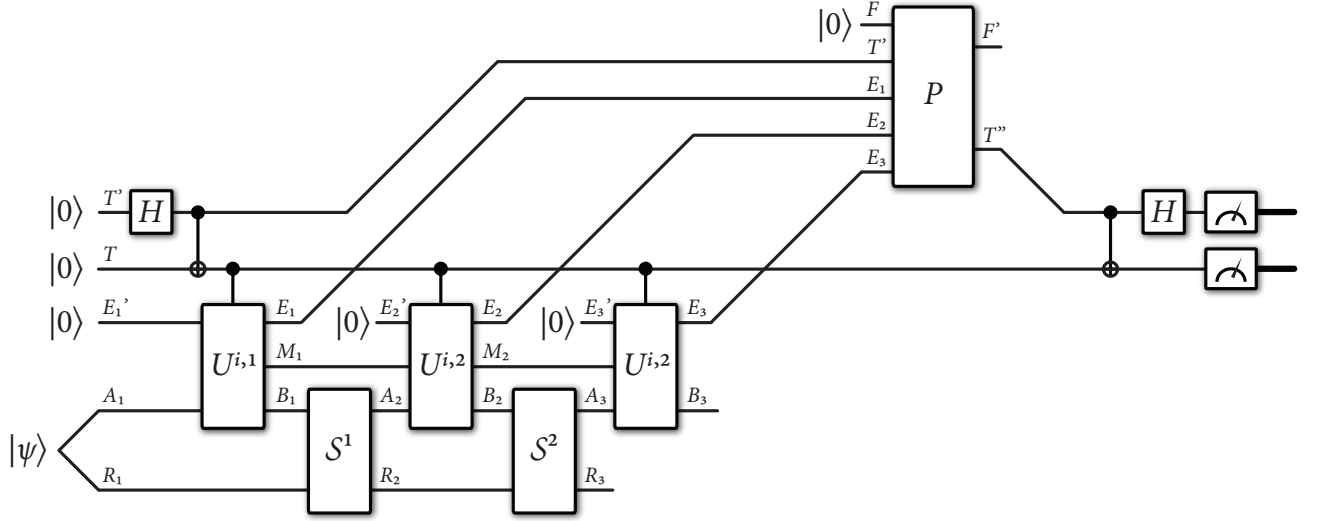


FIG. 10. This figure depicts Algorithm 9 for estimating the fidelity of quantum strategies $\mathcal{N}^{0,(n)}$ and $\mathcal{N}^{1,(n)}$ generated by quantum circuits $U_{A_1 E_1' \rightarrow M_1 B_1 E_1}^{i,1}$, $\{U_{M_{j-1} A_j E_j' \rightarrow M_j B_j E_j}^{i,j}\}_{j=2}^{n-1}$, and $U_{M_{n-1} A_n E_n' \rightarrow B_n E_n}^{i,n}$ for $i \in \{0, 1\}$ and $n = 3$. The min-prover prepares the state $|\psi\rangle_{RA}$ and acts with a co-strategy, while the max-prover acts with the unitary $P_{T'E_1 \dots E_n F \rightarrow T''F'}$.

in order to approximate an optimal input state for the channel fidelity.

Similarly, we can estimate the fidelity of strategies by employing a sequence of parameterized circuits to function as a co-strategy and then minimize over them, in conjunction with any of the previous methods for estimating fidelity of states.

G. Estimating maximum output fidelity of channels

In this section, we show how a simple variation of Algorithm 8, in which we combine the actions of the min-prover and max-prover into a single max-prover, leads to a QIP algorithm for estimating the following fidelity function of two quantum channels $\mathcal{N}_{A \rightarrow B}^0$ and $\mathcal{N}_{A \rightarrow B}^1$:

$$\sup_{\rho_A} F(\mathcal{N}_{A \rightarrow B}^0(\rho_A), \mathcal{N}_{A \rightarrow B}^1(\rho_A)), \quad (138)$$

where the optimization is over every input state ρ_A . This algorithm is based in part on Algorithm 4 but instead features an optimization over input states of the prover.

Algorithm 10 *The algorithm proceeds as follows:*

1. The verifier prepares a Bell state

$$|\Phi\rangle_{T'T} := \frac{1}{\sqrt{2}}(|00\rangle_{T'T} + |11\rangle_{T'T}) \quad (139)$$

on registers T' and T and prepares system E' in the all-zeros state $|0\rangle_{E'}$.

2. The prover transmits the system A of the state $|\psi\rangle_{RA}$ to the verifier.

3. Using the circuits $U_{AE' \rightarrow BE}^0$ and $U_{AE' \rightarrow BE}^1$, the verifier performs the following controlled unitary:

$$\sum_{i \in \{0,1\}} |i\rangle\langle i|_T \otimes U_{AE' \rightarrow BE}^i. \quad (140)$$

4. The verifier transmits systems T' and E to the prover.
5. The prover prepares a system F in the $|0\rangle_F$ state and acts on systems T' , E , and F with a unitary $P_{T'EF \rightarrow T''F'}$ to produce the output systems T'' and F' , where T'' is a qubit system.
6. The prover sends system T'' to the verifier, who then performs a Bell measurement

$$\{\Phi_{T''T}, I_{T''T} - \Phi_{T''T}\} \quad (141)$$

on systems T'' and T . The verifier accepts if and only if the outcome $\Phi_{T''T}$ occurs.

Figure 11 depicts Algorithm 10.

Theorem 6 *The acceptance probability of Algorithm 10 is equal to*

$$\frac{1}{2} \left(1 + \sup_{\rho_A} \sqrt{F}(\mathcal{N}_{A \rightarrow B}^0(\rho_A), \mathcal{N}_{A \rightarrow B}^1(\rho_A)) \right). \quad (142)$$

Proof. After Step 2 of Algorithm 10, the global state is

$$|\Phi\rangle_{T'T} |\psi\rangle_{RA} |0\rangle_{E'}. \quad (143)$$

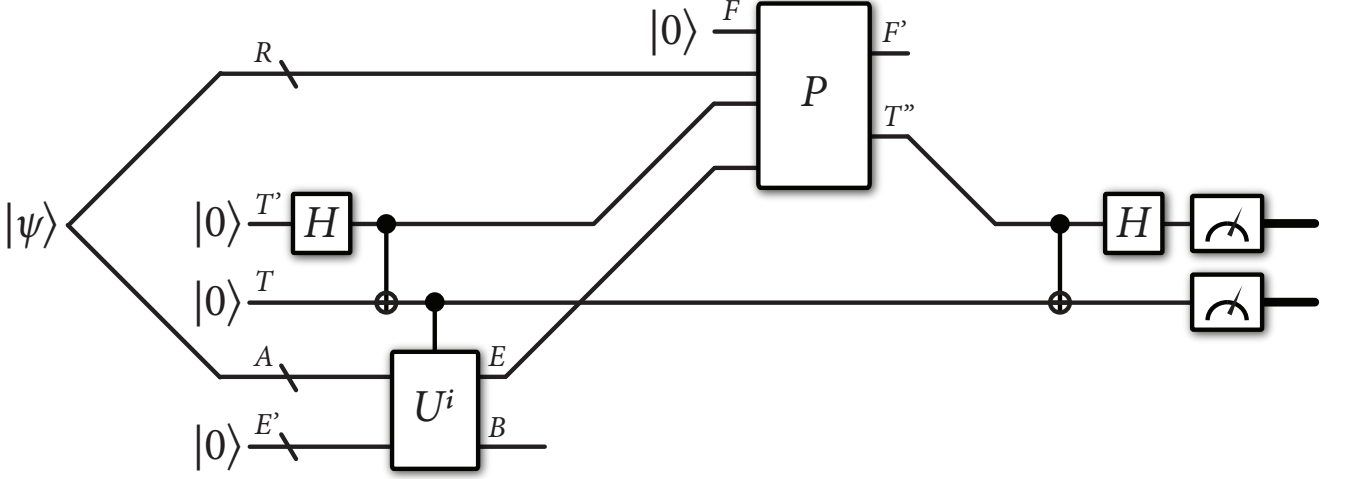


FIG. 11. This figure depicts Algorithm 10 for generating a state ρ_A that maximizes the fidelity of quantum channels generated by quantum circuits $U_{AE' \rightarrow BE}^0$ and $U_{AE' \rightarrow BE}^1$.

After Step 3, the global state is

$$\frac{1}{\sqrt{2}} \sum_{i \in \{0,1\}} |i\rangle_{T'} |i\rangle_T U_{AE' \rightarrow BE}^i |\psi\rangle_{RA} |0\rangle_{E'}. \quad (144)$$

After Step 5, it is

$$\frac{1}{\sqrt{2}} P \sum_{i \in \{0,1\}} |i\rangle_{T'} |i\rangle_T U_{AE' \rightarrow BE}^i |\psi\rangle_{RA} |0\rangle_{E'}, \quad (145)$$

where $P \equiv P_{T'EF \rightarrow T''F'}$. For a fixed state $|\psi\rangle_{RA}$ and unitary $P_{T'EF \rightarrow T''F'}$ of the prover, the acceptance probability is

$$\frac{1}{2} \left\| \left\langle \Phi \left|_{T''T} P \sum_{i \in \{0,1\}} |i\rangle_{T'} |i\rangle_T U_{AE' \rightarrow BE}^i |\psi\rangle_{RA} |0\rangle_{E'} \right. \right\rangle \right\|_2^2. \quad (146)$$

In a QIP algorithm, the prover chooses his actions in order to maximize the acceptance probability, so that the acceptance probability is

$$\frac{1}{2} \sup_{|\psi\rangle_{RA}} \left\| \left\langle \Phi \left|_{T''T} P \sum_{i \in \{0,1\}} |i\rangle_{T'} |i\rangle_T U_{AE' \rightarrow BE}^i |\psi\rangle_{RA} |0\rangle_{E'} \right. \right\rangle \right\|_2^2. \quad (147)$$

By the same reasoning employed in the proof of Theorem 2, we conclude that

$$\begin{aligned} & \frac{1}{2} \sup_P \left\| \left\langle \Phi \left|_{T''T} P \sum_{i \in \{0,1\}} |i\rangle_{T'} |i\rangle_T U_{AE' \rightarrow BE}^i |\psi\rangle_{RA} |0\rangle_{E'} \right. \right\rangle \right\|_2^2 \\ &= \frac{1}{2} \left(1 + \sqrt{F}(\mathcal{N}_{A \rightarrow B}^0(\rho_A), \mathcal{N}_{A \rightarrow B}^1(\rho_A)) \right), \quad (148) \end{aligned}$$

where ρ_A is the reduced state of ψ_{RA} (i.e., $\text{Tr}_R[\psi_{RA}] = \rho_A$). Now including the optimization over every pure state ψ_{RA} , we conclude the claim in (142). ■

H. Generalization to multiple states

In this section, we generalize Algorithm 4 to multiple states, by devising a quantum algorithm that tests how similar all the states of an ensemble are to each other.

Suppose that we are given an ensemble $\{p(x), \rho_S^x\}_{x \in \mathcal{X}}$ of states of system S , with $d = |\mathcal{X}|$, and we would like to know how similar they are to each other. Then we can perform a test like that given in Algorithm 4, but it is a multiple-state similarity test. The main difference is that the verifier prepares an initial entangled state that encodes the prior probabilities $\{p(x)\}_{x \in \mathcal{X}}$ and the algorithm employs d -dimensional control systems throughout, instead of qubit control systems. We suppose that, for all $x \in \mathcal{X}$, there is a circuit U_{RS}^x that generates a purification $|\psi^x\rangle_{RS}$ as follows:

$$|\psi^x\rangle_{RS} := U_{RS}^x |0\rangle_{RS}, \quad (149)$$

$$\rho_S^x = \text{Tr}_R[|\psi^x\rangle\langle\psi^x|_{RS}]. \quad (150)$$

Algorithm 11 *The algorithm proceeds as follows:*

1. The verifier prepares a state

$$|\Phi^p\rangle_{T'T} := \sum_{x \in \mathcal{X}} \sqrt{p(x)} |xx\rangle_{T'T} \quad (151)$$

on registers T' and T and prepares systems RS in the all-zeros state $|0\rangle_{RS}$.

2. Using the circuits in the set $\{U_{RS}^x\}_{x \in \mathcal{X}}$, the verifier performs the following controlled unitary:

$$\sum_{x \in \mathcal{X}} |x\rangle\langle x|_T \otimes U_{RS}^x. \quad (152)$$

3. The verifier transmits systems T' and R to the prover.

4. The prover prepares a system F in the $|0\rangle_F$ state and acts on systems T' , R , and F with a unitary $P_{T'RF \rightarrow T''F'}$ to produce the output systems T'' and F' , where T'' is a qudit system.
5. The prover sends system T'' to the verifier, who then performs a qudit Bell measurement

$$\{\Phi_{T''T}, I_{T''T} - \Phi_{T''T}\} \quad (153)$$

on systems T'' and T , where

$$\Phi_{T''T} = |\Phi\rangle\langle\Phi|_{T''T}, \quad (154)$$

$$|\Phi\rangle_{T''T} := \frac{1}{\sqrt{d}} \sum_{x \in \mathcal{X}} |xx\rangle_{T''T}. \quad (155)$$

The verifier accepts if and only if the outcome $\Phi_{T''T}$ occurs.

Theorem 7 *The acceptance probability of Algorithm 11 is equal to*

$$\frac{1}{d} \left[\sup_{\sigma_S} \sum_{x \in \mathcal{X}} \sqrt{p(x)} \sqrt{F(\rho_S^x, \sigma_S)} \right]^2, \quad (156)$$

where the optimization is over every density operator σ_S . This acceptance probability is bounded from above by

$$\frac{1}{d} + \frac{2}{d} \sum_{x, y \in \mathcal{X}: x < y} \sqrt{p(x)p(y)} \sqrt{F(\rho_S^x, \rho_S^y)}. \quad (157)$$

When $d = 2$, this upper bound is tight.

Proof. After Step 2 of Algorithm 11, the global state is

$$\sum_{x \in \mathcal{X}} \sqrt{p(x)} |xx\rangle_{T'T} |\psi^x\rangle_{RS}. \quad (158)$$

After Step 4, it is

$$P \sum_{x \in \mathcal{X}} \sqrt{p(x)} |xx\rangle_{T'T} |\psi^x\rangle_{RS} |0\rangle_F, \quad (159)$$

where $P \equiv P_{T'RF \rightarrow T''F'}$. Then, for a fixed unitary $P_{T'RF \rightarrow T''F'}$, the acceptance probability is

$$\begin{aligned} & \left\| \langle \Phi |_{T''T} P \sum_{x \in \mathcal{X}} \sqrt{p(x)} |xx\rangle_{T'T} |\psi^x\rangle_{RS} |0\rangle_F \right\|_2^2 = \\ & \sup_{|\varphi\rangle_{F'S}} \left| \langle \Phi |_{T''T} \langle \varphi |_{F'S} P \sum_{x \in \mathcal{X}} \sqrt{p(x)} |xx\rangle_{T'T} |\psi^x\rangle_{RS} |0\rangle_F \right|^2, \end{aligned} \quad (160)$$

where the optimization is over every pure state $|\varphi\rangle_{F'S}$ and we have used the fact that $\| |\phi\rangle \|_2^2 = \sup_{|\psi\rangle: \| |\psi\rangle \|_2 = 1} | \langle \psi | \phi \rangle |^2$. This implies that the acceptance probability is given by

$$\sup_{|\varphi\rangle_{F'S}, P} \left| \langle \Phi |_{T''T} \langle \varphi |_{F'S} P \sum_{x \in \mathcal{X}} \sqrt{p(x)} |xx\rangle_{T'T} |\psi^x\rangle_{RS} |0\rangle_F \right|^2. \quad (161)$$

Recall Uhlmann's theorem [Uhl76], which is the statement that

$$F(\omega_C, \tau_C) = \sup_{V_B} |\langle \varphi^\tau |_{BC} V_B \otimes I_C |\varphi^\omega\rangle_{BC} |^2, \quad (162)$$

where ω_C and τ_C are density operators with respective purifications $|\varphi^\omega\rangle_{BC}$ and $|\varphi^\tau\rangle_{BC}$ and the optimization is over every unitary V_B . Observing that the unitary $P_{T'RF \rightarrow T''F'}$ acts on systems $T'RF$ of $\sum_{x \in \mathcal{X}} \sqrt{p(x)} |xx\rangle_{T'T} |\psi^x\rangle_{RS} |0\rangle_F$ and systems $T''F'$ of $|\Phi\rangle_{T''T} |\varphi\rangle_{F'S}$, that their respective reduced states on systems TS are

$$\sum_{x \in \mathcal{X}} p(x) |x\rangle\langle x|_T \otimes \rho_S^x, \quad (163)$$

$$\pi_T \otimes \sigma_S, \quad (164)$$

where π_T is the maximally mixed state and $\sigma_S := \text{Tr}_{F'}[\varphi_{F'S}]$, and applying Uhlmann's theorem, we conclude that the acceptance probability is given by

$$\sup_{\sigma_S} F \left(\sum_{x \in \mathcal{X}} p(x) |x\rangle\langle x|_T \otimes \rho_S^x, \pi_T \otimes \sigma_S \right) \quad (165)$$

$$= \left[\sup_{\sigma_S} \sqrt{F} \left(\sum_{x \in \mathcal{X}} p(x) |x\rangle\langle x|_T \otimes \rho_S^x, \pi_T \otimes \sigma_S \right) \right]^2 \quad (166)$$

$$= \frac{1}{d} \left[\sup_{\sigma_S} \sum_{x \in \mathcal{X}} \sqrt{p(x)} \sqrt{F(\rho_S^x, \sigma_S)} \right]^2. \quad (167)$$

In the second equality, we made use of the direct-sum property of the root fidelity [KW20b, Proposition 4.29]. We note here that the analysis employed is the same as that used to show that the CLOSE-IMAGE problem is QIP(2)-complete [HMW13, HMW14].

We can also write the acceptance probability as

$$\begin{aligned} & \left\| \langle \Phi |_{T''T} P \sum_{x \in \mathcal{X}} \sqrt{p(x)} |xx\rangle_{T'T} |\psi^x\rangle_{RS} |0\rangle_F \right\|_2^2 \\ &= \frac{1}{d} \left\| \sum_{x \in \mathcal{X}} \sqrt{p(x)} P_{R \rightarrow F'}^x |\psi^x\rangle_{RS} \right\|_2^2 \end{aligned} \quad (168)$$

where we have defined

$$P_{R \rightarrow F'}^x := \langle x |_{T''} P_{T'RF \rightarrow T''F'} |x\rangle_{T'} |0\rangle_F. \quad (169)$$

The upper bound in (157) follows because

$$\begin{aligned} & \frac{1}{d} \left\| \sum_{x \in \mathcal{X}} \sqrt{p(x)} P_{R \rightarrow F'}^x |\psi^x\rangle_{RS} \right\|_2^2 \\ &= \frac{1}{d} \sum_{x, y \in \mathcal{X}} \sqrt{p(x)p(y)} \langle \psi^x |_{RS} (P_{R \rightarrow F'}^x)^\dagger P_{R \rightarrow F'}^y | \psi^y \rangle_{RS} \\ &= \frac{1}{d} \sum_{x \in \mathcal{X}} p(x) \langle \psi^x |_{RS} (P_{R \rightarrow F'}^x)^\dagger P_{R \rightarrow F'}^x | \psi^x \rangle_{RS} \end{aligned} \quad (170)$$

$$+ \frac{2}{d} \sum_{\substack{x,y \in \mathcal{X} \\ :x < y}} \sqrt{p(x)p(y)} \operatorname{Re}[\langle \psi^x |_{RS} (P^x)^\dagger P^y | \psi^y \rangle_{RS}] \quad (171)$$

$$\leq \frac{1}{d} + \sum_{x,y \in \mathcal{X} : x < y} \sqrt{p(x)p(y)} \sqrt{F}(\rho_S^x, \rho_S^y) \quad (172)$$

where the first equality follows by expanding the norm, the second by splitting the terms into those for which $x = y$ and $x \neq y$, and the inequality follows because $(P_{R \rightarrow F'}^x)^\dagger P_{R \rightarrow F'}^x \leq I_R$ and from reasoning similar to that in the proof of Theorem 2.

The final statement about tightness of the upper bound follows by picking P^x and P^y for $x \neq y$ to be isometries from Uhlmann's theorem, as was done at the end of the proof of Theorem 2. ■

Corollary 8 *The fact that the upper bound is achieved in Theorem 7 for $d = 2$ leads to the following identity for states ρ_S^0 and ρ_S^1 and probability $p \in [0, 1]$:*

$$\left[\sup_{\sigma_S} \sqrt{p} \sqrt{F}(\rho_S^0, \sigma_S) + \sqrt{1-p} \sqrt{F}(\rho_S^1, \sigma_S) \right]^2 = 1 + 2\sqrt{p(1-p)} \sqrt{F}(\rho_S^0, \rho_S^1), \quad (173)$$

where the optimization is over every density operator σ_S .

The acceptance probability in (156) is proportional to the secrecy measure discussed in [KRS09, Eq. (19)], which is the same as the max-conditional entropy of the following classical-quantum state:

$$\sum_{x \in \mathcal{X}} p(x) |x\rangle\langle x|_T \otimes \rho_S^x. \quad (174)$$

Indeed, it is a measure of secrecy because if an eavesdropper has access to system S and if $\rho_S^x \approx \sigma$ for all $x \in \mathcal{X}$ and if $p(x) \approx 1/d$, then it is difficult for the eavesdropper to guess the classical message in system T (also, the fidelity is close to one). According to [SDG+21, Remark 2.7] and the expression in (165), the acceptance probability in (156) is also a measure of the symmetric distinguishability of the classical-quantum state in (174), and thus gives this measure an operational meaning.

The upper bound in (157) on the acceptance probability has some conceptual similarity with known upper bounds on the success probability in state discrimination [Mon08, Qiu08], in the sense that we employ the fidelity of pairs of states in the upper bound. Finally, we note some similarities between the problem outlined here and coherent channel discrimination considered recently in [Wil20]. However, these two problems are ultimately different in their objectives.

I. Generalization to multiple channels and strategies

We now generalize Algorithms 8 and 11 to the case of testing the similarity of an ensemble of channels. The

resulting algorithm thus has applications in the context of private quantum reading [BDW18, DBW20], in which one goal of such a protocol is to encode a classical message into a channel selected randomly from an ensemble of channels such that it is indecipherable by an eavesdropper who has access to the output of the channel. We also remark at the end of this section about a generalization of Algorithms 9 and 12 to the case of an ensemble of n -turn quantum strategies.

Let us first consider the case of channels. In more detail, let $\{p(x), \mathcal{N}_{A \rightarrow B}^x\}_{x \in \mathcal{X}}$ be an ensemble of quantum channels. Set $d = |\mathcal{X}|$. We suppose that, for all $x \in \mathcal{X}$, there is a circuit $U_{AE' \rightarrow BE}^x$ that generates an isometric extension of the channel $\mathcal{N}_{A \rightarrow B}^x$, in the following sense:

$$\mathcal{N}_{A \rightarrow B}^x(\omega_A) = \operatorname{Tr}_E[U_{AE' \rightarrow BE}^x(\omega_A \otimes |0\rangle\langle 0|_{E'}) (U_{AE' \rightarrow BE}^x)^\dagger]. \quad (175)$$

The following algorithm employs competing provers, similar to how Algorithm 8 does.

Algorithm 12 *The algorithm proceeds as follows:*

1. The verifier prepares a state

$$|\Phi^p\rangle_{T'T} := \sum_{x \in \mathcal{X}} \sqrt{p(x)} |xx\rangle_{T'T} \quad (176)$$

on registers T' and T and prepares system E' in the all-zeros state $|0\rangle_{RS}$.

2. The min-prover transmits the system A of the state $|\psi\rangle_{RA}$ to the verifier.
3. Using the circuits in the set $\{U_{AE' \rightarrow BE}^x\}_{x \in \mathcal{X}}$, the verifier performs the following controlled unitary:

$$\sum_{x \in \mathcal{X}} |x\rangle\langle x|_T \otimes U_{AE' \rightarrow BE}^x. \quad (177)$$

4. The verifier transmits systems T' and E to the max-prover.
5. The max-prover prepares a system F in the $|0\rangle_F$ state and acts on systems T' , R , and F with a unitary $P_{T'E'F \rightarrow T''F'}$ to produce the output systems T'' and F' , where T'' is a qudit system.
6. The max-prover sends system T'' to the verifier, who then performs a qudit Bell measurement

$$\{\Phi_{T''T}, I_{T''T} - \Phi_{T''T}\} \quad (178)$$

on systems T'' and T , where $\Phi_{T''T}$ is defined in (154). The verifier accepts if and only if the outcome $\Phi_{T''T}$ occurs.

Theorem 9 *The acceptance probability of Algorithm 12 is equal to*

$$\frac{1}{d} \left[\inf_{\psi_{RA}} \sup_{\sigma_{RB}} \sum_{x \in \mathcal{X}} \sqrt{p(x)} \sqrt{F}(\mathcal{N}_{A \rightarrow B}^x(\psi_{RA}), \sigma_{RB}) \right]^2. \quad (179)$$

This acceptance probability is bounded from above by

$$\frac{1}{d} + \frac{2}{d} \times \inf_{\psi_{RA}} \sum_{\substack{x, y \in \mathcal{X}: \\ x < y}} \sqrt{p(x)p(y)} \sqrt{F(\mathcal{N}_{A \rightarrow B}^x(\psi_{RA}), \mathcal{N}_{A \rightarrow B}^y(\psi_{RA}))}. \quad (180)$$

When $d = 2$, this upper bound is tight.

Proof. We can employ the result of Theorem 7. For a fixed state ψ_{RA} of the min-prover, the acceptance probability is equal to

$$\frac{1}{d} \left[\sup_{\sigma_{RB}} \sum_{x \in \mathcal{X}} \sqrt{p(x)} \sqrt{F(\mathcal{N}_{A \rightarrow B}^x(\psi_{RA}), \sigma_{RB})} \right]^2, \quad (181)$$

as a consequence of Theorem 7. Thus, we arrive at the claim in (179) by minimizing over every state ψ_{RA} of the min-prover.

The upper bound in (180) follows from the upper bound in (157). Indeed, for a fixed state ψ_{RA} of the min-prover, the acceptance probability in (181) is bounded from above by

$$\frac{1}{d} + \frac{2}{d} \sum_{\substack{x, y \in \mathcal{X}: \\ x < y}} \sqrt{p(x)p(y)} \sqrt{F(\mathcal{N}_{A \rightarrow B}^x(\psi_{RA}), \mathcal{N}_{A \rightarrow B}^y(\psi_{RA}))}. \quad (182)$$

After taking infima, we arrive at (180).

The final statement follows from the same reasoning employed at the end of the proof of Theorem 7. ■

Corollary 10 *The following identity holds in the special case of two channels $\mathcal{N}_{A \rightarrow B}^0$ and $\mathcal{N}_{A \rightarrow B}^1$ and probability $p \in [0, 1]$:*

$$\left[\inf_{\psi_{RA}} \sup_{\sigma_{RB}} \left(\frac{\sqrt{p} \sqrt{F(\mathcal{N}_{A \rightarrow B}^0(\psi_{RA}), \sigma_{RB})}}{\sqrt{1-p} \sqrt{F(\mathcal{N}_{A \rightarrow B}^1(\psi_{RA}), \sigma_{RB})}} \right) \right]^2 = 1 + 2\sqrt{p(1-p)} \inf_{\psi_{RA}} \sqrt{F(\mathcal{N}_{A \rightarrow B}^0(\psi_{RA}), \mathcal{N}_{A \rightarrow B}^1(\psi_{RA}))}, \quad (183)$$

where the supremum is with respect to every density operator σ_{RB} .

Remark 11 *We note here that we can generalize the developments in this section and the previous one to the case of quantum strategies, in order to test how similar strategies in a set are to each other. Let $\{p(x), \mathcal{N}^{x,(n)}\}_{x \in \mathcal{X}}$ be an ensemble of quantum strategies, each of which has n turns. Then the acceptance probability of an algorithm that is the obvious generalization of Algorithms 9 and 12 is given by*

$$\frac{1}{d} \left[\inf_{\mathcal{S}^{(n-1)}} \sup_{\sigma} \sum_{x \in \mathcal{X}} \sqrt{p(x)} \sqrt{F(\mathcal{N}^{x,(n)} \circ \mathcal{S}^{(n-1)}, \sigma_{R_n B_n})} \right]^2, \quad (184)$$

where the infimum is with respect to every $(n-1)$ -turn pure co-strategy that leads to a quantum state $\mathcal{N}^{x,(n)} \circ \mathcal{S}^{(n-1)}$ (as discussed around (120)) and the supremum is with respect to every state $\sigma_{R_n B_n}$. The expression in (184) is a similarity measure for the strategies in the ensemble $\{p(x), \mathcal{N}^{x,(n)}\}_{x \in \mathcal{X}}$.

We can also generalize Algorithm 10 from Section II G, to estimate the following similarity measure for an ensemble $\{p(x), \mathcal{N}_{A \rightarrow B}^x\}_{x \in \mathcal{X}}$ of channels:

$$\frac{1}{d} \left[\sup_{\rho_A, \sigma_B} \sum_{x \in \mathcal{X}} \sqrt{p(x)} \sqrt{F(\mathcal{N}_{A \rightarrow B}^x(\rho_A), \sigma_B)} \right]^2, \quad (185)$$

where the optimization is over all density operators ρ_A and σ_B . As is the case with Algorithm 10, there is a single prover who is trying to make all of the channel outputs look like the same state. Again we suppose that there is a circuit $U_{AE' \rightarrow BE}^x$ that generates an isometric extension of the channel $\mathcal{N}_{A \rightarrow B}^x$, in the sense of (175).

Algorithm 13 *The algorithm proceeds as follows:*

1. *The verifier prepares a state*

$$|\Phi^p\rangle_{T'T} := \sum_{x \in \mathcal{X}} \sqrt{p(x)} |xx\rangle_{T'T} \quad (186)$$

on registers T' and T and prepares system E' in the all-zeros state $|0\rangle_{E'}$.

2. *The prover transmits the system A of the state $|\psi\rangle_{RA}$ to the verifier.*
3. *Using the circuits in the set $\{U_{AE' \rightarrow BE}^x\}_{x \in \mathcal{X}}$, the verifier performs the following controlled unitary:*

$$\sum_{x \in \mathcal{X}} |x\rangle\langle x|_T \otimes U_{AE' \rightarrow BE}^x. \quad (187)$$

4. *The verifier transmits systems T' and E to the max-prover.*
5. *The prover prepares a system F in the $|0\rangle_F$ state and acts on systems T' , R , and F with a unitary $P_{T'EF \rightarrow T''F'}$ to produce the output systems T'' and F' , where T'' is a qudit system.*
6. *The prover sends system T'' to the verifier, who then performs a qudit Bell measurement*

$$\{\Phi_{T''T}, I_{T''T} - \Phi_{T''T}\} \quad (188)$$

on systems T'' and T , where $\Phi_{T''T}$ is defined in (154). The verifier accepts if and only if the outcome $\Phi_{T''T}$ occurs.

Theorem 12 *The acceptance probability of Algorithm 12 is equal to*

$$\frac{1}{d} \left[\sup_{\rho_A, \sigma_B} \sum_{x \in \mathcal{X}} \sqrt{p(x)} \sqrt{F(\mathcal{N}_{A \rightarrow B}^x(\rho_A), \sigma_B)} \right]^2. \quad (189)$$

This acceptance probability is bounded from above by

$$\frac{1}{d} + \frac{2}{d} \times \sup_{\rho_A} \sum_{x,y \in \mathcal{X}: x < y} \sqrt{p(x)p(y)} \sqrt{F(\mathcal{N}_{A \rightarrow B}^x(\rho_A), \mathcal{N}_{A \rightarrow B}^y(\rho_A))}. \quad (190)$$

When $d = 2$, this upper bound is tight.

Proof. For a fixed state ψ_{RA} of the prover, the problem is equivalent to that specified by Algorithm 11, for the ensemble $\{p(x), F(\mathcal{N}_{A \rightarrow B}^x(\rho_A))\}_{x \in \mathcal{X}}$, where $\rho_A = \text{Tr}_R[\psi_{RA}]$. Thus, all of the statements from Theorem 7 apply for this fixed state. We arrive at the statement of the theorem after optimizing over all input states. ■

III. ESTIMATING TRACE DISTANCE, DIAMOND DISTANCE, AND STRATEGY DISTANCE

We now review several well known algorithms for estimating trace distance [Wat02], diamond distance [RW05], and strategy distance [GW07, Gut09, Gut12] by interacting with quantum provers. Later on, we replace the provers with parameterized circuits to see how well this approach can perform in estimating these distinguishability measures.

A. Estimating trace distance

The trace distance between quantum states ρ_S^0 and ρ_S^1 is defined as $\|\rho_S^0 - \rho_S^1\|_1$, where $\|A\|_1 = \text{Tr}[\sqrt{A^\dagger A}]$. It is a well known and operationally motivated measure of distinguishability for quantum states.

We suppose, as is the case in Section II C, that quantum circuits U_{RS}^0 and U_{RS}^1 are available for generating purifications of the states ρ_S^0 and ρ_S^1 . That is, for $i \in \{0, 1\}$,

$$\rho_S^i = \text{Tr}_R[U_{RS}^i |0\rangle\langle 0|_{RS} (U_{RS}^i)^\dagger]. \quad (191)$$

However, the purifying systems are not strictly necessary in the operation of the algorithm given below, which is an advantage over the algorithms from Section II C.

The following QSZK algorithm allows for estimating the trace distance [Wat02], in the sense that its acceptance probability is a simple function of the trace distance:

Algorithm 14 ([Hel67, Hel69, Hol72, Wat02])

The algorithm proceeds as follows:

1. The verifier picks a classical bit $i \in \{0, 1\}$ uniformly at random, prepares the state ρ_S^i , and sends system S to the prover.

2. The prover prepares a system F in the $|0\rangle_F$ state and acts on systems S and F with a unitary $P_{SF \rightarrow TF'}$ to produce the output systems T and F' , where T is a qubit system.
3. The prover sends system T to the verifier, who then performs a measurement on system T , with outcome j . The verifier accepts if and only if $i = j$.

This algorithm has been well known for some time [Hel67, Hel69, Hol72, Wat02] and its maximum acceptance probability is equal to

$$\max_{\Lambda: 0 \leq \Lambda \leq I} \frac{1}{2} \text{Tr}[\Lambda \rho_S^0] + \frac{1}{2} \text{Tr}[(I - \Lambda) \rho_S^1] = \frac{1}{2} \left(1 + \frac{1}{2} \|\rho_S^0 - \rho_S^1\|_1 \right). \quad (192)$$

This follows because the acceptance probability can be written as follows, for a fixed unitary $P \equiv P_{SF \rightarrow TF'}$ of the prover:

$$\begin{aligned} & \frac{1}{2} \sum_{i \in \{0,1\}} \text{Tr}[(|i\rangle\langle i|_T \otimes I_{F'}) P(\rho_S^i \otimes |0\rangle\langle 0|_F) P^\dagger] \\ &= \frac{1}{2} \sum_{i \in \{0,1\}} \text{Tr}[\langle 0|_F P^\dagger (|i\rangle\langle i|_T \otimes I_{F'}) P |0\rangle_F \rho_S^i] \end{aligned} \quad (193)$$

$$= \frac{1}{2} \sum_{i \in \{0,1\}} \text{Tr}[\Lambda_S^i \rho_S^i], \quad (194)$$

where we have defined the measurement operator Λ_S^i , for $i \in \{0, 1\}$, as

$$\Lambda_S^i := \langle 0|_F (P_{SF \rightarrow TF'})^\dagger (|i\rangle\langle i|_T \otimes I_{F'}) P_{SF \rightarrow TF'} |0\rangle_F, \quad (195)$$

and it is clear that $\sum_{i \in \{0,1\}} \Lambda_S^i = I_S$. By the Naimark extension theorem [Nai40] (see also [KW20b]), every measurement can be realized in this way, so that

$$\begin{aligned} & \max_P \frac{1}{2} \sum_{i \in \{0,1\}} \text{Tr}[(|i\rangle\langle i|_T \otimes I_{F'}) P(\rho_S^i \otimes |0\rangle\langle 0|_F) P^\dagger] \\ &= \max_{\Lambda: 0 \leq \Lambda \leq I} \frac{1}{2} \text{Tr}[\Lambda \rho_S^0] + \frac{1}{2} \text{Tr}[(I - \Lambda) \rho_S^1]. \end{aligned} \quad (196)$$

Thus, by replacing the actions of the prover with a parameterized circuit and repeating the algorithm, we can use a quantum computer to estimate a lower bound on the trace distance of the states ρ_S^0 and ρ_S^1 . An approach similar to this has been adopted in [CSZW20].

We note here that the following identity holds also [Hel67, Hel69, Hol72] (see also [KW20b, Theorem 3.13]):

$$\begin{aligned} & \min_{\Lambda: 0 \leq \Lambda \leq I} \frac{1}{2} \text{Tr}[\Lambda \rho_S^0] + \frac{1}{2} \text{Tr}[(I - \Lambda) \rho_S^1] \\ &= \frac{1}{2} \left(1 - \frac{1}{2} \|\rho_S^0 - \rho_S^1\|_1 \right). \end{aligned} \quad (197)$$

B. Estimating diamond distance

The diamond distance between quantum channels $\mathcal{N}_{A \rightarrow B}^0$ and $\mathcal{N}_{A \rightarrow B}^1$ is defined as [Kit97]

$$\begin{aligned} \|\mathcal{N}_{A \rightarrow B}^0 - \mathcal{N}_{A \rightarrow B}^1\|_{\diamond} &:= \\ \sup_{\rho_{RA}} \|\mathcal{N}_{A \rightarrow B}^0(\rho_{RA}) - \mathcal{N}_{A \rightarrow B}^1(\rho_{RA})\|_1, \end{aligned} \quad (198)$$

where the optimization is over every bipartite state ρ_{RA} and the system R can be arbitrarily large. By a well known data processing argument, the following equality holds

$$\begin{aligned} \|\mathcal{N}_{A \rightarrow B}^0 - \mathcal{N}_{A \rightarrow B}^1\|_{\diamond} &:= \\ \max_{\psi_{RA}} \|\mathcal{N}_{A \rightarrow B}^0(\psi_{RA}) - \mathcal{N}_{A \rightarrow B}^1(\psi_{RA})\|_1, \end{aligned} \quad (199)$$

where the optimization is over every pure bipartite state ρ_{RA} and the system R is isomorphic to the channel input system A . The diamond distance is a well known and operationally motivated measure of distinguishability for quantum channels [RW05, GLN05].

We suppose, as is the case in Section IID, that quantum circuits $U_{AE' \rightarrow BE}^0$ and $U_{AE' \rightarrow BE}^1$ are available for generating isometric extensions of the channels $\mathcal{N}_{A \rightarrow B}^0$ and $\mathcal{N}_{A \rightarrow B}^1$. That is, for $i \in \{0, 1\}$,

$$\mathcal{N}_{A \rightarrow B}^i(\cdot) = \text{Tr}_E[U_{AE' \rightarrow BE}^i((\cdot) \otimes |0\rangle\langle 0|_{E'}) (U_{AE' \rightarrow BE}^i)^\dagger]. \quad (200)$$

However, the environment systems are not strictly necessary in the operation of the algorithm given below, which is an advantage over the algorithms from Section IID.

The following QIP algorithm allows for estimating the diamond distance [RW05], in the sense that its acceptance probability is a simple function of the diamond distance:

Algorithm 15 ([RW05]) *The algorithm proceeds as follows:*

1. The prover prepares a pure state ψ_{RA} and sends system A to the verifier.
2. The verifier picks a classical bit $i \in \{0, 1\}$ uniformly at random, applies the channel $\mathcal{N}_{A \rightarrow B}^i$, and sends system B to the prover.
3. The prover prepares a system F in the $|0\rangle_F$ state and acts on systems R , B , and F with a unitary $P_{RBF \rightarrow TF'}$ to produce the output systems T and F' , where T is a qubit system.
4. The prover sends system T to the verifier, who then performs a measurement on system T , with outcome j . The verifier accepts if and only if $i = j$.

This algorithm has been well known for some time [RW05] and its maximum acceptance probability is equal to

$$\frac{1}{2} \left(1 + \frac{1}{2} \|\mathcal{N}_{A \rightarrow B}^0 - \mathcal{N}_{A \rightarrow B}^1\|_{\diamond} \right). \quad (201)$$

Thus, by replacing the actions of the prover with a parameterized circuit and repeating the algorithm, we can use a quantum computer to estimate a lower bound on the diamond distance of the channels $\mathcal{N}_{A \rightarrow B}^0$ and $\mathcal{N}_{A \rightarrow B}^1$.

C. Estimating strategy distance

We already provided the definition of a quantum strategy in Section IIE, and therein, we discussed the strategy fidelity (see Eq. (121)). The strategy distance [GW07, CDP08, Gut12] is conceptually similar, but it is defined with the trace distance as the underlying metric:

$$\begin{aligned} \|\mathcal{N}^{0,(n)} - \mathcal{N}^{1,(n)}\|_{\diamond_n} &:= \\ \sup_{\mathcal{S}^{(n-1)}} \|\mathcal{N}^{0,(n)} \circ \mathcal{S}^{(n-1)} - \mathcal{N}^{1,(n)} \circ \mathcal{S}^{(n-1)}\|_1, \end{aligned} \quad (202)$$

where the supremum is with respect to every co-strategy $\mathcal{S}^{(n-1)}$ that leads to the quantum states $\mathcal{N}^{0,(n)} \circ \mathcal{S}^{(n-1)}$ and $\mathcal{N}^{1,(n)} \circ \mathcal{S}^{(n-1)}$. The strategy distance is an operationally motivated measure of distinguishability for quantum strategies.

The following QIP algorithm allows for estimating the strategy distance [GW07], in the sense that its acceptance probability is a simple function of the strategy distance:

Algorithm 16 ([GW07]) *The algorithm proceeds as follows:*

1. The prover prepares a pure state ψ_{RA} and sends system A to the verifier.
2. The verifier picks a classical bit $i \in \{0, 1\}$ uniformly at random, applies the channel $\mathcal{N}_{A_1 \rightarrow M_1 B_1}^{i,1}$, and sends system B_1 to the prover.
3. The prover acts with the isometric channel $\mathcal{S}_{R_1 B_1 \rightarrow R_2 A_2}^1$ and then sends system A_2 to the verifier.
4. For $j \in \{2, \dots, n-1\}$, the verifier applies the channel $\mathcal{N}_{M_{j-1} A_j \rightarrow M_j B_j}^{i,j}$ and transmits system B_j to the prover, who subsequently acts with the isometric channel $\mathcal{S}_{R_j B_j \rightarrow R_{j+1} A_{j+1}}^j$ and then sends system A_{j+1} to the verifier.
5. The verifier applies the channel $\mathcal{N}_{M_{n-1} A_n \rightarrow B_n}^{i,n}$ and sends system B_n to the prover.
6. The prover prepares a system F in the $|0\rangle_F$ state and acts on systems R_n , B_n , and F with a unitary $P_{R_n B_n F \rightarrow TF'}$ to produce the output systems T and F' , where T is a qubit system.
7. The prover sends system T to the verifier, who then performs a measurement on system T , with outcome j . The verifier accepts if and only if $i = j$.

This algorithm has been well known since [GW07] and its maximum acceptance probability is equal to

$$\frac{1}{2} \left(1 + \frac{1}{2} \left\| \mathcal{N}^{0,(n)} - \mathcal{N}^{1,(n)} \right\|_{\diamond_n} \right). \quad (203)$$

Thus, by replacing the actions of the prover with a parameterized circuit and repeating the algorithm, we can use a quantum computer to estimate a lower bound on the strategy distance of the strategies $\mathcal{N}^{0,(n)}$ and $\mathcal{N}^{1,(n)}$. See [Gut12, KW20a] for semi-definite programs for evaluating the strategy distance of two strategies.

D. Estimating minimum trace distance of channels

In this section, we show how to estimate the following trace distance function of channels $\mathcal{N}_{A \rightarrow B}^0$ and $\mathcal{N}_{A \rightarrow B}^1$ by means of a short quantum game (SQG) algorithm:

$$\inf_{\rho_A} \left\| \mathcal{N}_{A \rightarrow B}^0(\rho_A) - \mathcal{N}_{A \rightarrow B}^1(\rho_A) \right\|_1, \quad (204)$$

where the optimization is over every input state ρ_A . The algorithm features a min-prover and a max-prover. Short quantum games were defined and studied in [GW05, Gut05].

Algorithm 17 *The algorithm proceeds as follows:*

1. *The min-prover prepares a state ψ_{RA} and sends system A to the verifier.*
2. *The verifier picks a classical bit $i \in \{0, 1\}$ uniformly at random, applies the channel $\mathcal{N}_{A \rightarrow B}^i$, and sends system B to the max-prover.*
3. *The max-prover prepares a system F in the $|0\rangle_F$ state and acts on systems R , B , and F with a unitary $P_{RBF \rightarrow TF'}$ to produce the output systems T and F' , where T is a qubit system.*
4. *The max-prover sends system T to the verifier, who then performs a measurement on system T , with outcome j . The verifier accepts if and only if $i = j$.*

For a fixed state ψ_{RA} of the min-prover, it follows from Algorithm 14 that the acceptance probability is equal to

$$\frac{1}{2} \left(1 + \frac{1}{2} \left\| \mathcal{N}_{A \rightarrow B}^0(\rho_A) - \mathcal{N}_{A \rightarrow B}^1(\rho_A) \right\|_1 \right), \quad (205)$$

where $\rho_A = \text{Tr}_R[\psi_{RA}]$. Since the min-prover plays first and his goal is to minimize the acceptance probability, it follows that the acceptance probability of Algorithm 17 is given by

$$\frac{1}{2} \left(1 + \frac{1}{2} \inf_{\rho_A} \left\| \mathcal{N}_{A \rightarrow B}^0(\rho_A) - \mathcal{N}_{A \rightarrow B}^1(\rho_A) \right\|_1 \right). \quad (206)$$

Another way to estimate the minimum trace distance of channels in (204) is to swap the roles of the max-prover and min-prover in Algorithm 17:

Algorithm 18 *The algorithm proceeds as follows:*

1. *The max-prover prepares a state ψ_{RA} and sends system A to the verifier.*
2. *The verifier picks a classical bit $i \in \{0, 1\}$ uniformly at random, applies the channel $\mathcal{N}_{A \rightarrow B}^i$, and sends system B to the min-prover.*
3. *The min-prover prepares a system F in the $|0\rangle_F$ state and acts on systems R , B , and F with a unitary $P_{RBF \rightarrow TF'}$ to produce the output systems T and F' , where T is a qubit system.*
4. *The min-prover sends system T to the verifier, who then performs a measurement on system T , with outcome j . The verifier accepts if and only if $i = j$.*

For a fixed state ψ_{RA} of the max-prover, it follows from (197) that the acceptance probability is equal to

$$\frac{1}{2} \left(1 - \frac{1}{2} \left\| \mathcal{N}_{A \rightarrow B}^0(\rho_A) - \mathcal{N}_{A \rightarrow B}^1(\rho_A) \right\|_1 \right), \quad (207)$$

where $\rho_A = \text{Tr}_R[\psi_{RA}]$. Since the max-prover plays first and his goal is to maximize the acceptance probability, it follows that the acceptance probability of Algorithm 17 is given by

$$\frac{1}{2} \left(1 - \frac{1}{2} \inf_{\rho_A} \left\| \mathcal{N}_{A \rightarrow B}^0(\rho_A) - \mathcal{N}_{A \rightarrow B}^1(\rho_A) \right\|_1 \right). \quad (208)$$

Although the quantities estimated by Algorithms 10 and 17 or 18 are similar (and related to each other by standard inequalities relating trace distance and fidelity [FvdG99]), the algorithms are very different in that the channel output is available at the end of Algorithm 10, whereas it is not at the end of Algorithms 17 and 18. This has implications for applications in which it is helpful to have access to the channel output, for example, when one is trying to find the fixed point of a quantum channel.

E. Generalization to multiple states, channels, and strategies

Each of the algorithms from the previous subsections has a generalization to multiple states, channels, and strategies. We go through them briefly here. The main idea is that, rather than randomly picking from a set of two resources, the verifier picks randomly from a set of multiple resources and then a prover has to guess which one was chosen. The main difference with the binary case is that there is not a closed-form expression for the acceptance probability in terms of a metric like the trace distance or derived metrics, but rather the optimization is phrased as a semi-definite program that can be solved numerically or used in some cases to obtain analytical solutions (for example, if there is sufficient symmetry).

Suppose that we are given an ensemble $\{p(x), \rho_S^x\}_{x \in \mathcal{X}}$ of quantum states. The verifier picks x randomly according to $p(x)$, prepares ρ_S^x , and the prover has to guess which state was prepared. The acceptance probability is given by

$$\sup_{\{\Lambda_S^x\}_{x \in \mathcal{X}}} \sum_{x \in \mathcal{X}} p(x) \text{Tr}[\Lambda_S^x \rho_S^x], \quad (209)$$

where the optimization is over every POVM $\{\Lambda_S^x\}_{x \in \mathcal{X}}$. In the case that $|\mathcal{X}| = 2$, this acceptance probability has the explicit form

$$\frac{1}{2} (1 + \|p\rho_S^0 - (1-p)\rho_S^1\|_1). \quad (210)$$

To account for multiple states, we modify Algorithm 14 as follows: the verifier's variable $i \in \{0, \dots, |\mathcal{X}| - 1\}$ is randomly selected and the prover's guess $j \in \{0, \dots, |\mathcal{X}| - 1\}$. System T therein is generalized to be a $\lceil \log_2 |\mathcal{X}| \rceil$ -qubit system. When $|\mathcal{X}|$ is a power of two, there is a perfect match between the number $|\mathcal{X}|$ of measurement outcomes and the dimension of system T . The verifier accepts if the outcome j equals the state i that was picked. If $|\mathcal{X}|$ is not a power of two, the following algorithm handles this case by coarse graining some of the measurement outcomes together. This is relevant because most quantum computers are qubit-based.

Algorithm 19 *The algorithm proceeds as follows:*

1. The verifier selects an integer $i \in \{0, \dots, |\mathcal{X}| - 1\}$ at random according to $p(i)$, prepares the state ρ_S^i , and sends system S to the prover.
2. The prover prepares a system F composed of $\lceil \log_2 |\mathcal{X}| \rceil$ qubits in the $|0\rangle_F$ state. The prover then acts on systems S and F with a unitary $P_{SF \rightarrow TF'}$, producing the output systems F' and T , where T is a system of $\lceil \log_2 |\mathcal{X}| \rceil$ qubits.
3. The prover sends system T to the verifier, who then performs a computational basis measurement on system T , with outcome $j \in \{0, \dots, 2^{\lceil \log_2 |\mathcal{X}| \rceil} - 1\}$.
4. The verifier accepts under two conditions.
 - $j \leq |\mathcal{X}| - 1$ and $i = j$.
 - $j > |\mathcal{X}| - 1$ and $i = 0$.

This algorithm is a direct generalization of Algorithm 14. To understand its connection to (209), consider that, for a fixed unitary $P_{SF \rightarrow TF'}$, its acceptance probability is given by

$$\begin{aligned} & \sum_{i \in \{0, \dots, |\mathcal{X}| - 1\}} p(i) \text{Tr}[(|i\rangle\langle i|_T \otimes I_{F'}) P(\rho_S^i \otimes |0\rangle\langle 0|_F) P^\dagger] \\ & + p(0) \sum_{j=|\mathcal{X}|}^{2^{\lceil \log_2 |\mathcal{X}| \rceil} - 1} \text{Tr}[(|j\rangle\langle j|_T \otimes I_{F'}) P(\rho_S^i \otimes |0\rangle\langle 0|_F) P^\dagger] \end{aligned} \quad (211)$$

$$\begin{aligned} & = \sum_{i \in \{0, \dots, |\mathcal{X}| - 1\}} p(i) \text{Tr}[\langle 0|_F P^\dagger (|i\rangle\langle i|_T \otimes I_{F'}) P |0\rangle_F \rho_S^i] \\ & + p(0) \sum_{j=|\mathcal{X}|}^{2^{\lceil \log_2 |\mathcal{X}| \rceil} - 1} \text{Tr}[\langle 0|_F P^\dagger (|j\rangle\langle j|_T \otimes I_{F'}) P |0\rangle_F \rho_S^i] \end{aligned} \quad (212)$$

$$= \sum_{i \in \{0, \dots, |\mathcal{X}| - 1\}} p(i) \text{Tr}[\Lambda_S^i \rho_S^i], \quad (213)$$

where we have defined the following measurement operators:

$$\begin{aligned} \Lambda_S^0 & := \langle 0|_F P^\dagger (|0\rangle\langle 0|_T \otimes I_{F'}) P |0\rangle_F \\ & + \sum_{j=|\mathcal{X}|}^{2^{\lceil \log_2 |\mathcal{X}| \rceil} - 1} \langle 0|_F P^\dagger (|j\rangle\langle j|_T \otimes I_{F'}) P |0\rangle_F, \end{aligned} \quad (214)$$

and for all $i \in \{1, \dots, |\mathcal{X}| - 1\}$:

$$\Lambda_S^i := \langle 0|_F P^\dagger (|i\rangle\langle i|_T \otimes I_{F'}) P |0\rangle_F. \quad (215)$$

As such, we coarse grain all measurement outcomes in $\{0, |\mathcal{X}|, |\mathcal{X}| + 1, \dots, 2^{\lceil \log_2 |\mathcal{X}| \rceil}\}$ into a single measurement outcome. By the Naimark extension theorem, every measurement with $|\mathcal{X}|$ outcomes can be realized in this way, so that maximizing the expression in (211) over every unitary P gives a value equal to that in (209).

On the one hand, if $|\mathcal{X}|$ is a power of two, then it follows that $|\mathcal{X}| = 2^{\lceil \log_2 |\mathcal{X}| \rceil}$ and the outcome $j > |\mathcal{X}| - 1$ never occurs. On the other hand, if $|\mathcal{X}|$ is not a power of two, then $|\mathcal{X}| < 2^{\lceil \log_2 |\mathcal{X}| \rceil}$ and the outcome $j > |\mathcal{X}| - 1$ does occur.

Now suppose that we are given an ensemble $\{p(x), \mathcal{N}_{A \rightarrow B}^x\}_{x \in \mathcal{X}}$ of quantum channels. Then a similar modification of Algorithm 15 has acceptance probability

$$\sup_{\psi_{RA}, \{\Lambda_{RB}^x\}_{x \in \mathcal{X}}} \sum_{x \in \mathcal{X}} p(x) \text{Tr}[\Lambda_{RB}^x \mathcal{N}_{A \rightarrow B}^x(\psi_{RA})], \quad (216)$$

where the optimization is over every state ψ_{RA} and POVM $\{\Lambda_{RB}^x\}_{x \in \mathcal{X}}$. In the case that $|\mathcal{X}| = 2$, this acceptance probability has the explicit form

$$\frac{1}{2} (1 + \|p\mathcal{N}_{A \rightarrow B}^0 - (1-p)\mathcal{N}_{A \rightarrow B}^1\|_\diamond). \quad (217)$$

Suppose we are given an ensemble $\{p(x), \mathcal{N}^{x, (n)}\}_{x \in \mathcal{X}}$ of n -turn quantum strategies. A similar modification of Algorithm 16 has acceptance probability

$$\sup_{\substack{\mathcal{S}^{(n-1)}, \\ \{\Lambda_{R^n B^n}^x\}_{x \in \mathcal{X}}}} \sum_{x \in \mathcal{X}} p(x) \text{Tr}[\Lambda_{R^n B^n}^x (\mathcal{N}^{x, (n)} \circ \mathcal{S}^{(n-1)})], \quad (218)$$

where the optimization is over every $(n-1)$ -turn pure co-strategy $\mathcal{S}^{(n-1)}$ and POVM $\{\Lambda_{R^n B^n}^x\}_{x \in \mathcal{X}}$ (recall (120) in this context). In the case that $|\mathcal{X}| = 2$, this acceptance probability has the explicit form

$$\frac{1}{2} \left(1 + \left\| p\mathcal{N}^{0, (n)} - (1-p)\mathcal{N}^{1, (n)} \right\|_{\diamond_n} \right), \quad (219)$$

where this is the strategy norm.

Finally, we can generalize Algorithms 17 and 18, with the acceptance probabilities respectively given by

$$\inf_{\rho_A} \sup_{\{\Lambda_B^x\}_{x \in \mathcal{X}}} \sum_{x \in \mathcal{X}} p(x) \text{Tr}[\Lambda_B^x \mathcal{N}_{A \rightarrow B}^x(\rho_A)], \quad (220)$$

$$\sup_{\rho_A} \inf_{\{\Lambda_B^x\}_{x \in \mathcal{X}}} \sum_{x \in \mathcal{X}} p(x) \text{Tr}[\Lambda_B^x \mathcal{N}_{A \rightarrow B}^x(\rho_A)]. \quad (221)$$

In the case that $|\mathcal{X}| = 2$, these acceptance probabilities become

$$\frac{1}{2} \left(1 + \inf_{\rho_A} \left\| p \mathcal{N}_{A \rightarrow B}^0(\rho_A) - (1-p) \mathcal{N}_{A \rightarrow B}^1(\rho_A) \right\|_1 \right), \quad (222)$$

$$\frac{1}{2} \left(1 - \inf_{\rho_A} \left\| p \mathcal{N}_{A \rightarrow B}^0(\rho_A) - (1-p) \mathcal{N}_{A \rightarrow B}^1(\rho_A) \right\|_1 \right). \quad (223)$$

IV. PERFORMANCE EVALUATION OF ALGORITHMS USING A NOISELESS AND NOISY QUANTUM SIMULATOR

In this section, we present results obtained from numerically simulating Algorithms 4–7 and Algorithm 14 on a noiseless quantum simulator and Algorithms 8, 15, and 19 on both a noiseless and noisy quantum simulator. In the first subsection, we introduce and discuss the circuit ansatz employed in these numerical experiments. In the next subsection, we discuss the form of the states and channels used for the numerical simulations. In the following subsections, we present the details of our numerical simulations of Algorithms 4–7 for fidelity of states, Algorithm 8 for the fidelity of channels, Algorithm 14 for trace distance of states, Algorithm 15 for diamond distance of channels, and Algorithm 19 for multiple state discrimination.

A. Ansatz

To estimate the relevant quantities in this work, we employ the hardware-efficient ansatz (HEA) [KMT⁺17]. The HEA is a problem-agnostic ansatz that depends on the architecture and the connectivity of the given hardware. In this work, we consider a fixed structure of the HEA. Let X , Y , and Z denote the Pauli matrices. We define one layer of the HEA to consist of the single-qubit rotations $e^{-i\theta/2Y} e^{-i\delta/2X}$, each of which acts on a single qubit and is parameterized by θ and δ , followed by CNOTs between neighboring qubits. A CNOT between the control qubit k and the target qubit ℓ is given by

$$e^{-i\pi/2(1 \otimes |1\rangle\langle 1|_k \otimes (X_\ell - I_\ell))} = |0\rangle\langle 0|_k \otimes I_\ell + |1\rangle\langle 1|_k \otimes X_\ell. \quad (224)$$

For our numerical experiments, we consider a sufficiently large number of layers of the HEA. In principle, both the circuit structure and the number of layers of the HEA can be made random and this randomness can lead to better performance of variational algorithms [BCV⁺21]. We leave the study of such ansatzes for future work.

The HEA is used both to create the states and channels, and to create a parameterized unitary that replaces the prover. In the former two cases, the rotation angles are fixed, but in the prover scenario, the angles are optimized over.

B. Test states and channels

To study the performance of our algorithms, we randomly select states and channels as follows. For n -qubit states, we apply m layers of the HEA with randomly selected angles for rotation around the x - and y -axes on $n+k$ qubits initialized to $|0\rangle$. This procedure prepares a pure state on $n+k$ qubits and hence, a mixed state on n qubits of rank $\leq 2^k$.

To realize an n -qubit channel $\mathcal{N}_{A \rightarrow B}$, we generate a unitary $U_{AE' \rightarrow BE}$ on $n+k$ qubits such that

$$\mathcal{N}_{A \rightarrow B}(\omega_A) := \text{Tr}_E [U_{AE' \rightarrow BE}(\omega_A \otimes |0\rangle\langle 0|_{E'}) (U_{AE' \rightarrow BE})^\dagger], \quad (225)$$

where systems E' and E are of size k . Due the Stinespring dilation theorem [Sti55], this is a general approach by which arbitrary channels can be realized.

For our experiments, we set U to be m layers of the HEA itself, with randomly selected angles for rotation around the x - and y -axes on $n+1$ qubits. Tracing out one of the qubits gives a channel on n qubits, as required.

Multiple algorithms in our work (see (5), (24), (108)) depend on having access to unitaries of the form

$$\sum_{i \in \{0,1\}} |i\rangle\langle i|_T \otimes U_S^i = |0\rangle\langle 0| \otimes U_S^0 + |1\rangle\langle 1| \otimes U_S^1. \quad (226)$$

These can be split into sequential application of the following two controlled unitaries

$$\begin{aligned} &|0\rangle\langle 0| \otimes I + |1\rangle\langle 1| \otimes U_S^1, \\ &|1\rangle\langle 1| \otimes I + |0\rangle\langle 0| \otimes U_S^0, \end{aligned} \quad (227)$$

of which our algorithms make use.

C. Fidelity of states

In this section, we discuss the performance of Algorithms 4–7 in the noiseless scenario to estimate the fidelity between two three-qubit mixed states. Algorithms 4–7 require different numbers of qubits for estimating the fidelity between ρ and σ . In particular,

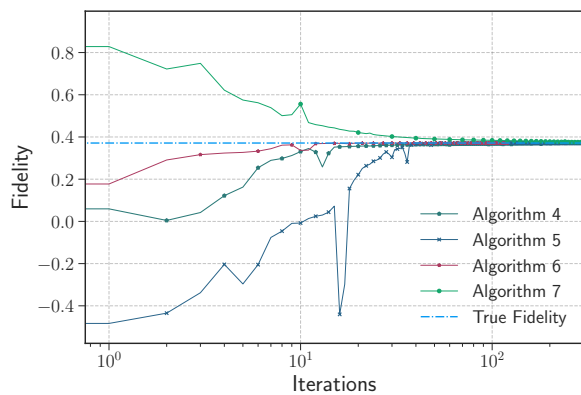


FIG. 12. Estimation of the fidelity between quantum states versus the number of iterations. We implement Algorithms 4–7 on a noiseless simulator to estimate the fidelity between two three-qubit mixed states, each of rank ≤ 4 . For each variational algorithm, we employ the HEA, as defined in Section IV A. In particular, we start with a random parameter vector $\vec{\theta}$ and then update it according to a gradient-based optimization procedure. The dashed-dotted curve represents the true fidelity between two randomly chosen quantum states. In each case, the optimization procedure converges to the true fidelity with high accuracy. Algorithms 4–7 achieve an absolute error in fidelity estimation of order 10^{-5} , 10^{-4} , 10^{-9} , and 10^{-3} , respectively.

Algorithm 4 requires eight qubits, along with access to controlled unitaries, as defined in (227). Algorithms 5, 6, and 7 require 13, 10, and 8 qubits, respectively. We recall that Algorithms 4–6 require purifications of both ρ and σ , while Algorithm 7 relies only on access to ρ and σ directly. Moreover, Algorithms 4 and 5 require measurements on two qubits, and Algorithm 6 requires Bell measurements on ten qubits. Finally, Algorithm 7 requires two single-qubit measurements.

We now summarize the HEA employed. For Algorithm 4, the prover unitary is created using five layers of the HEA, which acts on four qubits. Similarly, in Algorithm 5, we employ eight layers of the HEA that acts on six qubits. In Algorithm 6, the ansatz acts on two qubits, and we consider four layers of it. In Algorithm 7, the ansatz acts on four qubits, and we apply eight layers of it. For our implementations, we picked these circuit depths so that the cost function is minimized. A general framework is to allow the ansatz structure to be unfixed and instead variable, but we leave the detailed study of this for our algorithms to future work [BCV+21].

We begin the training with a random set of variational parameters. We evaluate the cost using a state vector simulator (noiseless simulator) [AAMA+21]. We then employ the gradient-descent algorithm to obtain a new set of parameters.¹ We note that in general, the true fidelity between states ρ and σ is not known. Thus the

stopping criterion for these algorithms is the number of iterations. For our numerical experiments, we set the total number of iterations to be 300. For each algorithm, we run ten instances of the algorithm and pick the best run for generating Figure 12.

In Figure 12, we plot the results of the numerical simulations. The dashed-dotted line represents the true fidelity between two random three-qubit quantum states ρ and σ , as described above. Each algorithm converges to the true fidelity with high accuracy within a finite number of iterations. As discussed above, for each algorithm, the HEA is of a different size. Thus, it is not straightforward to compare these different algorithms. In terms of the convergence rate, we find that Algorithm 6 converges to the true fidelity faster than all other algorithms. Algorithms 4–7 achieve an absolute error in fidelity estimation of order 10^{-5} , 10^{-4} , 10^{-9} , and 10^{-3} , respectively.

D. Trace distance of states

Using Algorithm 14, we estimate the normalized trace distance $\frac{1}{2}\|\rho - \sigma\|_1$ between two three-qubit states ρ and σ , each having rank ≤ 4 , as defined above in Section IV B. For our numerical experiments, we use a noiseless simulator. Algorithm 14 requires eight qubits in total and two single-qubit measurements. We employ ten layers of the HEA, which acts on four qubits. Similar to the fidelity-estimation algorithms detailed above, we begin with a random set of variational parameters and update them using the gradient-descent algorithm.

As the true normalized trace distance between ρ and σ is assumed to be unknown, we use a stopping criterion as the number of iterations, which we take to be 300 iterations. For Algorithm 14, we run ten instances of it and pick the best run for generating Figure 13.

In Figure 13, we plot the results of Algorithm 14. The dashed-dotted line represents the true normalized trace distance between two random three-qubit quantum states ρ and σ , as described above. The absolute error in trace-distance estimation is of order 10^{-4} .

E. Fidelity of channels

In this section, we discuss the performance of Algorithm 8 in both the noiseless and noisy scenarios. The channels in question are realized by using parameterized unitaries and tracing out ancilla qubits, as discussed in Section IV B. The algorithm employs a min-max optimization and thus requires two parameterized unitaries representing the min- and max-provers, respectively. The controlled unitaries consist of one layer of the HEA, with

¹ ArXiv ancillary files are available with the arXiv posting of our

paper. These contain all Python and Qiskit codes used to execute our simulations and generate the figures in our paper.

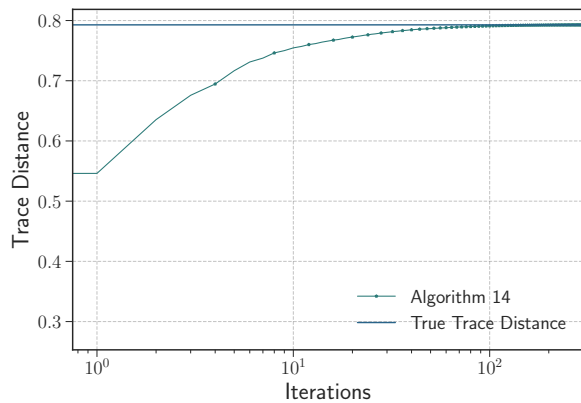


FIG. 13. Estimation of the normalized trace distance between quantum states versus the number of iterations. We implement Algorithm 14 on a noiseless simulator to estimate the normalized trace distance between three-qubit mixed states, each of rank four. Algorithm 14 achieves an absolute error in trace distance estimation of order 10^{-4} .

each consisting of random rotations about the x -axis, on two qubits, thereby realizing the $\mathcal{N}_{A \rightarrow B}^i$ channels acting on one qubit, for $i \in \{0, 1\}$.

We now summarize the HEA employed in generating the min- and max-provers. The min-prover unitary is generated using two layers of the HEA, which acts on two qubits. The max-prover unitary is generated using two layers of the HEA, which acts on three qubits. The rotation angles for both provers around the x - and y -axes are chosen at random. The particular choices of the number of layers are made so that the cost function is minimized.

We begin the training phase with a random set of variational parameters for both parameterized unitaries. For the noiseless simulation, we evaluate the cost using a state vector simulator (noiseless simulator) [AAMA⁺21]. For the noisy simulation, we use the qasm-simulator with the noise model from IBM-Jakarta. Since the number of parameters is significantly higher than the previous algorithms, to speed up the convergence, we employ both the simultaneous perturbation stochastic approximation (SPSA) method [Spa98] and the gradient descent method to obtain a new set of parameters.

The optimization is carried out in a zig-zag fashion, explained as follows. The minimizing optimizer implements the SPSA algorithm and is allowed to run until convergence occurs. Then, the maximizing optimizer, implementing the gradient descent algorithm, runs for one iteration. We note that in general, the true fidelity between the channels \mathcal{N}^0 and \mathcal{N}^1 is not known. Thus, the stopping criterion for these algorithms is the number of iterations. For our numerical experiments, we set the total number of iterations to be 6000, mostly used in the minimizing optimizer. The results of the numerical simulation are presented in Figure 14.

Note that the graph presented in Figure 14 shows that

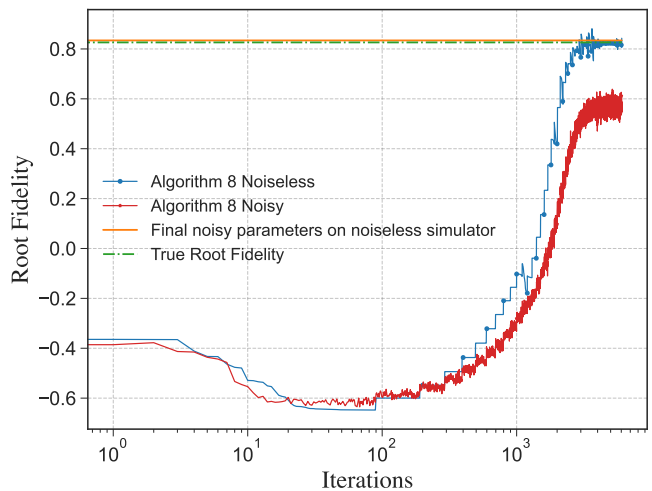


FIG. 14. Estimation of the normalized fidelity between quantum channels versus the number of iterations. We implement Algorithm 8 to estimate the normalized fidelity between two-qubit channels. The noiseless simulation achieves an absolute error in fidelity estimation of order 10^{-4} . The parameters obtained from the noisy simulation, with the noise model from IBM-Jakarta, achieve an absolute error of 10^{-2} on a noiseless simulator.

the convergence is highly non-monotonic, unlike the convergence behavior presented in previous graphs. Each iteration consists of a decrease in the function value, followed by a single increasing iteration. This is clearly indicative of the min-max optimization nature of the algorithm. Furthermore, unlike other algorithms, the optimization value in this algorithm can overshoot the true solution, due to the min-max nature of the optimization. However, the noiseless plot indicates that, once it overshoots the solution, it oscillates with decreasing amplitude and converges.

The noisy optimization converges as well, but it does not converge to the known value of the root fidelity of the two channels. However, the parameters found after convergence exhibit a noise resilience, as put forward in [SKCC20]; i.e., using the parameters obtained from the noisy optimization in a noiseless simulator gives a value much closer to the true value, as indicated by the solid orange line in Figure 14.

F. Diamond distance of channels

In this section, we discuss the performance of Algorithm 15 in the noiseless and noisy scenario. Algorithm 15 requires eight qubits. Similar to the previous section, the channels in question are realized using the procedure from Section IV B. The algorithm utilizes a max-max optimization and thus requires two parameterized unitaries representing the two max-provers. Each unitary $U_{AE' \rightarrow BE}^i$, for $i \in \{0, 1\}$, consists of one layer of the HEA with random rotations about the x - and y -

axes, on two qubits, each thereby realizing the one-qubit channel $\mathcal{N}_{A \rightarrow B}^i$.

We now summarize the HEA employed in generating the two provers. The first prover, called the state-prover because its goal is to realize an optimal distinguishing state, is generated using two layers of the HEA, which acts on two qubits. The second prover, called the max-prover, is generated using two layers of the HEA, which acts on three qubits. The rotation angles for both provers around the x - and y -axes are chosen at random. The particular choices of the number of layers are made so that the cost function is minimized.

We begin the training phase with a random set of variational parameters for both parameterized unitaries. In the noiseless simulation, we evaluate the cost using a state vector simulator (noiseless simulator). In the noisy setup, we use the qasm-simulator with the noise model from IBM-Jakarta. Similar to the previous section, we employ the SPSA optimization technique.

The optimization is carried out two parts—the first part uses the COBYLA optimizer [Pow94, VGO+20] (non-gradient based), and the second part uses the SPSA optimizer. In both stages, the optimization is carried out in a zig-zag fashion, explained as follows. The first stage allows for moving quickly into the neighbourhood of the actual solution, but then slows down dramatically. Once we approach the solution, we switch to a gradient based method that converges to the solution faster. In both stages, we allow the state-prover and the max-prover to be optimized for a fixed number of iterations in a zig-zag manner. This is because, in general, the true diamond distance between channels \mathcal{N}^0 and \mathcal{N}^1 is not known. Thus the stopping criterion for these algorithms is the number of iterations. For our numerical experiments, we set the total number of iterations to be 1600. The results of the numerical simulation are presented in Figure 15.

Note that the noiseless graph presented in Figure 15 shows that the convergence is highly monotonic, unlike the fidelity of channels (see Figure 14), because the optimization is a max-max one, as opposed to the min-max nature of Algorithm 8. The quick convergence, indicated by the lower number of iterations, is a consequence of this difference.

The noisy simulation converges as well, and similar to the previous section, the parameters exhibit a noise resilience. Once the COBYLA stage of the optimization is completed, the SPSA optimization is more noisy, due to the perturbative nature of the algorithm. Note that the COBYLA optimizer operates in batches of 30, giving an impression of smoothness.

G. Multiple state discrimination

In this section, we discuss the performance of Algorithm 19 in the noisy and noiseless scenarios. We consider a specific scenario of distinguishing three one-qubit

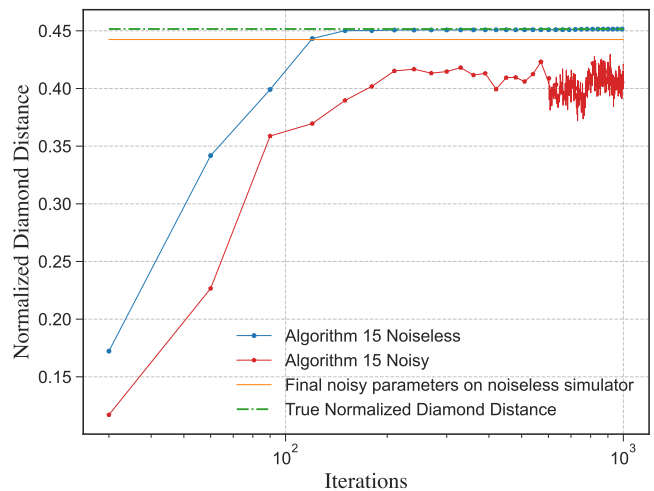


FIG. 15. Estimation of the normalized diamond distance between quantum channels versus the number of iterations. We implement Algorithm 15 to estimate the normalized diamond distance between one-qubit channels. Algorithm 15 achieves an absolute error in diamond distance estimation of order 10^{-4} . The parameters obtained from the noisy simulation, with the noise model from IBM-Jakarta, achieve an absolute error of 10^{-2} on a noiseless simulator.

mixed states. Recall from Section IV B that the one-qubit states are generated by using two layers of the HEA on two qubits. We execute this on a qubit system, and hence we use Algorithm 19. The algorithm requires twelve qubits in total and three two-qubit measurements. The measurement is realized using a parameterized unitary and ancilla qubits. By Naimark’s extension [Nai40], an arbitrary POVM can be realized using this procedure, so that there is no loss in expressiveness. The parameterized unitary required employs two layers of the HEA, which acts on three qubits.

To speed up convergence, we use the SPSA algorithm for the optimization. As the true value of the optimal acceptance probability between the three states is assumed to be unknown, we use a stopping criterion as the number of iterations, which we take to be 250 iterations.

In Figure 16, we plot the results of Algorithm 19. The dashed-dotted line represents the optimal acceptance probability of the three states, calculated using the SDP. The noiseless simulation converges to the known optimal acceptance probability. The noisy optimization converges as well, but it does not converge to the known optimal acceptance probability. However, similar to the previous sections, the parameters exhibit noise resilience, as indicated by the solid orange line in Figure 16.

V. GENERATING FIXED POINTS OF QUANTUM CHANNELS

In this section, we discuss how Algorithm 10 can generate a fixed-point state or an approximate fixed-point

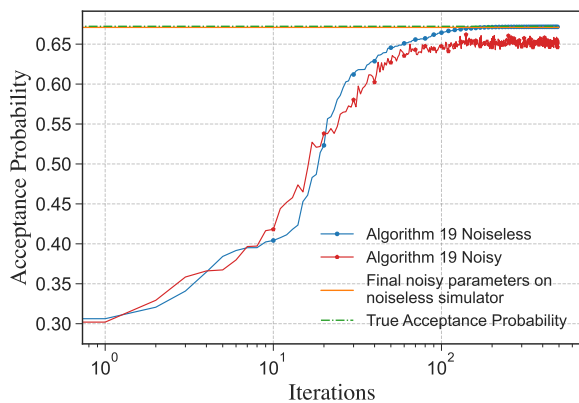


FIG. 16. Estimation of the optimal acceptance probability for Algorithm 19. The noiseless simulation achieves an absolute error of order 10^{-4} . The parameters obtained from the noisy simulation, with the noise model from IBM-Jakarta, achieve an absolute error of 10^{-3} on a noiseless simulator.

state of a quantum channel. There are various associated subtleties in such a scenario that we consider.

As a special case of Algorithm 10, we can select $\mathcal{N}_{A \rightarrow B}^0$ to be a channel \mathcal{N} with its output and input systems having the same dimension (i.e., $|A| = |B|$), and we can select the second channel $\mathcal{N}_{A \rightarrow B}^1$ to be the identity channel. In this case, the quantity in (138) is always equal to one. This follows from the well known fact that every quantum channel with matching input and output systems has a fixed point state [EHK78] (see also [Deu91, Wol12]) and because the prover's goal is to maximize the acceptance probability. That is, for every such channel \mathcal{N} , there exists a state ρ such that

$$\mathcal{N}(\rho) = \rho, \quad (228)$$

and so the prover can simply send this state. Related to this, there is a faithfulness property that holds. If the acceptance probability is equal to one, then it follows that

$$\sup_{\rho} F(\mathcal{N}(\rho), \rho) = 1, \quad (229)$$

and we conclude that there exists a state ρ satisfying (228) because the fidelity is continuous and the set of density operators is convex and compact.

What is interesting in this case is that Algorithm 10 outputs a fixed point of the channel \mathcal{N} . Fixed points of quantum channels are important not only for understanding thermalization in a physical process [BCL⁺21] (a fixed point can be understood as an equilibrium state of the channel) but also in the Deutschian theory of closed timelike curves [Deu91].

We can also modify this approach slightly and employ Algorithm 13. In this case, the verifier can employ the following ensemble of channels

$$\left\{ \frac{1}{L}, \mathcal{N}^\ell \right\}_{\ell=0}^{L-1}, \quad (230)$$

where \mathcal{N}^ℓ here is defined as

$$\mathcal{N}^\ell = \underbrace{\mathcal{N} \circ \dots \circ \mathcal{N}}_{\ell \text{ times}}. \quad (231)$$

In this case, the acceptance probability of Algorithm 13 is given by

$$\left[\frac{1}{L} \sup_{\rho, \sigma} \sum_{\ell=0}^{L-1} \sqrt{F(\mathcal{N}^\ell(\rho), \sigma)} \right]^2. \quad (232)$$

This is again equal to one because the prover can transmit a fixed point to the verifier, which satisfies

$$\mathcal{N}^\ell(\rho) = \rho \quad \forall \ell \in \{0, \dots, L-1\}. \quad (233)$$

Similarly, in this case, a faithfulness property holds as well. If the expression in (232) is equal to one, then there exists a state ρ satisfying (233). Furthermore, Algorithm 13 outputs a fixed point satisfying (232).

The cases outlined above are simple. The situation becomes more subtle when the verifier tries to use the state sent by the prover to solve a computational problem, as is the case in quantum computation in the presence of Deutschian closed timelike curves [AW09]. In this case, there are different goals, which are 1) to pass the test of the verifier in Algorithm 13, as well as 2) to have the decision qubit be as close as possible to the $|1\rangle\langle 1|$ state. In this case, the prover need not send an exact fixed point, but only send an approximate fixed point, satisfying

$$F(\rho, \mathcal{N}(\rho)) \geq 1 - \varepsilon, \quad (234)$$

or

$$\left[\frac{1}{L} \sup_{\sigma} \sum_{\ell=0}^{L-1} \sqrt{F(\mathcal{N}^\ell(\rho), \sigma)} \right]^2 \geq 1 - \varepsilon, \quad (235)$$

where $\varepsilon \in (0, 1)$. The prover can do this to optimize the overall acceptance probability of the QIP algorithm. Somewhat counter-intuitively, approximate fixed points need not be close to exact fixed points, as illustrated by the following example. Suppose that \mathcal{N} is a classical channel that takes $1 \rightarrow 1$ deterministically, but then takes $0 \rightarrow 0$ with probability $1 - \varepsilon$ and $0 \rightarrow 1$ with probability ε . In this case, 1 is the exact fixed point of this stochastic process, but 0 is an approximate fixed point satisfying (234). However, 0 is completely distinguishable from 1 (the fidelity of these two classical states is equal to zero).

In Appendix A, we discuss various issues related to fixed points and approximate fixed points of quantum channels when attempting to understand quantum interactive proofs and the computational complexity of Deutschian closed timelike curves.

VI. CONCLUSION

In this paper, we have delineated several algorithms for estimating distinguishability measures on quantum computers. All of the measures are based on trace distance or

fidelity, and we have considered them for quantum states, channels, and strategies. Many of the algorithms rely on interaction with a quantum prover, and in these cases, we have replaced the prover with a parameterized quantum circuit. As such, these methods are not guaranteed to converge for all possible states, channels, and strategies. It is an interesting open question to determine conditions under which the algorithms are guaranteed to converge and run efficiently.

We have also simulated several of the algorithms in both the noiseless and noisy scenarios. We found that the simulations converge well for all states and channels considered, and for all algorithms simulated. As more advanced quantum computers become available (with more qubits and greater reliability), it would be interesting to simulate our algorithms for states and channels involving larger numbers of qubits. All of our Python code is written in a modular way, such that it will be straightforward to explore this direction.

Going forward from here, it remains open to determine methods for estimating other distinguishability measures such as the Petz–Rényi relative entropy [Pet85, Pet86] and the sandwiched Rényi relative entropy [MLDS⁺13, WWY14] of channels [LKDW18] and strategies [WW19]. More generally, one could consider distinguishability measures beyond these. One desirable aspect of the algorithms appearing in this paper is that they provide a one-shot interpretation for the various distinguishabil-

ity measures as the maximum acceptance probability in a quantum interactive proof (with the trace-distance based algorithms and interpretations being already known from [Wat02, RW05, GW07, Gut09, Gut12]). However, it is unclear to us whether one could construct a quantum interactive proof for which the maximum acceptance probability is related to the Petz– or sandwiched Rényi relative entropy of a channel or a strategy.

Note added: While finalizing the results of our initial arXiv post [ARSW21], we noticed the arXiv post [BBC21], which is related to the contents of Section III. Ref. [BBC21] is now published as [BBC22].

ACKNOWLEDGMENTS

We acknowledge insightful discussions with Todd Brun, Patrick Coles, Zoe Holmes, Margarite LaBorde, Dhrumil Patel, and Aliza Siddiqui. We thank Robert Salzmann and John Watrous for discussions related to fixed points and thank JW for reminding us of the example after (235). We also thank him and Scott Aaronson for discussions related to Deutschian CTCs. SR and MMW acknowledge support from the National Science Foundation under Grant No. 1907615. KS acknowledges support from the Department of Defense.

-
- [AAMA⁺21] M. D. Sajid Anis, Abby-Mitchell, Héctor Abraham, AduOffei, Rochisha Agarwal, et al. Qiskit: An open-source framework for quantum computing, 2021.
- [Aar05] Scott Aaronson. NP-complete problems and physical reality. *ACM SIGACT News*, 36(1):30–52, March 2005. arXiv:quant-ph/0502072.
- [AJL06] Dorit Aharonov, Vaughan Jones, and Zeph Landau. A polynomial quantum algorithm for approximating the jones polynomial. In *Proceedings of the thirty-eighth annual ACM symposium on Theory of computing*, pages 427–436. ACM, 2006. arXiv:quant-ph/0511096.
- [AOST17] Jayadev Acharya, Alon Orlitsky, Ananda Theertha Suresh, and Himanshu Tyagi. Estimating renyi entropy of discrete distributions. *IEEE Transactions on Information Theory*, 63(1):38–56, January 2017. arXiv:1408.1000.
- [ARSW21] Rochisha Agarwal, Soorya Rethinasamy, Kunal Sharma, and Mark M. Wilde. Estimating distinguishability measures on quantum computers. August 2021. arXiv:2108.08406v1.
- [AW09] Scott Aaronson and John Watrous. Closed timelike curves make quantum and classical computing equivalent. *Proceedings of the Royal Society A: Mathematical, Physical and Engineering Sciences*, 465(2102):631–647, February 2009. arXiv:0808.2669.
- [BBC21] Paolo Braccia, Leonardo Banchi, and Filippo Caruso. Quantum noise sensing by generating fake noise. July 2021. arXiv:2107.08718v1.
- [BBC22] Paolo Braccia, Leonardo Banchi, and Filippo Caruso. Quantum noise sensing by generating fake noise. *Physical Review Applied*, 17:024002, February 2022.
- [BCL⁺21] Ivan Bardet, Angela Capel, Angelo Lucia, David Pérez-García, and Cambyse Rouzé. On the modified logarithmic Sobolev inequality for the heat-bath dynamics for 1D systems. August 2021. arXiv:1908.09004.
- [BCLK⁺21] Kishor Bharti, Alba Cervera-Lierta, Thi Ha Kyaw, Tobias Haug, Sumner Alperin-Lea, Abhinav Anand, Matthias Degroote, Hermann Heimonen, Jakob S. Kottmann, Tim Menke, Wai-Keong Mok, Sukin Sim, Leong-Chuan Kwek, and Alán Aspuru-Guzik. Noisy intermediate-scale quantum (NISQ) algorithms. January 2021. arXiv:2101.08448.
- [BCV⁺21] M. Bilkis, M. Cerezo, Guillaume Verdon, Patrick J. Coles, and Lukasz Cincio. A semi-agnostic ansatz with variable structure for quantum machine learning. March 2021. arXiv:2103.06712.
- [BCWdW01] Harry Buhrman, Richard Cleve, John Watrous, and Ronald de Wolf. Quantum fingerprinting. *Physical Review Letters*, 87(16):167902, September 2001. arXiv:quant-ph/0102001.
- [BDW18] Stefan Bäuml, Siddhartha Das, and Mark M. Wilde. Fundamental limits on the capacities of bipartite quantum interactions. *Physical Review Letters*, 121(25):250504, December 2018. arXiv:1812.08223.
- [BHW09] Todd A. Brun, Jim Harrington, and Mark M. Wilde. Localized closed timelike curves can perfectly distinguish quantum states. *Physical Review Letters*, 102(21):210402, May 2009. arXiv:0811.1209.

- [Bru04] Todd A. Brun. Measuring polynomial functions of states. *Quantum Information and Computation*, 4(5):401–408, September 2004. arXiv:quant-ph/0401067.
- [BWW13] Todd A. Brun, Mark M. Wilde, and Andreas Winter. Quantum state cloning using Deutschian closed time-like curves. *Physical Review Letters*, 111(19):190401, November 2013. arXiv:1306.1795.
- [CAB⁺20] M. Cerezo, Andrew Arrasmith, Ryan Babbush, Simon C. Benjamin, Suguru Endo, Keisuke Fujii, Jarrod R. McClean, Kosuke Mitarai, Xiao Yuan, Lukasz Cincio, and Patrick J. Coles. Variational quantum algorithms. December 2020. arXiv:2012.09265.
- [CDP08] Giulio Chiribella, Giacomo Mauro D’Ariano, and Paolo Perinotti. Memory effects in quantum channel discrimination. *Physical Review Letters*, 101(18):180501, October 2008. arXiv:0803.3237.
- [CDP09] Giulio Chiribella, Giacomo Mauro D’Ariano, and Paolo Perinotti. Theoretical framework for quantum networks. *Physical Review A*, 80(2):022339, August 2009. arXiv:0904.4483.
- [CHM⁺16] Tom Cooney, Christoph Hirche, Ciara Morgan, Jonathan P. Olson, Kaushik P. Seshadreesan, John Watrous, and Mark M. Wilde. Operational meaning of quantum measures of recovery. *Physical Review A*, 94(2):022310, August 2016. arXiv:1512.05324.
- [CPCC20] M. Cerezo, Alexander Poremba, Lukasz Cincio, and Patrick J. Coles. Variational quantum fidelity estimation. *Quantum*, 4:248, March 2020. arXiv:1906.09253.
- [CSZW20] Ranyiliu Chen, Zhixin Song, Xuanqiang Zhao, and Xin Wang. Variational quantum algorithms for trace distance and fidelity estimation. December 2020. arXiv:2012.05768.
- [DBW20] Siddhartha Das, Stefan Bäuml, and Mark M. Wilde. Entanglement and secret-key-agreement capacities of bipartite quantum interactions and read-only memory devices. *Physical Review A*, 101(1):012344, January 2020. arXiv:1712.00827.
- [Deu91] David Deutsch. Quantum mechanics near closed timelike lines. *Physical Review D*, 44(10):3197–3217, November 1991.
- [EHK78] David E. Evans and Raphael Høegh-Krohn. Spectral properties of positive maps on C^* -algebras. *Journal of the London Mathematical Society*, s2-17(2):345–355, April 1978.
- [FC95] Christopher A. Fuchs and Carlton M. Caves. Mathematical techniques for quantum communication theory. *Open Systems & Information Dynamics*, 3(3):345–356, 1995. arXiv:quant-ph/9604001.
- [Fuc96] Christopher Fuchs. *Distinguishability and Accessible Information in Quantum Theory*. PhD thesis, University of New Mexico, December 1996. arXiv:quant-ph/9601020.
- [FvdG99] Christopher A. Fuchs and Jeroen van de Graaf. Cryptographic distinguishability measures for quantum-mechanical states. *IEEE Transactions on Information Theory*, 45(4):1216, May 1999. arXiv:quant-ph/9712042.
- [GEC13] Juan Carlos Garcia-Escartin and Pedro Chamorro-Posada. SWAP test and Hong-Ou-Mandel effect are equivalent. *Physical Review A*, 87(5):052330, May 2013. arXiv:1303.6814.
- [GHMW15] Gus Gutoski, Patrick Hayden, Kevin Milner, and Mark M. Wilde. Quantum interactive proofs and the complexity of separability testing. *Theory of Computing*, 11(3):59–103, March 2015. arXiv:1308.5788.
- [GLN05] Alexei Gilchrist, Nathan K. Langford, and Michael A. Nielsen. Distance measures to compare real and ideal quantum processes. *Physical Review A*, 71(6):062310, June 2005. arXiv:quant-ph/0408063.
- [GRS18] Gus Gutoski, Ansis Rosmanis, and Jamie Sikora. Fidelity of quantum strategies with applications to cryptography. *Quantum*, 2:89, September 2018. arXiv:1704.04033.
- [Gut05] Gus Gutoski. Short quantum games. Master’s thesis, University of Calgary, September 2005. arXiv:quant-ph/0604183.
- [Gut09] Gus Gutoski. *Quantum strategies and local operations*. PhD thesis, University of Waterloo, 2009. arXiv:1003.0038.
- [Gut12] Gus Gutoski. On a measure of distance for quantum strategies. *Journal of Mathematical Physics*, 53(3):032202, March 2012. arXiv:1008.4636.
- [GW05] Gus Gutoski and John Watrous. Quantum interactive proofs with competing provers. In *Proceedings of the 22nd Symposium on Theoretical Aspects of Computer Science (STACS 2005)*, volume 3404 of *Lecture Notes in Computer Science*, pages 605–616, Stuttgart, Germany, February 2005. arXiv:cs/0412102.
- [GW07] Gus Gutoski and John Watrous. Toward a general theory of quantum games. In *Proceedings of 39th ACM Symposium on the Theory of Computing*, pages 565–574, June 2007. arXiv:quant-ph/0611234.
- [GW13] Gus Gutoski and Xiaodi Wu. Parallel approximation of min-max problems. *Computational Complexity*, 22(2):385–428, June 2013. arXiv:1011.2787.
- [Hel67] Carl W. Helstrom. Detection theory and quantum mechanics. *Information and Control*, 10(3):254–291, 1967.
- [Hel69] Carl W. Helstrom. Quantum detection and estimation theory. *Journal of Statistical Physics*, 1:231–252, 1969.
- [HHL09] Aram W. Harrow, Avinatan Hassidim, and Seth Lloyd. Quantum algorithm for linear systems of equations. *Physical Review Letters*, 103(15):150502, October 2009. arXiv:0811.3171.
- [HMW13] Patrick Hayden, Kevin Milner, and Mark M. Wilde. Two-message quantum interactive proofs and the quantum separability problem. In *Proceedings of the 18th Annual IEEE Conference on Computational Complexity*, pages 156–167, Palo Alto, California, USA, June 2013.
- [HMW14] Patrick Hayden, Kevin Milner, and Mark M. Wilde. Two-message quantum interactive proofs and the quantum separability problem. *Quantum Information and Computation*, 14(5 & 6):384–416, April 2014. arXiv:1211.6120.
- [Hoe63] Wassily Hoeffding. Probability inequalities for sums of bounded random variables. *Journal of the American Statistical Association*, 58(301):13–30, March 1963.
- [Hol72] Alexander S. Holevo. An analog of the theory of statistical decisions in noncommutative theory of probability. *Trudy Moskovskogo Matematicheskogo Obshchestva*, 26:133–149, 1972. English translation: *Trans. Moscow Math Soc.* 26, 133–149 (1972).
- [JJUW11] Rahul Jain, Zhengfeng Ji, Sarvagya Upadhyay, and John Watrous. QIP = PSPACE. *Journal of the ACM*, 58(6):1–27, December 2011. arXiv:0907.4737.
- [JVHW15] Jiantao Jiao, Kartik Venkat, Yanjun Han, and Tsachy Weissman. Minimax estimation of functionals of discrete distributions. *IEEE Transactions*

- on *Information Theory*, 61(5):2835–2885, May 2015. arXiv:1406.6956.
- [JW07] Dominik Janzing and Pawel Wocjan. A simple PromiseBQP-complete matrix problem. *Theory of Computing*, 3(1):61–79, 2007.
- [Kit97] Alexei Kitaev. Quantum computations: algorithms and error correction. *Russian Mathematical Surveys*, 52(6):1191–1249, 1997.
- [KL01] Emanuel Knill and Raymond Laflamme. Quantum computing and quadratically signed weight enumerators. *Information Processing Letters*, 79(4):173–179, August 2001. arXiv:quant-ph/9909094.
- [KMT⁺17] Abhinav Kandala, Antonio Mezzacapo, Kristan Temme, Maika Takita, Markus Brink, Jerry M. Chow, and Jay M. Gambetta. Hardware-efficient variational quantum eigensolver for small molecules and quantum magnets. *Nature*, 549(7671):242–246, 2017. arXiv:1704.05018.
- [KRS09] Robert Koenig, Renato Renner, and Christian Schaffner. The operational meaning of min- and max-entropy. *IEEE Transactions on Information Theory*, 55(9):4337–4347, September 2009. arXiv:0807.1338.
- [KW00] Alexei Kitaev and John Watrous. Parallelization, amplification, and exponential time simulation of quantum interactive proof systems. In *Proceedings of the 32nd ACM Symposium on Theory of Computing*, pages 608–617, May 2000.
- [KW20a] Vishal Katariya and Mark M. Wilde. Evaluating the advantage of adaptive strategies for quantum channel distinguishability. January 2020. arXiv:2001.05376.
- [KW20b] Sumeet Khatri and Mark M. Wilde. *Principles of Quantum Communication Theory: A Modern Approach*. November 2020. arXiv:2011.04672v1.
- [KW21] Vishal Katariya and Mark M. Wilde. Geometric distinguishability measures limit quantum channel estimation and discrimination. *Quantum Information Processing*, 20:78, April 2021. arXiv:2004.10708.
- [LKDW18] Felix Leditzky, Eneet Kaur, Nilanjana Datta, and Mark M. Wilde. Approaches for approximate additivity of the Holevo information of quantum channels. *Physical Review A*, 97(1):012332, January 2018. arXiv:1709.01111.
- [LLB18] Sang Min Lee, Jinhyoung Lee, and Jeongho Bang. Learning unknown pure quantum states. *Physical Review A*, 98(5):052302, Nov 2018. arXiv:1805.06580.
- [LLSL21] Sheng-Jie Li, Jin-Min Liang, Shu-Qian Shen, and Ming Li. Variational quantum algorithms for trace norms and their applications. *Communications in Theoretical Physics*, 2021. Accepted manuscript.
- [MLDS⁺13] Martin Müller-Lennert, Frédéric Dupuis, Oleg Szehr, Serge Fehr, and Marco Tomamichel. On quantum Rényi entropies: a new generalization and some properties. *Journal of Mathematical Physics*, 54(12):122203, December 2013. arXiv:1306.3142.
- [Mon08] Ashley Montanaro. A lower bound on the probability of error in quantum state discrimination. In *2008 IEEE Information Theory Workshop*, pages 378–380, 2008.
- [Nai40] Mark Aronovich Naimark. Spectral functions of a symmetric operator. *Izv. Akad. Nauk SSSR Ser. Mat.*, 4(3):277–318, 1940.
- [Pet85] Dénes Petz. Quasi-entropies for states of a von Neumann algebra. *Publ. RIMS, Kyoto University*, 21:787–800, 1985.
- [Pet86] Dénes Petz. Quasi-entropies for finite quantum systems. *Reports in Mathematical Physics*, 23:57–65, 1986.
- [Pow94] M. J. D. Powell. *A Direct Search Optimization Method That Models the Objective and Constraint Functions by Linear Interpolation*, pages 51–67. Springer Netherlands, Dordrecht, 1994.
- [PRM13] Jacques L. Pienaar, Timothy C. Ralph, and Casey R. Myers. Open timelike curves violate Heisenberg’s uncertainty principle. *Physical Review Letters*, 110(6):060501, February 2013. arXiv:1206.5485.
- [Qiu08] Daowen Qiu. Minimum-error discrimination between mixed quantum states. *Physical Review A*, 77(1):012328, January 2008. arXiv:0707.3970.
- [Ros09] Bill Rosgen. *Computational Distinguishability of Quantum Channels*. PhD thesis, University of Waterloo, September, 2009. arXiv:0909.3930.
- [RW05] Bill Rosgen and John Watrous. On the hardness of distinguishing mixed-state quantum computations. *Proceedings of the 20th IEEE Conference on Computational Complexity*, pages 344–354, June 2005. arXiv:cs/0407056.
- [SCC19] Yigit Subasi, Lukasz Cincio, and Patrick J Coles. Entanglement spectroscopy with a depth-two quantum circuit. *Journal of Physics A: Mathematical and Theoretical*, 52(4):044001, January 2019. arXiv:1806.08863.
- [SDG⁺21] Robert Salzmann, Nilanjana Datta, Gilad Gour, Xin Wang, and Mark M. Wilde. Symmetric distinguishability as a quantum resource. *New Journal of Physics*, 23:083016, August 2021. arXiv:2102.12512.
- [Sio58] Maurice Sion. On general minimax theorems. *Pacific Journal of Mathematics*, 8(1):171–176, March 1958.
- [SKCC20] Kunal Sharma, Sumeet Khatri, M Cerezo, and Patrick J Coles. Noise resilience of variational quantum compiling. *New Journal of Physics*, 22(4):043006, apr 2020.
- [Spa98] James C. Spall. An overview of the simultaneous perturbation method for efficient optimization, 1998.
- [Sti55] W. F. Stinespring. Positive functions on C^* -algebras. *Proceedings of the American Mathematical Society*, 6:211–216, 1955.
- [SW12] Naresh Sharma and Naqeeb Ahmad Warsi. On the strong converses for the quantum channel capacity theorems. May 2012. arXiv:1205.1712.
- [SW15] Kaushik P. Seshadreesan and Mark M. Wilde. Fidelity of recovery, squashed entanglement, and measurement recoverability. *Physical Review A*, 92(4):042321, October 2015. arXiv:1410.1441.
- [TV21] Kok Chuan Tan and Tyler Volkoff. Variational quantum algorithms to estimate rank, quantum entropies, fidelity and Fisher information via purity minimization. March 2021. arXiv:2103.15956.
- [Uhl76] Armin Uhlmann. The “transition probability” in the state space of a C^* -algebra. *Reports on Mathematical Physics*, 9(2):273–279, April 1976.
- [VGO⁺20] Pauli Virtanen, Ralf Gommers, Travis E. Oliphant, Matt Haberland, et al. SciPy 1.0: Fundamental Algorithms for Scientific Computing in Python. *Nature Methods*, 17:261–272, 2020.
- [VW16] Thomas Vidick and John Watrous. Quantum proofs. *Foundations and Trends in Theoretical Computer Science*, 11(1–2):1–215, March 2016. arXiv:1610.01664.
- [Wat02] John Watrous. Limits on the power of quantum statistical zero-knowledge. *Proceedings of the 43rd Annual IEEE Symposium on Foundations of Computer Science*, pages 459–468, November 2002. arXiv:quant-

- ph/0202111.
- [Wat09a] John Watrous. Quantum computational complexity. *Encyclopedia of Complexity and System Science*, 2009. arXiv:0804.3401.
- [Wat09b] John Watrous. Semidefinite programs for completely bounded norms. *Theory of Computing*, 5(11):217–238, November 2009. arXiv:0901.4709.
- [Wat09c] John Watrous. Zero-knowledge against quantum attacks. *SIAM Journal on Computing*, 39(1):25–58, 2009. arXiv:quant-ph/0511020.
- [Wat13] John Watrous. Simpler semidefinite programs for completely bounded norms. *Chicago Journal of Theoretical Computer Science*, 2013(8):1–19, July 2013. arXiv:1207.5726.
- [Wat18] John Watrous. *The Theory of Quantum Information*. Cambridge University Press, 2018.
- [Wil17] Mark M. Wilde. *Quantum Information Theory*. Cambridge University Press, second edition, 2017.
- [Wil20] Mark M. Wilde. Coherent quantum channel discrimination. In *Proceedings of the 2020 IEEE International Symposium on Information Theory (ISIT)*, pages 1915–1920, June 2020. arXiv:2001.02668.
- [Wol12] Michael M. Wolf. Quantum channels & operations: Guided tour. Lecture notes available at <http://www-m5.ma.tum.de/foswiki/pub/M5/Allgemeines/MichaelWolf/QChannelLecture.pdf>, July 2012.
- [WW19] Xin Wang and Mark M. Wilde. Resource theory of asymmetric distinguishability for quantum channels. *Physical Review Research*, 1(3):033169, December 2019. arXiv:1907.06306.
- [WWY14] Mark M. Wilde, Andreas Winter, and Dong Yang. Strong converse for the classical capacity of entanglement-breaking and Hadamard channels via a sandwiched Rényi relative entropy. *Communications in Mathematical Physics*, 331(2):593–622, October 2014. arXiv:1306.1586.
- [WZC⁺21] Qisheng Wang, Zhicheng Zhang, Kean Chen, Ji Guan, Wang Fang, and Mingsheng Ying. Quantum algorithm for fidelity estimation. March 2021. arXiv:2103.09076.
- [YAT⁺15] Xiao Yuan, Syed M Assad, Jayne Thompson, Jing Yan Haw, Vlatko Vedral, Timothy C Ralph, Ping Koy Lam, Christian Weedbrook, and Mile Gu. Replicating the benefits of Deutschian closed timelike curves without breaking causality. *npj Quantum Information*, 1(1):15007, November 2015. arXiv:1412.5596.
- [YF17] Haidong Yuan and Chi-Hang Fred Fung. Fidelity and Fisher information on quantum channels. *New Journal of Physics*, 19(11):113039, November 2017. arXiv:1506.00819.
- [Zha11] Fuzhen Zhang. *Matrix Theory: Basic Results and Techniques*. Springer, 2011.
- [Zha12] Shengyu Zhang. *BQP-Complete Problems*, pages 1545–1571. Springer Berlin Heidelberg, Berlin, Heidelberg, 2012.

Appendix A: Approximate fixed points and Deutschian closed timelike curves

The computational complexity of computation assisted by Deutschian closed timelike curves (CTCs) was solved

in [AW09], in which these authors showed that the power of classical and quantum computing are equivalent and equal to PSPACE, which is the class of decision problems solvable with polynomial memory. Let us briefly review these results. In the Deutschian model of CTCs [Deu91], we suppose that chronology-respecting qubits in a state ρ can interact with chronology-violating qubits in a state σ according to a unitary transformation U . Let S denote the quantum system for the chronology-respecting qubits, and let C denote the quantum system for the chronology-violating qubits. Then the output state of the transformation is as follows:

$$\text{Tr}_C[U_{SC}(\rho_S \otimes \sigma_C)U_{SC}^\dagger]. \quad (\text{A1})$$

In an effort to avoid grandfather and unproved theorem paradoxes, Deutsch postulates that nature imposes the following self-consistency condition on the state of the CTC qubits:

$$\sigma_C = \text{Tr}_S[U_{SC}(\rho_S \otimes \sigma_C)U_{SC}^\dagger]. \quad (\text{A2})$$

At a first glance, this condition might seem innocuous, but its implications for quantum information processing are dramatic, essentially due to the fact that (A2) allows for non-linear evolutions, which are disallowed in standard quantum mechanics. Indeed, quantum processors assisted by Deutschian CTCs can violate the uncertainty principle [BHW09, PRM13], can break the no-cloning theorem [BWW13, YAT⁺15], and can solve computational problems believed to be difficult [AW09].

The connection of Deutschian CTCs (D-CTCs) with fixed points of channels is that the condition in (A2) demands that the state of the CTC system be a fixed point of the quantum channel $\mathcal{N}_{U,\rho}$:

$$\omega_C \rightarrow \mathcal{N}_{U,\rho}(\omega_C) := \text{Tr}_S[U_{SC}(\rho_S \otimes \omega_C)U_{SC}^\dagger]. \quad (\text{A3})$$

Thus, this is how Section V connects with Deutschian CTCs.

The class of computational problems efficiently decidable by a quantum computer assisted by D-CTCs is called BQP_{CTC} , and it is formally defined as follows. Set $\delta \in (0, 1/2)$. Let G be a universal set of quantum gates. A quantum D-CTC algorithm is a deterministic polynomial time algorithm that takes as input a string $x \in \{0, 1\}^n$ and produces an encoding of a unitary quantum circuit U using gates from G . This unitary acts on two systems of qubits, called S and C as discussed above, which consist of $p(n)$ and $q(n)$ qubits, respectively, where $p(n)$ and $q(n)$ are polynomials. The system S is initialized to the all-zeros state $|0\rangle\langle 0|_S^{\otimes p(n)}$, and the system C is initialized to a state σ_C satisfying the causal self-consistency condition in (A2) with $\rho_S = |0\rangle\langle 0|_S^{\otimes p(n)}$. That is, σ_C is such that

$$\mathcal{N}_{U,|0\rangle\langle 0|_S^{\otimes p(n)}}(\sigma_C) = \sigma_C. \quad (\text{A4})$$

Let \mathcal{M} be a measurement of the last qubit of S in the computational basis. The algorithm accepts the input x

if

$$\mathcal{M}(\text{Tr}_C[U_{SC}(|0\rangle\langle 0|_S^{\otimes p(n)} \otimes \sigma_C)U_{SC}^\dagger]) \quad (\text{A5})$$

results in the output 1 with probability at least $1 - \delta$ for every state σ_C satisfying (A2). The algorithm rejects if (A5) results in output 1 with probability no larger than δ for every state σ_C satisfying (A2). The algorithm decides the promise problem $A = A_{\text{yes}} \cup A_{\text{no}} \subseteq \{0, 1\}^*$ (where $A_{\text{yes}} \cap A_{\text{no}} = \emptyset$) if the algorithm accepts every input $x \in A_{\text{yes}}$ and rejects every input $x \in A_{\text{no}}$. BQP_{CTC} is the class of all promise problems that are decided by some quantum D-CTC algorithm.

It is already known from [AW09] that $\text{BQP}_{\text{CTC}} = \text{PSPACE}$, and it is also known that $\text{QIP} = \text{PSPACE}$ [JJUW11]. Thus, it immediately follows from these results that $\text{BQP}_{\text{CTC}} = \text{QIP}$. Here, we discuss an attempt at a direct proof that $\text{BQP}_{\text{CTC}} \subseteq \text{QIP}$, which ideally would be arguably simpler to see than by examining the proofs of the equalities $\text{BQP}_{\text{CTC}} = \text{PSPACE}$ and $\text{QIP} = \text{PSPACE}$ individually. However, there are some difficulties in establishing this direct proof. We note here that this is related to an open question posed in [Aar05, Section 8], the spirit of which is to find a direct proof of the containment $\text{BQP}_{\text{CTC}} \subseteq \text{QIP}$.

Consider the following purported algorithm for simulating BQP_{CTC} in QIP:

Algorithm 20 *The algorithm proceeds as follows:*

1. *The verifier prepares a state*

$$|\Phi\rangle_{T'T} := \sum_{\ell=0}^{L-1} \sqrt{\frac{1}{L}} |\ell\rangle_{T'T} \quad (\text{A6})$$

on registers T' and T and prepares system S^L in the all-zeros state $|0\rangle_{S^L}$.

2. *The prover transmits the system C of the state $|\psi\rangle_{RC}$ to the verifier.*

3. *Using the circuit U_{SC} , the verifier performs the following controlled unitary:*

$$\sum_{\ell=0}^{L-1} |\ell\rangle\langle \ell|_T \otimes U_{S_1^L C}^\ell, \quad (\text{A7})$$

where

$$U_{S_1^L C}^\ell := \underbrace{(U_{S_\ell C \rightarrow S_\ell C} \circ \cdots \circ U_{S_1 C \rightarrow S_1 C})}_{\ell \text{ times}} \quad (\text{A8})$$

4. *The verifier transmits systems T' and S^L to the max-prover.*

5. *The prover prepares a system F in the $|0\rangle_F$ state and acts on systems T' , S^L , and F with a unitary $P_{T', S^L F \rightarrow T'' F'}$ to produce the output systems T'' and F' , where T'' is a qudit system.*

6. *The prover sends system T'' to the verifier, who then performs a qudit Bell measurement*

$$\{\Phi_{T''T}, I_{T''T} - \Phi_{T''T}\} \quad (\text{A9})$$

on systems T'' and T , where $\Phi_{T''T}$ is defined in (154). The verifier then initializes a system S_{L+1} to the all-zeros state $|0\rangle_{S_{L+1}}$, performs the unitary $U_{S_{L+1}C}$, and measures the decision qubit of system S_{L+1} . The verifier accepts if and only if the outcome $\Phi_{T''T}$ occurs and the decision qubit is measured to be in the $|1\rangle$ state.

Proposition 2 *The acceptance probability of Algorithm 20 is equal to*

$$\left[\sup_{\rho_C, \sigma_G} \frac{1}{L} \sum_{\ell=0}^{L-1} \sqrt{F} \left(\begin{array}{c} |1\rangle\langle 1|_D \otimes \sigma_G, \\ U_{SC}(|0\rangle\langle 0|_S \otimes \mathcal{N}^\ell(\rho_C))U_{SC}^\dagger \end{array} \right) \right]^2, \quad (\text{A10})$$

where

$$\mathcal{N}(\omega_C) := \text{Tr}_S[U_{SC}(|0\rangle\langle 0|_S \otimes \omega_C)U_{SC}^\dagger]. \quad (\text{A11})$$

Proof. This follows by employing reasoning similar to that for [Ros09, Lemma 4.2] (see also [KW00]). This reasoning is also very similar to the reasoning used around (160)–(167). For a fixed state $|\psi\rangle_{RC}$ of the prover, the global state after Step 6 of Algorithm 20, but before the measurements, is

$$P U_{S_{L+1}C} \sum_{\ell=0}^{L-1} \sqrt{\frac{1}{L}} |\ell\rangle_{T'T} U_{S_1^L C}^\ell |0\rangle_{S_{L+1}} |\psi\rangle_{RC}, \quad (\text{A12})$$

where $P \equiv P_{T', S^L F \rightarrow T'' F'}$. Then, by splitting the systems $S_{L+1}C$ into the decision qubit D and denoting all other qubits by G , the acceptance probability is given by

$$\begin{aligned} & \left\| \sum_{\ell=0}^{L-1} \sqrt{\frac{1}{L}} |\ell\rangle_{T'T} U_{S_1^L C}^\ell |0\rangle_{S_{L+1}} |\psi\rangle_{RC} \right\|_2^2 \\ &= \sup_{|\varphi\rangle_{F'G}} \left| \langle \Phi_{T''T} \langle 1|_D \langle \varphi|_{F'G} P U_{S_{L+1}C} \times \right. \\ & \quad \left. \sum_{\ell=0}^{L-1} \sqrt{\frac{1}{L}} |\ell\rangle_{T'T} U_{S_1^L C}^\ell |0\rangle_{S_{L+1}} |\psi\rangle_{RC} \right|. \end{aligned} \quad (\text{A13})$$

Considering that the reduced state of $\sum_{\ell=0}^{L-1} \sqrt{\frac{1}{L}} |\ell\rangle_{T'T} U_{S_1^L C}^\ell |0\rangle_{S_{L+1}} |\psi\rangle_{RC}$, after tracing over all systems sent to the prover, is

$$\frac{1}{L} \sum_{\ell=0}^{L-1} |\ell\rangle\langle \ell|_T \otimes \mathcal{N}^\ell(\rho_C), \quad (\text{A14})$$

where $\rho_C := \text{Tr}_R[\psi_{RC}]$, and the reduced state of $|\Phi\rangle_{T''T} |1\rangle_D |\varphi\rangle_{F'G}$, after tracing over all systems not transmitted by the prover, is

$$\frac{1}{L} \sum_{\ell=0}^{L-1} |\ell\rangle\langle \ell|_T \otimes |1\rangle\langle 1|_D \otimes \sigma_G, \quad (\text{A15})$$

where $\sigma_G := \text{Tr}_{F'}[\varphi_{F'G}]$, we conclude by Uhlmann's theorem that (A13) is equal to

$$\begin{aligned} & \sup_{\sigma_G} F \left(\frac{1}{L} \sum_{\ell=0}^{L-1} |\ell\rangle\langle\ell|_T \otimes \mathcal{N}^\ell(\rho_C), \frac{1}{L} \sum_{\ell=0}^{L-1} |\ell\rangle\langle\ell|_T \otimes |1\rangle\langle 1|_D \otimes \sigma_G \right) \\ &= \left[\sup_{\sigma_G} \frac{1}{L} \sum_{\ell=0}^{L-1} \sqrt{F} \left(\begin{array}{c} |1\rangle\langle 1|_D \otimes \sigma_G, \\ U_{SC}(|0\rangle\langle 0|_S \otimes \mathcal{N}^\ell(\rho_C))U_{SC}^\dagger \end{array} \right) \right]^2. \end{aligned} \quad (\text{A16})$$

We conclude the expression in the statement of the theorem after optimizing over all input states of the prover. ■

In order to establish that BQP_{CTC} is contained in QIP, it is necessary to map yes-instances of the former to yes-instances of the latter, and the same for the no-instances. Accomplishing the first part of the task is straightforward. A yes-instance of BQP_{CTC} implies that there exists a fixed-point state ρ_C such that

$$\text{Tr} \left[(|1\rangle\langle 1|_D \otimes I_G) U_{SC}(|0\rangle\langle 0|_S \otimes \rho_C) U_{SC}^\dagger \right] \geq 1 - \delta. \quad (\text{A17})$$

Thus, the prover transmits such a fixed-point state ρ_C to the verifier, and we find that the acceptance probability is not smaller than

$$\begin{aligned} & \left[\sup_{\sigma_G} \frac{1}{L} \sum_{\ell=0}^{L-1} \sqrt{F} \left(\begin{array}{c} |1\rangle\langle 1|_D \otimes \sigma_G, \\ U_{SC}(|0\rangle\langle 0|_S \otimes \mathcal{N}^\ell(\rho_C))U_{SC}^\dagger \end{array} \right) \right]^2 \\ & \geq \sup_{\sigma_G} F \left(|1\rangle\langle 1|_D \otimes \sigma_G, U_{SC}(|0\rangle\langle 0|_S \otimes \rho_C) U_{SC}^\dagger \right) \end{aligned} \quad (\text{A18})$$

$$\geq \sup_{|\varphi\rangle_{F'G}} |\langle 1|_D \langle \varphi|_{F'G} U_{SC} |0\rangle_S |\psi\rangle_{RC}|^2 \quad (\text{A19})$$

$$= \|\langle 1|_D U_{SC} |0\rangle_S |\psi\rangle_{RC}\|_2^2 \quad (\text{A20})$$

$$= \text{Tr} \left[(|1\rangle\langle 1|_D \otimes I_G) U_{SC}(|0\rangle\langle 0|_S \otimes \rho_C) U_{SC}^\dagger \right] \quad (\text{A21})$$

$$\geq 1 - \delta. \quad (\text{A22})$$

The first inequality follows because $\mathcal{N}^\ell(\rho_C) = \rho_C$ for all ℓ .

It is less clear how to handle the case of a no-instance of BQP_{CTC} , because the definition of this complexity class only specifies the behavior of the circuit when ρ_C is an exact fixed point of \mathcal{N} . Algorithm 20 attempts to verify whether the prover sends a fixed point, but it only actually verifies whether the prover sends a state that is an approximate fixed point. The acceptance probability of Algorithm 20 is given by (A10) and is bounded from above by

$$\begin{aligned} & \sup_{\rho_C, \sigma_G} F \left(|1\rangle\langle 1|_D \otimes \sigma_G, U_{SC}(|0\rangle\langle 0|_S \otimes \overline{\mathcal{N}}_L(\rho_C)) U_{SC}^\dagger \right) \\ & \leq \sup_{\rho_C} \langle 1|_D \text{Tr}_G [U_{SC}(|0\rangle\langle 0|_S \otimes \overline{\mathcal{N}}_L(\rho_C)) U_{SC}^\dagger] |1\rangle_D, \end{aligned} \quad (\text{A23})$$

where the bounds follow from concavity of root fidelity and the data-processing inequality for fidelity. In the above, $\overline{\mathcal{N}}_L$ is the Cesaro mean channel:

$$\overline{\mathcal{N}}_L(\omega_C) := \frac{1}{L} \sum_{\ell=0}^{L-1} \mathcal{N}^\ell(\omega_C). \quad (\text{A24})$$

This channel has the property that the sequence $\{\overline{\mathcal{N}}_L\}_L$ converges to the fixed-point projection channel $\mathcal{P} := \lim_{L \rightarrow \infty} \overline{\mathcal{N}}_L$ of \mathcal{N} , so that $\mathcal{P}(\omega_C)$ is guaranteed to be a fixed point of \mathcal{N} for every input state ω_C [Wol12]. It is not clear how to obtain a channel independent bound that relates the convergence of $\overline{\mathcal{N}}_L$ to \mathcal{P} , as a function of L alone. Furthermore, it is likely not possible that the closeness of $\overline{\mathcal{N}}_L$ to \mathcal{P} could generally be inverse polynomial in L ; for if it were, then one could simulate BQP_{CTC} in BQP, because the verifier could apply the map $\overline{\mathcal{N}}_L$ and generate a fixed point of the channel without the help of the prover. However, we now know that $\text{BQP}_{\text{CTC}} = \text{PSPACE}$ [AW09], and it is widely believed that $\text{PSPACE} \neq \text{BQP}$. In the case of a no-instance of BQP_{CTC} , it is thus not clear how to relate the acceptance probability of Algorithm 20 to the acceptance probability of the no-instance of BQP_{CTC} . We leave this as a curious open question.